THE UNIVERSITY
of EDINBURGH

Investigating the role of MyD88-NF-κB signalling in regulating the inflammatory response to the emerging pre-neoplastic cells

Isabel Ribeiro Bravo

PhD Inflammation

The University of Edinburgh

2019

Abstract

Chronic inflammation has long been considered an enabling characteristic of the cancer microenvironment. The release of growth and survival factors, extracellular matrix-modifying enzymes and other bioactive molecules by inflammatory cells into the tumour microenvironment contributes to the acquisition of cancer hallmark capabilities. It is now known that oncogenes can activate signals that promote the formation of an inflammatory microenvironment, even in the absence of external stimuli, placing inflammation as an early phenomenon in the timeline of tumour development. The over-expression of an oncogene in pre-neoplastic cells has been shown to promote the release of cytokines and other pro-inflammatory markers and consequent recruitment of neutrophils and macrophages. The recruitment of neutrophils has been previously associated with increased proliferation of oncogene-transformed cells, however, the mechanisms by which neutrophils exercise this trophic role are yet poorly understood.

Nuclear factor *kappa* B (NF-κB) transcription factors are crucial elements for the regulation of inflammation, immune response as well as cellular stress response. Activation of NF-κB signalling pathway leads to the expression of mitogenic and anti-apoptotic factors, thus having the potential to promote tumorigenesis.

MyD88 is an adaptor protein that mediates TLR/IL-1-R activation of the NF-κB pathway. MyD88 has been shown to play both positive and negative roles in cancer development. It is unclear however, whether the MyD88-NF-κB signalling pathway plays a role during the earliest stages of preneoplastic development of tumour initiation.

To better understand the role of MyD88-NF-κB in oncogene driven inflammation during preneoplastic cell development, I was involved in the development of a zebrafish (*Danio rerio*) tissue specific inducible model which allowed the temporal control of $HRas^{G12V}$ oncogene expression for generation of pre-neoplastic cells (PNCs) and the detection of the earliest signalling

events that initiate the process of tumour development. Using reporter lines, generated elsewhere, I demonstrate the activation of MyD88-NF-κB signalling pathway in both PNCs and recruited neutrophils. I also evaluate the effect of its downregulation, through the expression of the murine dominant negative mutant of IκBα, on PNCs proliferation and modulation of recruited neutrophil behaviour.

Alongside the study of NF-κB as an inducer of tumour initiation, I also provide evidence of heterogeneity within the neutrophil population recruited to the PNCs and the different behaviours they exhibit.

This work demonstrates the potential of zebrafish for the study of tumour initiation highlighting the involvement of NF-κB signalling pathway in the establishment of an inflammatory milieu that allows the progression of this first stage of tumorigenesis.

Lay Abstract

Chronic inflammation has long been considered an enabling characteristic of cancer. Inflammatory cells can be activated to infiltrate tumours and release signals which exacerbate the aggressiveness of the disease. Nuclear factor *kappa* B (NF-κB) is known as one of the main components to regulate the release of these signals and was shown to have enhanced activity in several malignancies of distinct origins. Even though much is known in well-established tumours, the difficulty of early detection of tumour masses rendered the study of inflammation in tumour initiation inaccessible.

The use of zebrafish (*Danio rerio*) larvae as a model organism has rapidly gained popularity within this field of study. The possibility for genetic manipulation coupled with the larvae's translucency allows a non-invasive in vivo approach for the study of the initial stages of tumour development.

This work characterizes the development of a new model, which allows the live detection of the earliest events that initiate the process of tumour development in the zebrafish larval skin. Live imaging studies revealed the involvement of NF-κB in the regulation of the inflammatory response during tumour initiation. Genetically blocking NF-κB activation confirmed its tumour promoting role at a very early stage of tumour development.

Acknowledgments

I would like to thank my supervisors for their much appreciated help during this project. To my primary supervisor, Dr. Yi Feng, my most sincere gratitude for the continuous encouragement, guidance and patience throughout the last five years. Many thanks to Professor Adriano Rossi for the valued advice and support, especially during the writing process.

I would like thank all the members of the Feng Laboratory, past and present. My biggest appreciation goes to my oldest companion in the trenches, the outsource of my conscience, the Sam to my Frodo, my "work wife", Lisa Kelly, with whom sharing this journey has been the greatest pleasure. A big thank you to Nikolay Ogryzko who gave true meaning to the term "NF-κB Dream Team". His constant support with experimental design and troubleshooting has been instrumental for my latest progress.

I would like to thank Shonna Johnston, Will Ramsay and Mari Pattison at the QMRI Flow Cytometry and Cell Sorting Facility for their help with the flow cytometry experiments. I would also like to a knowledge the staff of the QMRI zebrafish facility, past and present, and the technical staff at the Centre for Inflammation Research.

Finally, I would like to thank all my friends and family for their moral support. A special mention to Dyana Markose, Ross Mills, David Taggart, Jordan Portman, Luke Way and Natasha Gibson for making Edinburgh my Home, and to my parents, Ni and Paulo, for their continued encouragement, even from a distance.

Signed Declaration

I declare that this thesis has been composed solely by myself and that it has not been submitted, in whole or in part, in any previous application for a degree. Except where otherwise by reference or acknowledgment, the work presented is entirely my own.

.....

Isabel Ribeiro Bravo

Table of Contents

List of Figures and Tables

Supplementary video 1 PNC rearrangement and protrusion extension

Supplementary video 2 PNC movement

Supplementary video 3 Neutrophil recruitment 12-36hpi

Supplementary video 4 NF-κB activity in PNCs 10-24hpi

Supplementary video 5 Neutrophil close interaction with PNCs at 24hpi

Supplementary video 6 Recruited neutrophils exhibit variable levels of *myd88* expression at 24hpi

Abbreviations

4-OHT: 4-Hydroxytamoxifen

Abp140: Actin Binding Protein 140

AKT: Protein Kinase B

ANOVA: Analysis of variance

AP1: Activator Protein 1

APC: Adenomatous polyposis coli

ARC: Activity Regulated Cytoskeleton Associated Protein

BCl10: B-Cell lymphoma/leukemia 10

BCL-(2/X_L): B-cell lymphoma (2/extra-large)

BLT2: Leukotriene B4 receptor 2

BMP: Bone morphogenetic protein

BRCA1: Breast cancer type 1 susceptibility protein

CAFs: cancer associated fibroblasts

CARMA: CARD- and membrane-associated guanylate kinase-like domain-containing protein

CDKN2A: Cyclin Dependent Kinase Inhibitor 2

CFP: Cyan Fluorescent Protein

CHT: Caudal Hematopoietic Tissue

COX-2: Cyclooxygenase-2

Cry: Crystallin

Ct: Cycle Threshold

CXCL(1/2/5/8/18b): C-X-C motif chemokine ligand

CXCR(1/2): C-X-C motif chemokine receptor

DAMPs: Damage-associated molecular patterns

DDR: DNA Damage Response

DMBA: 7,12-Dimethylbenz[a]anthracene

DMSO: Dimethyl Sulfoxide

(c)DNA: (complimentary) Deoxyribonuclease Acid

dpf: days post fertilization

Dpp: Decapentaplegic

DSB: Double Strand Breaks

DsRed: Red Fluorescent Protein

Duox: Dual Oxidase

ECM: extracellular matrix

EdU: 5-ethynyl-2'-deoxyuridine

EDTA: Ethylenediaminetetraacetic acid

EGF(R): Epidermal Growth Factor (Receptor)

eGFP: enhanced Green Fluorescent Protein

EMT: Epithelial-to-Mesenchymal Transition

ErBB2/HER2: human epidermal growth factor receptor 2

ERK: Extracellular signalling-related kinase

ER^{T2}: human estrogen receptor α

FACS: Fluorescence-activated cell sorting

GAPs: GTPase-activating proteins

G-CSF: granulocyte-colony stimulating factor

GDF-15: Growth/differentiation factor 15

GDP: Guanosine diphosphate

GEFs: guanine nucleotide exchange factors

Grb2: Growth factor receptor-bound protein 2

GSK3β: Glycogen synthase kinase 3 beta

HBEGF: Heparin-Binding EGF-Like Growth Factor

HMGB1: High mobility group box 1

hpi: hours post induction

HPV16: human papillomavirus type 16

HSP: Heat Shock Protein

HSPCs: hematopoietic stem and progenitor cells

(c)IAPs: (cellular) inhibitor of apoptosis proteins

IFN(α): Interferon

IκB(α/SR): inhibitor of kappa B (super-repressor)

IKK(α/β/γ): inhibitor of kappa B kinase

IL(1/1α/1β/6/12/18/23)(R): Interleukin (Receptor)

$IPLA_2$: Calcium-independent phospholipase A2

IRAK(4/1/2): Interleukin-1 receptor-associated kinase

JNK: c-Jun N-terminal kinase

krt4: keratin 4

krtt1c19e: keratin type 1 c19e

LPS: Lipopolysaccharide

LTB_4: Leukotriene B4

lyz: lysozyme C

MALT1: Mucosa-associated lymphoid tissue lymphoma translocation protein 1

MAPK: Mitogen-activated protein kinase

MDSCs: myeloid-derived suppressor cells

MEK: Methyl Ethyl Ketone

MMP(9): Metalloproteinase

MNK1: MAP kinase-interacting serine/threonine-protein kinase 1

MyD88: Myeloid Differentiation Primary Response 88

NF-κB: nuclear factor kappa-light-chain-enhancer of activated B cells

(i)NO(S): (inducible) nitric oxide (synthase)

NSAIDs: Nonsteroidal anti-inflammatory drugs

PAMPs: pathogen-associated molecular patterns

PAR4: Protease-Activated Receptor 4

PBS: Phosphate buffered saline

(q)(RT)PCR: (quantitative) (reverse transcription) polymerase chain reaction

PDK1: Phosphoinositide-dependent kinase-1

PNC: Pre-neoplastic cell

PGE2: Prostaglandin E2

PI3K: Phosphoinositide 3-kinase

PKC(α/δ): Protein kinase C

PTEN: Phosphatase and tensin homolog

RAGE: receptor for advanced glycation endproducts

(H/K/N)Ras(4A/4B): (Harvey/Kirsten/Neuroblastoma) Rat Sarcoma Viral proto-oncogene

RalB: Ras Like Proto-Oncogene B

RalGEFs: Ras like guanine nucleotide exchange factors

RB1: retinoblastoma gene

(m)RNA: (messenger) Ribonucleic Acid

ROS: Reactive oxygen species

RT: Room Temperature

SEM: Standard Error of the Mean

SOD(2): Superoxide dismutase

SOS: Son of Sevenless

STAT3: Signal transducer and activator of transcription 3

TAN: Tumour associated neutrophil

TBK1: TANK Binding Kinase 1

TGF-β: Transforming growth factor β

Tiam: T-lymphoma invasion and metastasis-inducing protein 1

TIR: Toll/interleukin-1 receptor

TLR(3/4): Toll-like Receptor

TNF: Tumour necrosis factor

(A/G/U)TP: (Adenosine/Guanosine/Uridine) Triphosphate

TPA: 12-O-tetradecanoyl-phorbol-13-acetate

TP53: Tumour protein p53

TRAF6: TNF receptor-associated factor 6

TRK: Tyrosine Kinase Receptors

TUNEL: Terminal deoxynucleotidyl transferase dUTP nick end labelling

UAS: Upstream activating sequence

Upd: Unpaired

VEGF: Vascular endothelial growth factor

Wg: Wingless

WT: Wild type

Yki: Transcriptional coactivator yorkie

1 Introduction

1.1 Introduction to Cancer

Cancer is a group of more than 100 distinct diseases which can originate in nearly all cell types and organs of the human body, with the most common organs affected being lung, female breast, bowel or prostate [1]. The underlying characteristic of all cancers is an abnormal and uncontrolled proliferative and invasive phenotype whereby cells expand beyond normal tissue boundaries and ultimately metastasize to distant organs of the body [2]. With millions of new cases arising every year, cancer is responsible for 1 in 7 deaths worldwide [3].

Since the early twentieth century, when Theodore Boveri observed that cancer cells were often affected with chromosomal anomalies [4], increasing cumulative evidence established that genetic mutations carried within a cell's genome, is the central driving mechanism of all cancers. While a small proportion of cancers can be hereditary, 90% of cancers are associated with newly acquired somatic mutations as a result of environmental factors [5]. A variety of risk factors have been implicated as potential causes for tumour development. Considering cancer arises as the result of somatic mutations accumulated through the course of one's life, the risk of developing this disease increases with age. Consequently, 36% of all cancer patients diagnosed each year in the UK are over 75 years old [1]. Environmental factors, such as, exposure to ionising radiation or mutagenic chemicals, can directly affect a cell's genetic integrity. However, many cancers are often associated with some sort of chronic inflammation. Tobacco smoking is implicated in approximately 33% of cancer cases. 35% of cases are associated with obesity and poor diet. Chronic viral infections are also associated with certain types of cancer [1,5]. Considering that some risk factors are associated with unhealthy behaviour and life style, it is believed that nearly 40% of cancer cases in the UK are preventable [1].

Even though all cancers share a common pathogenesis and genetic mutations as the central driving mechanism, cancer is a highly heterogeneous group of diseases. The multitude of environmental factors, the great variety of gene mutations, often with context dependent functional impact, makes each disease unique with distinct severities and prognosis [6–8]. Early detection and treatment greatly increase the chances of survival. However, by the time patients present visible symptoms and report to the clinic, the disease has already progressed to a well-established tumour and, occasionally, with metastases in distant organs, limiting the available treatment options. Therefore, there is limited compiled evidence of the early events of carcinogenesis. Given the importance of early detection in improving patient outcomes, several funding bodies are starting to prioritize scientific research for the development of platforms for early detection and preventive therapies [9,10].

1.2 Cancer as a Complex Multistage Disease

The development of cancer is a stepwise process with increasing complexity. Tumour development is initiated with the acquisition of mutations in one or more somatic cells which give them a proliferative or survival advantage, or confer an increased susceptibility to further mutations. With each mutation a cell's aberrant phenotype becomes more prominent and its malignant state is enhanced. These aberrant cells promote tumour formation by uncontrolled clonal expansion developing cell masses which expand beyond normal tissue boundaries [2]. As the disease progresses, cancer cells acquire great plasticity. As such, some cells may detach from the primary tumour and spread to surrounding and distant organs where they seed the development of metastases.

As a tumour develops, cancer cells are believed to acquire a mutator phenotype, becoming more susceptible to additional stochastic mutations and chromosomal rearrangements [11,12]. In agreement with this concept, sequencing analysis of several tumour types has estimated that most cancers

present 1000 to 20000 somatic point mutations and hundreds of insertions, deletions and chromosomal rearrangements [13].

As such, cancer can be considered an evolutionary process whereby progressive hereditary genetic alterations that accompany tumour development give rise to a heterogeneous population of abnormal cells subject to natural selection. Some cells with metabolic or immunologic disadvantage die, while cells that survive and proliferate more efficiently thrive constituting the dominant subpopulation until a more advantageous phenotype appears [2,14,15].

While genetic mutations are considered the driving mechanism for cancer development, not all mutations acquired by somatic cancer cells have a consequent effect on tumour progression. These alterations can be classified as driver mutations or passenger mutations. Driver mutations grant the cells carrying them a proliferative or survival advantage allowing these cells to outcompete their neighbours. Passenger mutations do not confer any advantage to the tumour formation but happen to be present in cancer cells that are positively selected through the presence of driver mutations [2].

Cancer driver mutations often involve genes that regulate homeostatic cell processes such as cell polarity, cell cycle progression and proliferation, DNA repair and cell death signalling pathways. These genes fall into two different categories: oncogenes and tumour suppressor genes. Oncogenes arise from gain-of-function mutations in genes which encode proteins involved in the positive regulation of cell growth and proliferation, proto-oncogenes [16]. Such genes include RAS, EGFR, v-SRC, c-MYC, WNT and ERBB2. Tumour suppressor genes arise from loss-of function mutations in genes which control anti-tumorigenic mechanisms such as DNA repair and mitotic checkpoints, cell senescence and cell death [16]. TP53, PTEN, BRCA1, RB1 and APC are examples of tumour suppressor genes. As such, driver mutations will either directly enable a cell to proliferate or survive, or make it more resistant to the mechanisms which hold its proliferation or survival in check.

While nearly 300 driver genes have been identified [7], their functional impact is confined to a select number of signalling pathways implicated in

mechanisms such as cell growth and proliferation, stemness (pluripotency) and differentiation, cell survival/death and cell cycle progression, DNA repair and genomic integrity [8]. Some of these signalling pathways are often associated with specific types of cancer. But a few genes and their respective pathways are altered in high frequency across most cancer types. These genes include the tumour suppressor genes TP53 and CDKN2A which are involved in the DNA Damage Response and cell cycle regulation, respectively. Gain-of-function mutations in RAS and EGFR, promoting cell growth and proliferation, are also amongst the most common genetic alterations [8,12,17]. Although both the general principles of the mechanisms driving tumour development and the concept of cancer as an evolutionary disease are well established, the complexity and diversity between and within different cancer types restrict the study of important aspects of this disease. For instance, the classification of mutations found in cancer cells is constantly being updated as newly discovered cancer genes are added. Moreover, it is not always clear which mutations in those genes are, in fact, “drivers” and at which stage during tumorigenesis they are acquired [6,7,18]. As such, a long-standing question in cancer research has been to determine the minimum number of mutations required for the initiation of the tumorigenesis process to take place [13]. A recent study by Martincorena and colleagues in 2017 addressed this question, concluding that a surprisingly low number of driver mutations, ranging from 1 to 10 depending on the type of tissue, are required for tumorigenesis [19].

The complexity of cancer disease is further exacerbated by the involvement of other cell types within the tumour microenvironment. Transformed cells often exhibit paracrine signalling and engage surrounding resident and recruited cells to redirect their intracellular circuitry to nurture tumour development. Through the course of tumour development paracrine signalling promotes activation of resident fibroblasts and the recruitment of inflammatory cells. As tumour density increases, the recruitment of endothelial cells and vessel sprouting are extremely important for the establishment of a vascular system to meet the tumour needs for nutrients and oxygen. In this context it is important to consider tumours as complex tissues which include not only

mutant cancer cells but also the surrounding tumour associated stroma, involved in heterotypic interactions with one another to promote tumour progression [20–23].

With the purpose of formulating a commonality within the diversity and complexity of cancers for a better understanding of the development of such malignancies, Hanahan and Weinberg envisioned the concept of phenotypic capabilities required in most cancers, which they named hallmarks of cancer [20,23]. This concept comprises the principle that various driver mutations and subsequent altered pathways acquired by cancer cells, as well as the activity of the surrounding normal cell types, present a multitude of mechanisms for the development of the same underlying features required for the progression of the disease (Figure 1.2.1) [20,22,23].

While these phenotypic capabilities have been extensively studied in well-established tumours, how they arise and whether they are required for the early stages of tumour development is still not fully understood.

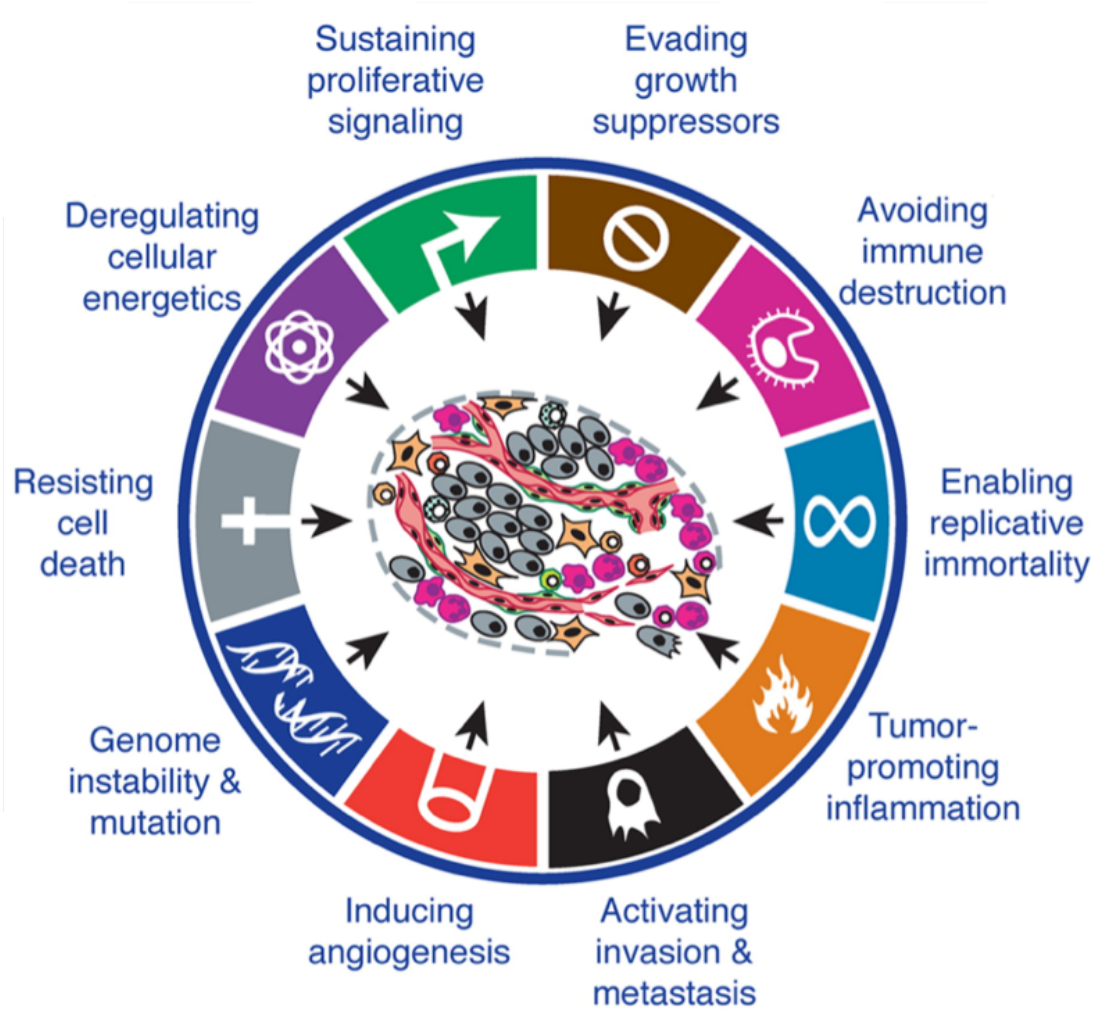

Figure 1.2.1 Hallmarks of Cancer. Phenotypic capabilities required in most cancers for tumour development and progression to metastatic disease as envisioned by Hanahan and Weinberg.

(Figure reused from Cell, Volume 144, Issue 5, Douglas Hanahan and Robert Weinberg, Hallmarks of Cancer: The Next Generation, P646-674., Copyright (2011), with permission from Elsevier)

1.3 Ras Signalling and Its Role in Cancer

Ras proteins are ubiquitous small GTPases which act as signal-relay proteins for several external stimuli, such as growth factors. Amongst the many important cell mechanisms they regulate are cell proliferation, differentiation, survival, motility [24]. In humans, the family of Ras proteins is composed of four highly homologous isoforms: HRas, NRas, KRas4A and KRas4B. These proteins are mainly present on the cytosolic surface of the plasma membrane. Specific isoforms were shown to exert signal relay in other membrane-bound organelles , namely Golgi apparatus (HRas and NRas) and endosomes (HRas and KRas) [25].

Ras functions as a binary switch, transitioning between the inactive GDP-bound and the active GTP-bound conformation. Because GDP is generally tightly bound and Ras intrinsic GTPase activity is very slow, this conformational switch is dependent and regulated by other GTPases [26,27]. Specifically, guanine nucleotide exchange factors (GEFs) bind to GDP-bound Ras mediating a conformational change which weakens Ras affinity to GDP, leading to the latter's release and the former's passive binding to GTP, which is more abundant in the cytosol, and consequent activation [28,29]. Conversely, GTPase-activating proteins (GAPs) bind to GTP-bound Ras and accelerate GTP hydrolysis by stabilising its high-energy transition state through the insertion of a catalytic residue, switching Ras back to its inactive GDP-bound form [28,30]. Given that the signalling network downstream of Ras and, consequently, the final signal output of a cell is greatly determined by the intensity and duration of Ras activity [24,31], a tight regulation of GEFs and GAPs is in place to mediate the appropriate Ras responsiveness to a multitude of stimuli. While this regulation is extremely important, it is mainly dependent on the mechanism of translocation, as GEFs and GAPs bind and promote Ras conformational changes by being recruited to the plasma membrane in close proximity with Ras proteins [26]. For instance, the activation of a cell through the binding of growth factors to Tyrosine Kinase Receptors (TRK), leads to receptor autophosphorylation, creating an intracellular docking site for adaptor

proteins. Amongst these adaptor proteins, Grb2 is recruited in association with Sos, a GEF protein, allowing for activation of Ras proteins and subsequent effector pathways [32].

To date, more than 10 different Ras effector pathways have been identified. The best characterized effector pathway is the Raf-MEK-ERK kinase cascade, whereby activated ERK can interact with several cytosolic and nuclear proteins, such as transcription factors, and ultimately, have a great effect on a cell transcriptional activity [33–36]. Another Ras downstream effector pathway involves the activation of PI3Ks and activation of downstream PDK1 and Akt kinases [36–38]. Ras-GTP can also bind and activate the signalling cascades of RALGEFs [39], Tiam [40], Phospholipase Cε [41], amongst others. Collectively, all Ras effector pathways act synergistically to mediate cellular responses to external stimuli regulating a wide range of cellular processes, including cell cycle progression and cell growth, survival and apoptosis, cell adhesion and cell motility, and vesicle trafficking (Figure 1.3.1).

Whilst all isoforms share regulatory mechanisms and can virtually bind to all Ras downstream effectors, their functions in embryo development and cellular homeostasis are not completely redundant [42]. The mechanisms attributing specific functions to each isoform are not fully understood and still under extensive investigation. It has been suggested that the functional singularities of Ras isoforms are related to differences in subcellular localization [25,43] and in their efficiency at activating distinct downstream effectors [44]. Tissue dependent variable expression levels of each isoform could also explain their non-redundant functionalities [45]. However, given the complexity of Ras signalling networks and how they are differently regulated in a tissue specific manner, in vivo evidence of the unique isoform functions is less clear [42,46].

Gain-of-function Ras mutations are amongst the most common tumour drivers, present in approximately one third of all human cancers [46]. These mutations often involve a single amino acid substitution at positions G12, G13 or Q61 which results in the loss of intrinsic and GAP dependent GTPase activity [47]. As a result of these mutations Ras proteins remain constitutively in the active GTP-bound conformation leading to the continuous activation of their

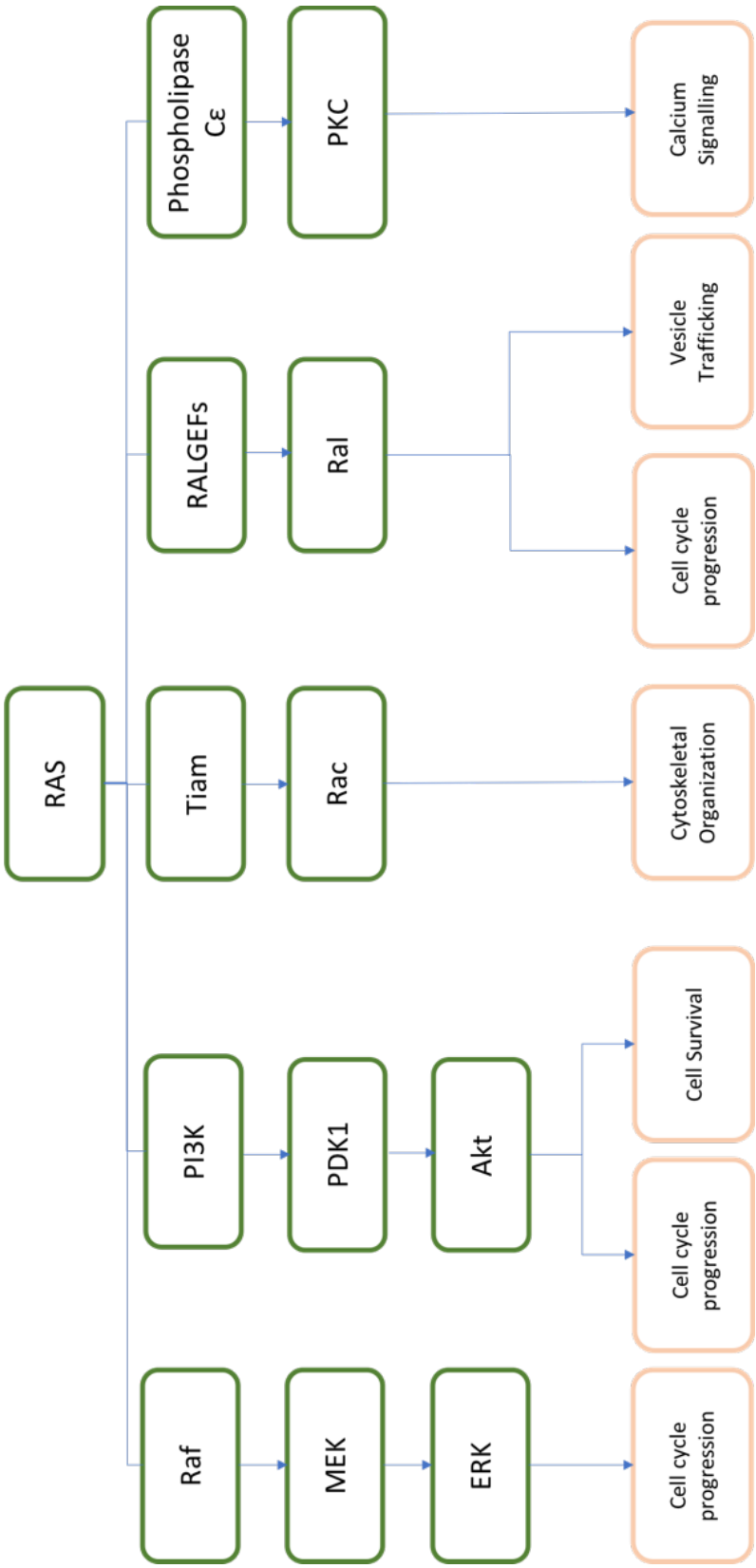

Figure 1.3.1 Ras signalling pathway. Downstream Ras effector pathways implicated in Ras mediated oncogenesis and the main mechanisms they regulate.

downstream effectors. Substitutions in each of the three positions have oncogenic potential in all Ras isoforms, however, each Ras isoform mutated at specific positions with distinct substitutions, prevail in different types of cancer. Namely, KRas mutations are most frequently found in adenocarcinomas [46,48], NRas mutations predominate in melanoma and haematopoietic malignancies [46,49], HRas mutations are often associated with skin squamous cell carcinoma and cancer of the urinary bladder [24,46,50].

Oncogenic Ras can contribute to the transformed cell phenotype in various ways. Considering the role of Ras proteins as regulators of a cell's response to mitogenic signals, it is not surprising that constitutively active Ras has an effect on the control of a transformed cell's proliferation. In fact, not long after its discovery, oncogenic Ras has been shown to be sufficient for cell cycle progression and increased proliferation of quiescent cells [51,52]. Several downstream effectors of Ras seem to contribute to this effect by promoting overexpression of cyclinD1 [53]. PI3K signalling further contributes to a cell's proliferative capacity by inhibiting GSK3β dependent proteolysis of CyclinD1 [54]. The central role of CyclinD1 in oncogenic Ras induced proliferation and tumorigenesis has also been established in vivo, whereby CyclinD1-deficient mice failed to develop and maintain different types of tumours [55–57].

Oncogenic Ras can further potentiate its own mitogenic effects by generating an autocrine loop through the overexpression of several growth factors, such as HBEGF, and the respective receptors [58,59].

The role of oncogenic Ras in cell viability is rather complex as it has been shown to mediate both, anti- and pro-apoptotic mechanisms. For instance, activation of PI3K and Raf pathways promotes cell survival through the upregulation of anti-apoptotic factors, such as ARC [60], and downregulation of pro-apoptotic proteins, including PAR4 [61]. Inversely, oncogenic Ras was also shown to promote apoptosis through a variety of mechanisms, such as activation of various tumour suppressor pathways [62,63]. While the mechanisms regulating the balance of these opposing signals are not yet fully understood, they seem to be context dependent. Nevertheless, in vivo

experimental data suggest that during tumorigenesis, oncogenic Ras favours a pro-survival signalling output in the presence and absence of tumour suppressors [64,65]. This is corroborated by the high incidence of Ras mutations found in human cancers.

The pro-tumorigenic role of constitutively active Ras is not limited to cell proliferation and survival as constitutively active Ras has also been shown to contribute to cell plasticity and migration through the alteration of cell junctions and the actin cytoskeleton [66]. The downstream effects of oncogenic Ras signalling are also felt beyond the cancer cell and promote alterations in the tumour microenvironment. Oncogenic Ras can contribute to the establishment of an inflammatory microenvironment with the release of cytokines and chemokines, such as, IL-1α, IL1-β, IL-6, CXCL8, amongst others [67–69]. These inflammatory mediators are believed to exert a pro-tumorigenic effect mainly through paracrine signalling. More specifically, secreted IL-6 was shown to promote angiogenesis by inducing expression of vascular endothelial growth factor (VEGF) [68,70]. Ras-induced CXCL8 expression promotes tumour infiltration of inflammatory cells, namely neutrophils, and consequent recruitment of endothelial cells, facilitating angiogenesis [69]. Ras induced upregulation of pro-angiogenic factors promote tumour vascularization. This is only achieved with the release of proteases which mediate extensive remodelling of the extracellular matrix (ECM) softening the physical entrapment of paracrine factors and tumour cells [71]. Therefore, aberrant Ras signalling contributes to all stages of cancer progression.

1.4 Tumour Associated Inflammation

The connection between cancer and inflammation has long been considered. In the nineteenth century, Rudolf Virchow established this link for the first time upon the observation that tumours were frequently found in tissues with chronic inflammation and were often infiltrated with inflammatory cells [5,72]. Since then, increasing evidence confirmed the importance of inflammation in

the generation of a pro-tumorigenic microenvironment that nurtures tumour formation.

Chronic inflammation is known to increase the risk of cancer. The implication that a chronic inflammatory microenvironment can increase mutation rate, in addition to enhancing the proliferation of mutated cells, elucidates how a number of inflammatory conditions predispose individuals to cancer development [5]. Moreover, inflammation can also be triggered after tumour initiation in a process now recognised as “tumour elicited inflammation”. Several mechanisms can contribute to that effect. A few oncoproteins have been shown to drive an inflammatory response through the activation of signalling pathways that promote the upregulation and release of proinflammatory cytokines and chemokines [67,69,72–77]. Inflammation can also be promoted by hypoxia and cancer cell necrosis due to insufficient blood supply at the core of a tumour mass. In some tissues where the epithelium exerts a protective barrier against the external environment, the development of a disorganised tumour mass can cause barrier deterioration and microbial invasion which can also elicit an inflammatory response [78]. The intensity of set inflammation may vary depending on the type of tumour, ranging from tumours with low leucocyte density, only detected with the appropriate antibodies, to highly chronic inflammatory setting [23]. Regardless of the intensity of the inflammatory microenvironment, it is now accepted most cancers exhibit an inflammatory component which impacts every step of tumorigenesis, from initiation to metastatic progression. In fact, the long term intake of non-steroidal anti-inflammatory drugs (NSAIDs) has a well-recognised preventive effect against several types of cancer [79]. As such, “tumour promoting inflammation” has been recognized as one of the hallmarks of cancer [23].

Many cell types, within the tumour microenvironment, can contribute to the establishment of an inflammatory setting. These include, not only, infiltrating immune cells, such as neutrophils, macrophages, monocytes, NK cells and T and B lymphocytes, but also the cancer cells and cancer associated fibroblasts [23].

Mechanistically, inflammation can promote tumorigenesis in various ways, contributing for the development of multiple hallmark capabilities. The release of inflammatory mediators into the microenvironment can promote tumour cell proliferation and cell survival. Inflammatory cells are also major contributors for tumour vascularization through the release of pro-angiogenic factors and ECM modifiers. Inflammation can equally contribute to tumour progression through the release of mutagenic factors, such as reactive oxygen species (ROS), which contribute to genetic instability [80–82].

Finally, inflammation can also have an effect on tumour immune surveillance. Most infiltrating immune cells can exhibit both pro- and anti-tumorigenic functions and the balance between the immune mediators that promote tumour progression opposing anti-tumour immune mediators is the ultimate determinant for tumour progression or rejection [83]. Inflammation polarizes this balance towards a tumour promoting immunity by enhancing the release pro-tumorigenic mediators and by down-regulating immune surveillance causing a dysfunctional anti-tumour immunity. Overall, tumour associated inflammation functions, not only as a potentiator of tumour progression, but also as a protective environment against immune surveillance [83].

1.5 The NF-κB and MyD88 Signalling Pathways

Nuclear Factor-kappa B (NF-κB) is a family of DNA binding proteins which promote transcriptional activation of a multitude of inflammatory and mitogenic factors. Given the multitude of external and internal stimuli which can activate the NF-κB signalling pathway, as well as the wide range of target genes it regulates, NF-κB is considered to play a central role in immune and inflammatory responses [84].

The NF-κB family of transcription factors include 5 subunits: Rel (cRel), p65 (RelA), RelB, p105/p50 and p100/p52. These subunits act as homodimers and heterodimers for transcriptional regulation. With the exception of RelB, which can only form heterodimers with p50 and p52, all other subunits can combine in many different dimers. Nevertheless, the most common combination is the

heterodimer p65-p50 [85,86]. It is generally agreed that NF-κB activity leads to transcriptional activation. However the assembly of p50 and p52 homodimers can act as transcriptional inhibitors [86–88]. The different combinations of subunits which have variable affinities to distinct NF-κB binding sites in gene regulatory sequences, and have different mechanisms of action, allow for the diversity of responses regulated by NF-κB [89,90].

In unstimulated cells, NF-κB dimers are mainly bound to the inhibitor proteins from the IκB family, which interfere with the nuclear localization signal (NLS) present on NF-κB dimers and thus sequester NF-κB in the cytoplasm. Alongside IκBs, NF-κB can also be inhibited by the p100 and p105 proteins, precursors to NF-κB p50 and p52 subunits, which also contain an inhibitory domain promoting the retention of their partners in the cytoplasm [91]. However, while p105 processing into p50 is constitutive, the processing of p100 into p52 is regulated [92]. Upon cell stimulation with extracellular stimuli, two main pathways lead to nuclear translocation of NF-κB dimers and transcriptional activation: the classical (canonical) pathway and the alternative (noncanonical) pathway [93]. Both pathways involve similar mechanisms including activation of an IκB Kinase (IKK) complex and proteasomal release of the NF-κB dimer NLS, although being activated through different cell surface receptors and targeting different cytoplasmic adaptors and NF-κB subunits (Figure 1.5.1) [93].

In the classical (canonical) pathway the IKK complex is composed of the catalytic subunits IKKα, IKKβ, and the regulatory subunit IKKγ or NEMO [94,95]. This complex, when active, phosphorylates IκBs targeting their polyubiquitination and subsequent proteasomal degradation. The release of the NF-κB dimer (mainly p65-p50 in this pathway) from their inhibitor protein allows their translocation to the nucleus where they can regulate gene transcription [96]. The alternative (noncanonical) pathway activates IKKα homodimers which phosphorylate p100, often in a p100-RelB dimer [97]. Once phosphorylated, p100 is processed to p52 through ubiquitination and proteasomal degradation of its inhibitory C-terminal half. The resulting p52-

RelB dimer can then translocate to the nucleus to activate gene transcription [92].

While the alternative pathway is mostly associated with development of secondary lymphoid organs, B cell maturation and adaptive immunity, the classical pathway is considered a central regulator of innate immunity and inflammatory responses. The classical pathway can be rapidly activated by pro-inflammatory cytokines, PAMPs and DAMPs acting via TNF, IL-1 and Toll-Like receptors. Activation occurs within minutes and results in expression of multiple inflammatory and innate immune genes [91,98].

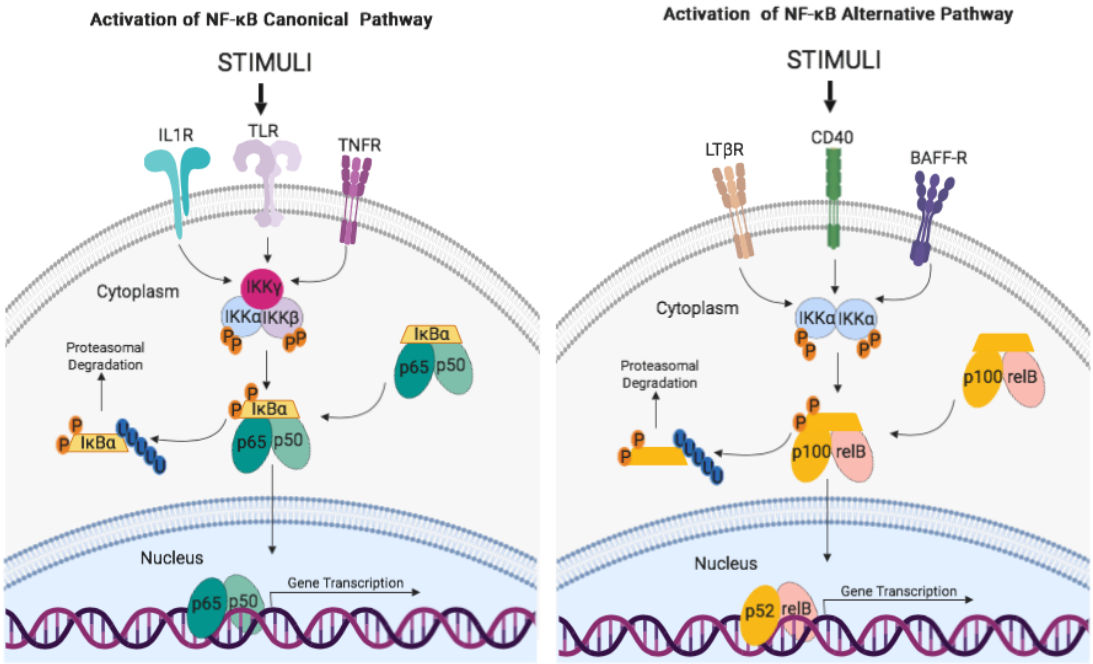

Figure 1.5.1 NF-κB signalling pathway, Schematic representation of the canonical and alternative pathway for NF-κB activation. (Created with Biorender.com)

The activation of the classical NF-κB pathway occurs mainly through the intracellular adaptor protein MyD88. This protein mediates the intracellular signalling of IL-1R, IL-18R and all Toll-like receptors (TLRs), with the exception of TLR3 [99–102]. MyD88 binds to the cytoplasmic TIR domain of activated receptors and recruits IRAK4 [99,102]. IRAK4 autophosphorylation, as a result of clustering of MyD88-IRAK4 within the receptor complex, promotes the

nucleation of the Mydossome with recruitment of IRAK1 and IRAK2 [103]. The Mydossome assembly promotes recruitment and activation of other adaptor proteins, including several E3 ubiquitin ligases, such as TRAF6, which catalyses K63-linked polyubiquitylation of adjacent proteins [104]. K63-linked polyubiquitin is recognised by the regulatory subunit IKKγ of the IKK complex, which when recruited, induces proximity between the two IKK catalytic subunits required for their trans-autophosphorylation and consequent activation [104–107].

Characteristic target genes of NF-κB signalling include cytokines (such as IL-1, IL-6 and TNF), chemokines (such as CXCL1, CXCL2 and CXCL8), pro-inflammatory enzymes (such as COX-2), metalloproteases (MMPs), mitogenic signals (such as CyclinD1 and Myc), pro-survival signals (such as BCL-X_L, BCL-2, SOD2 and cIAPs), inducible nitric oxide synthase (iNOS), NF-κB negative regulators (IκBα and A20) amongst others [84,85,93].

1.6 The Importance of MyD88-NF-κB Signalling in Tumour Development

NF-κB is found constitutively active in most cancers, although the mechanisms for activation of this signalling pathway greatly vary depending on the type of malignancy. Gain of function mutations in several NF-κB subunits and IκBs encoding genes have been found in a variety of cancers [108–110]. Similarly, cancer driver mutations are also found in genes coding upstream regulators of the NF-κB pathway, including TRAF proteins and MyD88 [111–115]. These genetic alterations are mainly restricted to haematological malignancies. Nevertheless, the majority of NF-κB-positive tumours are solid tumours of epithelial nature [116].

With regards to epithelial tumours, several studies have revealed a connection between oncogenic Ras and NF-κB activation. Several *in vitro* studies have implicated a variety of oncogenic Ras downstream effector pathways in the activation of NF-κB signalling and the requirement of NF-κB activity for cellular

transformation [69,117–124]. The main mechanism through which NF-κB activity seems to mediate cellular transformation is by the suppression of a p53-independent oncogenic Ras induced apoptosis [120,125]. This effect seems to also be observed *in vivo*. Suppression of NF-κB signalling leads to an increase in apoptosis and reduced formation of $KRas^{G12D}$ induced lung tumours independent of p53 status [126,127].

NF-κB activity can have additional pro-tumorigenic effects by stimulating the production of regeneration enhancing inflammatory cytokines and chemokines and growth factors, promoting proliferation of tumour cells . As such, increased NF-κB activity on its own is sufficient for hyperproliferation and dysplasia of the mouse epidermis [128]. Inversely, mice with keratinocyte-specific p65 deletion are resistant to DMBA/TPA-induced skin carcinogenesis. In this model, NF-κB activity has a twofold pro-tumorigenic effect by protecting keratinocytes from DNA damage-induced death and by facilitating the establishment of a proinflammatory microenvironment which promotes epidermal hyperplasia [129].

NF-κB dependent cytokine and chemokine production is important to maintain NF-κB activation but also to engage other signalling pathways in the process of tumorigenesis. IL-1α and IL-1β are important pro-inflammatory cytokines, which can be produced by cancer cells and promote activation of the NF-κB and MAPK pathways. IL-1α, for instance, was shown to be extremely important for a sustained NF-κB activity in $HRas^{G12V}$ transformed keratinocytes through the establishment of an autocrine loop through IL-1α-IL-1R-MyD88 signalling [130]. The importance of this autocrine loop in skin tumorigenesis is further validated by the reduced tumour size arisen from MyD88-deficient $HRas^{G12V}$ transformed keratinocytes transplanted into nude mice. MyD88 deficiency did not affect tumour cell proliferation or survival but diminished the paracrine function of tumour cells, in such manner that tumours displayed impaired vascularization [130].

Recruited inflammatory cells and cancer associated fibroblasts (CAFs) are also major contributors to the establishment of a pro-tumorigenic inflammatory

microenvironment in skin carcinomas, through NF-κB-dependent release of cytokines and chemokines [131].

Sporadic colorectal cancer is also highly dependent on MyD88-NF-κB signalling for tumorigenesis [132]. This type of cancer is often initiated by loss of the APC tumour suppressor gene and consequent activation of β-catenin [133,134]. This results in the downregulation of mucin 2 production and aberrant expression of tight junction proteins, resulting in intestinal epithelial barrier deterioration [78]. As such, the inflammatory microenvironment characteristic of this type of tumours is initiated when intestinal epithelial barrier deterioration allows the invasion of microbial products, which in turn activate resident myeloid cells in a TLR-MyD88 dependent manner. Myeloid cells are major contributors for the release of IL-23, IL-1β and IL-6 into the tumour microenvironment [78][135]. These cytokines are important for tumorigenesis as they promote, directly and through altered adaptive immune gene expression, tumour cell proliferation and activation of stem cell markers gene expression by activating NF-κB and other inflammatory signalling pathways [78,135,136].

MyD88-NF-κB signalling has also been implicated in tumorigenesis through the activation of immune cell polarization and immunosuppressive behaviour. For instance, mobilization and activation of myeloid derived suppressor cells (MDSCs) can occur through the activation of IL-1R-MyD88-NF-κB pathway [137]. Pro-tumorigenic “M2” macrophage polarization was also shown to rely on the same signalling pathway [138,139].

While generally accepted as having a pro-tumorigenic role, NF-κB has also been shown to exert a tumour suppressor effect in some circumstances. Namely, in diethyl nitrosamine (DEN) driven hepatocellular carcinoma NF-κB suppression results in increased hepatocyte death and subsequent compensatory proliferation of surviving hepatocytes leading to enhanced tumorigenesis [140]. Inactivation of NF-κB in murine skin results in spontaneous development of squamous cell carcinomas through the increase of keratinocyte apoptosis and TNF-dependent inflammation [141–144].

Therefore, the impact of NF-κB in cancer development is extremely complex, having specific effects which may vary depending on cell type, mechanism of tumour induction, type of inflammatory response involved in tumour promotion or stage of tumour development.

1.7 Neutrophil Recruitment and Their Conflicting Roles in Tumour Development

Neutrophils constitute the most abundant leukocytes in circulation and represent an organism's first line of defence against infection and tissue damage. These inflammatory cells exert their role in host defence through a multitude of mechanisms ranging from phagocytosis to the release of antimicrobial materials. They can also modulate other innate and adaptive immune responses by the release of cytokines and chemokines and through antigen presentation [145].

While extensively studied in their role in acute inflammatory responses, neutrophils were considered, for a long time, simple bystanders in the mechanisms of carcinogenesis and tumour development [146,147]. However, since the establishment of inflammation as one of Hanahan and Weinberg's hallmarks of cancer [23], a newfound appreciation for neutrophils and their role in tumorigenesis has arisen.

Several studies have established that neutrophils rely on CXCR2 and CXCR1 dependent chemotaxis to be recruited to the tumour microenvironment [148–152]. A number of chemokines upregulated in the tumour stroma have been suggested as potential mediators of this neutrophil chemotaxis. CXCL8, a known transcriptional target of oncogenic Ras, is known to promote neutrophil infiltration [69,74]. CXCL5 was also found to induce neutrophil recruitment in hepatocellular carcinoma [153]. As activated neutrophils are also great sources of chemokines they can potentiate neutrophil infiltration through a positive feedback mechanism whereby they further promote the recruitment of additional neutrophils [147]. Other mechanisms have also been implicated in neutrophil chemotaxis. Hydrogen peroxide, for instance, is one of the initial

signals promoting neutrophil recruitment to oncogenic Ras transformed cells, as it has been shown in a zebrafish model [154].

In the tumour stroma, tumour associated neutrophils (TANs) constitute a heterogeneous population with conflicting phenotypes. Depending on their polarization, neutrophils can exhibit an N1 anti-tumorigenic effect or an N2 pro-tumorigenic effect [155]. A recent study has further characterized the diversity within the neutrophil population in tumour bearing individuals and established three distinct populations according to their density and maturity. According to the study, mature high density neutrophils resembling neutrophils of tumour free animals have an anti-tumorigenic effect. Inversely, low density neutrophils are pro-tumorigenic and include a subpopulation of mature (fully formed lobulated nucleus) neutrophils and a population of immature neutrophils, similar to granulocytic MDSCs [156]. While the characteristic differences of these subpopulations are well defined, TANs are able to transition between populations in response to tumour derived factors. For example, high density neutrophils are capable of becoming low density neutrophils upon treatment with TGF-β. Additionally, the low density neutrophil population was found to expand with disease progression [156].

In line with these findings, others have also suggested that TAN polarization bias is correlated with the stage of tumorigenesis. TANs from early tumours were shown to be more cytotoxic and produce higher levels of TNF, NO and H_2O_2. This effect was progressively reduced with tumour progression and in late stage disease TANs mainly exhibited a tumour promoting immunosuppressive effect with evident N2 polarized transcriptional signature [157–159].

Nevertheless, recent studies have shown a pro-tumorigenic role of neutrophils from an early neoplastic stage [149,150,154,160,161]. Some neutrophil-derived biomolecules, such as, elastase [162] and MMP9 [163], have been shown to exert a direct effect at promoting tumour cell proliferation. However, the regulatory mechanisms involved to this effect are still not fully understood.

1.8 Zebrafish as a Model Organism in Cancer Research

Zebrafish (*Danio rerio*) are freshwater tropical fish native to southeast Asia. The use of this animal as a model organism for research purposes began in the 1960s and for many years it was mainly confined to the field of developmental genetics.

In 1982, the discovery that zebrafish are susceptible to tumour formation upon exposure to carcinogens widened the scope of scientific areas to which zebrafish could be useful to include cancer research [164].

Since then, various studies contributed to the confirmation that the role of oncogenes and tumour suppressor genes, as the underlying mechanism of carcinogenesis, was conserved across species [165–167]. Following the development of powerful transgenesis technologies, a multitude of zebrafish models of cancer have been created and contributed to the better understanding of all stages of the disease [168,169].

Due to their genetic tractability and optical transparency, zebrafish larvae exhibit an unprecedented suitability for the study of tumour initiation and early progression. As such, a variety of studies using zebrafish as a model organism have uncovered important mechanisms of early tumour development in different types of cancer, including melanoma [154,170,171], hepatocellular carcinoma (HCC) [160,172], pancreatic adenocarcinoma [173,174] and glioma [149].

The epidermis of the developing zebrafish comprises a periderm of terminally differentiated keratinocytes and a basal layer with both differentiated keratinocytes and epidermal stem cells sitting on a basement membrane, much like the mammalian embryonic epidermis [175–178]. While zebrafish larval skin is structurally different from mammalian adult epidermis, the identification of zebrafish orthologues for mammalian keratinocyte stem cell specific markers (*tp63*) and for keratin isoforms suggests there is genetic conservation between the zebrafish and mammals [179–181]. The establishment of this structure as the main organ for gas exchange coupled with the differentiation of specialized cell types for ion transport and mucous

secretion confer the larval skin epidermis morphological and functional similarities with other mammalian epithelial structures such as lung, prostate, mammary gland, colon and kidney [176,178,182,183]. Therefore, findings obtained from the study of zebrafish larval skin can also be loosely extrapolated to the mechanisms of tumour initiation in epithelial tissues coating mammalian internal organs, which are inaccessible to high resolution *in vivo* studies.

1.9 Zebrafish as a Model Organism for the Study of Inflammation and Neutrophil Biology

Fish immunology has long been a subject of scientific inquiry. From an evolutionary perspective, fish comprise a relevant comparative outgroup to understand the evolution of vertebrate immune systems [184]. Furthermore, the increasing understanding of fish immune systems and their multiple similarities to mammalian systems has propelled the use of teleost model organisms, namely zebrafish, for the study of disease processes such as infection and cancer [185].

The inflammatory response is the primary manifestation of the innate immune system. Given their predominant abundance in circulation and their immediate mobilization to sites of infection and tissue damage, neutrophils are considered central effectors of inflammation.

Zebrafish neutrophils, also known as heterophil granulocytes, are detected for the first time in the developing larva at 33 hpf. By 48 hpf neutrophils are fully functional and constitute the majority of the zebrafish larva leucocyte population [186,187]. Similarly to mammalian neutrophils, these granulocytes contain primary and secondary granules and high levels of myeloid specific peroxidase [187]. Zebrafish neutrophils also share several biochemical and functional features with mammalian neutrophils. Namely, they are capable of phagocyte and consequently kill bacteria [188]. Their antimicrobial activity is also evident by their ability to generate NADPH oxidase-dependent oxidative stress [189] and to release neutrophil extracellular traps (NETs) [190].

At the molecular level, zebrafish innate immunity exhibit a higher level of complexity than mammalian systems. Key inflammatory factors such as TLRs, MyD88 and other adaptor proteins, and transcription factors involved in the NF-κB signalling pathway, are highly conserved. Conversely, other components of zebrafish innate immunity, namely, complement system, pattern recognition receptors and some cytokines, have been through significant expansion and consequent phylogenetic divergence from other vertebrates [191–195]. The increased molecular complexity of zebrafish innate immunity allows for increased functional flexibility and redundancy, which may be important for efficient protection against exposure to microorganisms before adaptive immunity is fully functional [184].

Given the late maturation of zebrafish adaptive immune system, which is not complete until approximately three weeks post fertilization [196], zebrafish larval stages are specially suitable for the study of the direct role of innate immunity and inflammation in disease progression, providing a window in which the innate immunity can be studied in the absence of T and B cell responses. These studies are facilitated by the availability of various tissue specific fluorescent reporter transgenic lines, labelling distinct innate immune cell populations, namely, neutrophils [197–199] and macrophages [200,201], which allow for high resolution *in vivo* observations of these inflammatory cells' behaviour upon an inflammatory insult.

1.10 Hypothesis and Aims of the Project

While it has been established inflammation is an important component of a tumour microenvironment, the role of specific regulatory pathways has shown to be extremely complex with context dependent effects. Due to the limited available tools that allow the study of early stages of tumour development, the role of the inflammatory mechanisms during that stage are even more elusive. The hypothesis for this project is that MyD88-NF-κB dependent signalling is involved in the mechanisms that support the pre-neoplastic cell induced inflammation and early tumour development.

The aims of the project are to:

- Develop and characterize a model for conditional generation of pre-neoplastic epithelial cell in the basal skin cell layer of the larval zebrafish.

- Characterize the inflammatory response induced by pre-neoplastic cells.

- Assess the role of MyD88-NF-κB for the establishment of the neutrophilic inflammatory response.

- Establish the cell specific role of MyD88-NF-κB signalling in pre-neoplastic cell progression.

2 Materials and Methods

2.1 Media and Solutions

All reagents were acquired from Sigma-Aldrich, unless otherwise stated.

Embryo Medium

- 0.5μM NaCl
- 0.17μM KCl
- 0.33μM CaCl
- 0.33μM $MgS0_4$
- 0.1% Methylene Blue

0.3x Danieau's Solution

- 58mM NaCl
- 0.7mM KCl
- 0.4mM $MgSO_4$
- 0.6mM $Ca(NO_3)_2$
- 5.0mM HEPES Adjust pH to 7.6

Induction Solution

- 0.3x Danieau's Solution
- 0.5%(v/v) DMSO
- 5μM 4-Hydroxyamoxifen (4-OHT) (10mM stock in EtOH)

LB Broth

- 10G Tryptone
- 5G Yeast Extract
- 5G NaCl
- 1ML 1M NaOH
- 1L H_2O Adjust pH to 7.0

LB Agar

LB Broth

15 g/L Bacto Agar

PBS

137mM NaCl

2.7mM KCl

10mM Na_2HPO_4

1.8mM KH_2PO_4 Adjust pH to 7.4

Fixative solution

PBS

4%(w/v) Paraformaldehyde (PFA)

PBST

PBS

0.5%(v/v) Triton X-100

Calcium-free Ringers Solution

5mM HEPES

2.9mM KCl

116mM NaCl

TAE (10x)

48.4G Tris

3.7G EDTA

11.4ML Acetic Acid

1L dH_20

2.2 Expression Constructs Generation

Expression constructs were generated according to the Tol2kit [202] using MultiSite Gateway Three-Fragment Vector Construction Kit (Invitrogen, 12537-023). All reagents and plasmids were acquired from Invitrogen, unless otherwise stated.

For generation of DNA fragments of interest, PCR was performed using primers as depicted in Table 2.1. pTol2-5xUAS:mCherry-HRas^{G12V}, kindly provided by Masazumi Tada (University College London, UK), was used as DNA template. PCR reaction was set up as stated in Table 2.2 and run in a Mastercycler Nexus Gradient GSX1 Thermal Cycler (Eppendorf) according to Table 2.3.

PCR products were purified using the DNA Clean & Concentrator™ Kit (Zymo Research, D4003) according to manufacturer's instructions. To generate pME vectors, equimolar amounts of *attB* PCR product and pDONR 221 vector were mixed in TE Buffer with 2μL BP Clonase II Enzyme Mix in a total volume of 10μL. To generate expression constructs, equimolar amounts of destination vector, and 5', middle and 3' entry vectors (Table 2.4) were combined in TE Buffer with 2μL LR Clonase II Plus Enzyme Mix in a total volume of 10μL. Following an over-night incubation at 25°C, enzyme was degraded in a 10-min incubation at 37°C after addition of 1 μL of Proteinase K solution (2μg/μL). Plasmids were isolated by bacterial transformation and plasmid purification as described below.

Table 2.1 Primer sequences used for PCR amplification of insert of interest for Multisite Gateway cloning

PCR Product	Primers
attB1-mCherry-HRas^{G12V}-attB2	**Fw:** 5'-GGGGACAAGTTTGTACAAAAAAGCAGGCTGCCGCCACCATGGTGA-3' **Rv:** 5'-GGGGACCACTTTGTACAAGAAAGCTGGGTTCAGGAGAGCACACAC-3'
attB1-mCherry-CAAX-attB2	**2 consecutive PCR reactions (PCR1:FW+Rv1; PCR2: FW+Rv2)** **Fw:** 5'-GGGGACAAGTTTGTACAAAAAAGCAGGCTGCCGCCACCATGGTGA-3' **Rv1:** 5'-TCAGGAGAGCACACACTTGCAGCTCATGCAGCCGGGGCCACTCTCATCAGGAGGGTTCAGCTTAGATCTTCCTCCTCCCTTGTACAGCTCGTCCATG-3' **Rv2:** 5'-GGGGACCACTTTGTACAAGAAAGCTGGGTTCAGGAGAGCACACACTTGCAGCTC-3'

Table 2.2 PCR reaction mix for amplification of DNA fragment of interest for Multisite Gateway cloning

5x Q5 Reaction Buffer (New England Biolabs)	10 μL
10mM dNTPs (Roche)	1 μL
10μM Fw Primer	1 μL
10μM Rv Primer	1 μL
DNA Template	50-100 ng
Q5 High-Fidelity DNA Polymerase (New England Biolabs)	0.5 μL
Nuclease Free Water	To 50 μL

Table 2.3 PCR cycling conditions for amplification of insert of interest for Multisite Gateway cloning

Step	**Temperature**	**Duration**	**Cycles**
Initial Denaturation	95°C	2 min	
Denaturation	95°C	30 sec	30
Annealing	Primer Optimised	30 sec	cycles
Extension	72°C	2 min	
Final Extension	72°C	7 min	
Hold	10°C		

Table 2.4 Entry vectors used for generation of expression constructs with Multisite Gateway cloning

Final Construct	p5'E vector	pME vector	p3'E vector	Destination vector
UAS:mCherry-HRas^{G12V}	p5'E: 6xUAS (A kind gift from Dr. Dirk Sieger)	pME: mCherry-HRas^{G12V}	p3'E: polyA (Tol2kit)	pDestTol2CG2 (Tol2kit)
UAS:mCherry-CAAX	p5'E: 6xUAS	pME: mCherry-CAAX	p3'E: polyA	pDestTol2CG2

2.3 Bacterial Transformation and Plasmid Purification

All imported and newly generated plasmids went through bacterial transformation for plasmid propagation. All reagents were acquired from Invitrogen, unless otherwise stated. One Shot™ ccdB Survival™ 2 T1R Competent Cells were used for transformation with empty vectors. One Shot TOP10 chemically competent *E. coli* were transformed with remaining plasmids. Frozen bacteria vials were thawed on ice. 1-4 μL of plasmid were carefully added to the vial and gently mixed. After a 30 min incubation on ice cells were heat-shocked at 42°C for 30 seconds, immediately followed by a 2 min incubation on ice. 250 μL of S.O.C. medium was then added and vials were incubated at 37 °C, 200 rpm for 1 hour. Transformed bacteria were plated in the appropriate antibiotics selective LB agar plates and incubated at 37°C over-night. Individual, isolated colonies were picked and grown in selective LB Broth with the appropriate antibiotics at 37 °C, 200 rpm over-night. Following bacterial growth in LB selective medium, plasmids were purified with Qiagen Plasmid Purification Kits according to manufacturer's instructions. For sequencing, diagnostic digests and cloning purposes, a 5mL culture volume was used and processed with the QIAprep Spin Miniprep Kit. For high purity,

larger volumes of plasmids necessary for microinjections, 25-50 mL culture volume was used and processed with the QIAGEN Plasmid Midi Kit. Plasmid DNA concentration was measured using NANODROP™ 1000 spectrophotometer. Integrity of all purified plasmids was verified by restriction digestion. Following 2h incubation with appropriate restriction enzyme (New England Biolabs) and respective buffer at the temperature for optimal enzymatic activity, digested plasmids were mixed with gel loading dye (New England Biolabs) and run on an agarose gel (1-1.6% (w/v) agarose, 1xTAE) electrophoresis with a PowerPac™ Basic Power Supply (BioRad) at 100V with 1xTAE as conductive buffer. PCR amplified inserts were further verified by sequencing analysis of entry vectors with M13 Forward and T7 Reverse primers using the Mix2seq service from Eurofins Genomics. Predicted sequences of each plasmid were generated in Ape – A plasmid Editor (version 2.0.51) and analysed in SnapGene Viewer (version 4.1).

2.4 Transposase mRNA Synthesis

Transposase mRNA was synthesised using pT3TS/Tol2 plasmid [203] as a template. Plasmid DNA was linearized with BamHI (New England Biolabs, R0136S) and purified with DNA Clean & Concentrator kit (Zymo Research, D4033) according to the manufacturer's instructions. Capped mRNA *in vitro* transcription was performed using the mMessage mMachine T3 Transcription Kit (Invitrogen, AM1348) according to the manufacturer's instructions. 1μg of linearized plasmid was mixed with 1x reaction buffer, 1x NTP/CAP mix and 2 μL of T3 enzyme mix in a 20 μL reaction solution and incubated for 2 hours at 37°C. The DNA template was then degraded in a 15-min incubation at 37°C after addition of 1 μL of TURBO DNase (2U/μL). Transcribed RNA was recovered by Lithium Chloride precipitation in which RNA was kept in a 18 mM EDTA, 2.5 M Lithium Chloride solution at -20°C for 1 hour and pelleted by centrifugation at 4 °C, 14000rpm for 15 minutes. Pellet was then washed with 70% Ethanol and re-centrifuged with the same parameters. After removal of

70% Ethanol, pellet was air-dried for 5 minutes and resuspended in Nuclease-Free Water (Invitrogen, AM9930).

2.5 Zebrafish Husbandry

Adult zebrafish (*Danio rerio*) were maintained and handled following previously described protocols [204] and in accordance with the UK Home Office Regulations. Wild-type zebrafish of the Tuebingen (TUE) strain, maintained by the CBS Aquatics Facility at The University of Edinburgh, were used, unless otherwise stated. Transgenic zebrafish lines used throughout the project (Table 2.5) were maintained under Home Office license held by Dr. Yi Feng. Fertilized zebrafish eggs were collected, washed and transferred to fresh embryo medium. Eggs were checked for viability and staged according to time post fertilization [205]. Embryos were maintained for up to 5 dpf at 28.5^{o}C. For screening purposes, embryos were kept under anaesthesia with embryo medium containing 0.02% buffered 3-aminobenzoic acid ethyl ester (Tricaine/MS-222). Desired phenotype was detected using a Leica M205 FA Fluorescence Stereo Microscope.

Table 2.5 Zebrafish transgenic lines used throughout the project

Transgenic Zebrafish Line	Reference
Tg(krtt1c19e:KalTA4-ER^{T2})	Unpublished, generated in Paul Martin's Laboratory with construct generated in the Feng Laboratory (Supplementary Figure 1)
Tg(krt4:KalTA4-ER^{T2})	Unpublished, generated in Paul Martin's Laboratory with construct generated in the Feng Laboratory [206]
Tg(6xNFκB:eGFP)sh235	[207]
Tg(myd88:DsRed2)zf164	[208]

Tg(UAS:IκBSR)	Unpublished, generated by Yi Feng in Paul Martin's Laboratory
Tg(lyz:IκBSR)	Unpublished, generated by Nikolay Ogryzko in the Feng Laboratory
Tg(lyz:DsRed2)nz50	[198]
Tg(lyz:lifeact-mTurquoise2a)	Unpublished, generated during this project
Tg(krtt1c19e:KalTA4-ER^{T2}); Tg(myd88:DsRed2)zf164	Unpublished, generated during this project
Tg(krtt1c19e:KalTA4-ER^{T2}); Tg(lyz:lifeact-mTurquoise2a)	Unpublished, generated during this project
Tg(krtt1c19e:KalTA4-ER^{T2}); Tg(lyz:DsRed2)nz50	Unpublished, generated during this project
Tg(krt4:KalTA4-ER^{T2}); Tg(lyz:DsRed2)nz50	Unpublished, generated during this project
Tg(krt4:KalTA4-ER^{T2}); Tg(6xNFκB:eGFP)sh235	Unpublished, generated during this project

2.6 Generation of Transgenic Zebrafish

2.6.1 Microinjection of Zebrafish Eggs

Adult zebrafish were set up in pair mating tanks overnight. To avoid premature mating, male and female zebrafish were kept separated by dividers. The following morning dividers were lifted to allow mating. Fertilized eggs were immediately collected and aligned on a plate, against a slide. Microinjections were performed using a borosilicate glass capillary needle (World Precision Instruments 1B100F-4) connected to a Pico-Liter Injector (Warner Instruments, PLI-90A). One-cell-stage embryos were co-injected into the blastodisc with 7.5 pg of plasmid DNA and 40 pg of capped Tol2 transposase mRNA in a volume of 0.5 nL 1X Danieau's solution. DNA constructs used for

microinjection throughout the project are listed in Table 2.6. Injected eggs were incubated as previously described.

Table 2.6 Constructs used for microinjection throughout the project

Construct	Origin
UAS:eGFP-HRas^{G12V}	Generated by Thomas Ramezani in the Feng Laboratory
UAS:eGFP-CAAX	Generated by Lisa Kelly in the Feng Laboratory
UAS:mCherry-HRas^{G12V}	Generated during this project
UAS:mCherry-CAAX	Generated during this project
***lyz*:lifeact-mTurquoise2a**	Generated by Thomas Ramezani in the Feng Laboratory

2.6.2 Generation of Transgenic Stable Lines

Wilde-type adult zebrafish were mated and fertilized eggs were injected with *lyz*:lifeact-mTurquoise2a DNA construct (Supplementary Figure 2) as previously described. 3dpf injected larvae were screened for mTurquoise expression in neutrophils and selected larvae were raised to adulthood. Once zebrafish reached sexual maturity they were crossed with Wild-type for identification of founder fish with germ line integration and stable transmission to their offspring. Two founders were identified and larvae with transgene expression were raised to adulthood constituting F1 generation. Stable transgenic line was established based on the F2 generation with the strongest reporter gene expression.

Double transgenic lines were generated through line crosses. Male and female adult zebrafish from each transgenic line were set up in pair mating tanks overnight and eggs were collected the following morning. 3dpf larvae were screened and selected double positive larvae were raised to adulthood.

2.6.3 Generation of Zebrafish Larvae with Transient KalTA4-ER^{T2}/UAS Mediated Gene Expression

KalTA4-ER^{T2} transgene carrier adult zebrafish were mated according to experimental requirements and fertilized eggs were injected with DNA constructs containing UAS driven transgene (Supplementary Figure 3), as previously described. Injected embryos were screened at 2dpf for desired phenotype and selected embryos were transferred to induction solution and kept in the dark for the duration of the experiment. When appropriate, embryos were screened and selected for desired proportion of HRas^{G12V}/CAAX expressing cells. Embryos were transferred into fresh induction solution every 24 hours.

2.7 Drug Treatment

Embryos were screened at 7hpi and treated with 5 μM Trametinib (Selleckchem, S2673) or 0.5% (v/v) DMSO by immersion at 28.5 °C for specified time intervals, determined by experimental requirements.

2.8 Live Image Acquisition and Analysis

For all live imaging studies, larvae were mounted on lateral view in 1% low melting point agarose (LMP) (Invitrogen, 16520-050) in 0.3x Danieau's solution, in a glass-bottomed dish, filled with induction solution containing 0.02% Tricaine. Screening and full body imaging was performed under a Leica M205 FA Fluorescence Stereo Microscope. Detailed images were taken using confocal microscopy as specified below and, when necessary, analysed with the image analysis software IMARIS (version 9.2.1).

2.8.1 Characterization of Cell Morphology

Tg(krtt1c19e:KalTA4-ER^{T2}) adult zebrafish were in crossed and fertilized eggs were injected with UAS:eGFP-HRas^{G12V} or UAS:eGFP-CAAX followed by induction as described previously. Larvae were screened at appropriate time-points for eGFP (PNCs/CAAX cells) expression. A selected subset from each group were mounted as described above. Images were taken on a Zeiss LSM-780 inverted confocal laser scanning microscope with a 40x oil immersion objective lens using the 488nm laser. Zen 2011 software was used for image collection. Aggregates of eGFP positive cells were categorised according to cell shape.

2.8.2 Analysis of NF-κB Activity in PNCs

Tg(krt4:KalTA4-ER^{T2}); Tg(NFκB:eGFP) adult zebrafish were in-crossed and fertilized eggs were injected with UAS:mCherry-HRas^{G12V} or UAS:mCherry-CAAX followed by induction as described previously. Larvae were screened at 8hpi for eGFP (NF-κB reporter) and mCherry (PNCs/CAAX cells) expression. A selected subset from each group were mounted as described above. Images were taken on a Leica TCS SP5 confocal laser scanning microscope attached to an inverted DMI 6000 CS microscope base with an HC PLAN APO 20x dry objective lens in 30 min intervals for a duration of 14 hours (10-24 hpi) using the 488nm and 594 nm lasers.

For drug treatment experiments, drug was added, when mounting the larvae, to mounting media and induction solution. Larvae were kept in mounting media during drug treatment, in between image collection time-points. Images were taken on a Leica TCS SP8 confocal laser scanning attached to an inverted, motorised DMi8 research microscope base with a HC PL APO 20x CS2 dry objective lens at 9hpi and 18hpi using the 488nm and 596 nm lasers. Leica Application Suite Advance Fluorescence (LAS AF) software was used for image collection in both experiments.

Time-lapse videos and images were analysed with the image analysis software IMARIS (version 9.2.1) as follow. HRas^{G12V}/CAAX positive cells were isolated using the Surfaces module based on absolute mCherry intensity and eGFP mean intensity within each Surface was measured. eGFP mean intensity in the lateral line was calculated with the Spots module. When needed, analysis was restricted to areas of interest for efficient separation of HRas^{G12V}/CAAX positive cells from lateral line and neuromasts, which exhibit constitutive eGFP (NF-κB reporter) expression. To account for variation due to differences in transgene copy number mean intensity values within each larva were normalized to eGFP expression level in the lateral line at the earliest time-point. Fold Change was calculated as the ratio between eGFP mean intensity at 24hpi and 10hpi. Quantification of eGFP/mCherry double positive cells at 10hpi and 24hpi was performed manually by optical sectioning, whereby each slice within a z-stack was individually analysed to assure the correct assessment of cells in distinct focal planes.

2.8.3 Analysis of *myd88* Gene Expression in PNCs

Tg(krtt1c19e:KalTA4-ER^{T2}); Tg(myd88:DsRed2) adult zebrafish were in-crossed and fertilized eggs were injected with UAS:eGFP-HRas^{G12V} or UAS:eGFP-CAAX followed by induction as described previously. Larvae were screened at appropriate time-points for DsRed (*myd88* gene reporter) and eGFP (PNCs/CAAX cells) expression. A selected subset from each group were mounted as described above. Images were taken on a Zeiss LSM-780 inverted confocal laser scanning microscope with a 40x oil immersion objective lens at 12hpi, 24 hpi, 36hpi and 48hpi using the 488nm and 561nm lasers. Zen 2011 software was used for image collection. Each larva was imaged in up to three different areas of the trunk.

Images were analysed with the image analysis software IMARIS (version 9.2.1) as follow. Quantification of DsRed/eGFP double positive cells at different time-points was performed manually by optical sectioning. HRas^{G12V}/CAAX positive cells were isolated using the Surfaces module based

on absolute eGFP intensity. The Distance Transformation XTension allowed for the generation of an additional channel where intensity translated the distance to $HRas^{G12V}$/CAAX generated Surfaces. Neighbouring Cells were isolated using the Surfaces module based on the Distance Transformation Channel with a 25 intensity value as the top threshold. This allowed the generation of 25 μm wide surfaces surrounding the $HRas^{G12V}$/CAAX positive cells. DsRed mean intensity within each Surface was measured at different time-points.

2.8.4 Analysis of NF-κB Activity in Neutrophils

Tg(krt4:KalTA4-ER^{T2}); Tg(NFκB:eGFP) adult zebrafish were out-crossed to *Tg(lyz:DsRed2)* adult zebrafish and fertilized eggs were injected with UAS:eGFP-$HRas^{G12V}$ followed by induction as described previously. Larvae were screened at 22hpi for DsRed (neutrophils) eGFP (PNCs/CAAX cells; NF-κB reporter) expression. A selected subset were mounted as described above. Images were taken on a Leica TCS SP5 confocal laser scanning attached to a DMI 6000 CS inverted microscope with a HC PLAN APO 20x dry objective lens in 1 min 30 sec intervals for a duration of 2 hours (24-26 hpi) using the 488nm and 543nm lasers. Leica Application Suite Advance Fluorescence (LAS AF) software was used for image collection.

Time-lapse videos were analysed with the image analysis software IMARIS (version 9.2.1) as follow. Neutrophils were isolated using the Surfaces module based on absolute DsRed intensity and tracked using a Brownian movement based algorithm. Cell tracking was manually checked and corrected when necessary. When more than one neutrophil converged into the same surface, the latter was cut at the appropriate intersection planes and tracks were rearranged accordingly. Individual neutrophils were analysed according to eGFP mean intensity.

2.8.5 Neutrophil Recruitment

Tg(krtt1c19e:KalTA4-ER^{T2}); Tg(lyz:DsRed2) adult zebrafish were in-crossed and fertilized eggs were injected with UAS:eGFP-HRas^{G12V} or UAS:eGFP-CAAX followed by induction as described previously. Larvae were screened at 10hpi for DsRed (neutrophils) and eGFP (PNCs/CAAX cells) expression. A selected subset from each group were mounted as described above. Images were taken on a Leica TCS SP8 confocal laser scanning attached to an inverted, motorised DMi8 research microscope base with a HC PL APO 20x CS2 dry objective lens in 15 min intervals for a duration of 24 hours (12-36 hpi) using the 488nm and 561nm lasers. Leica Application Suite Advance Fluorescence (LAS AF) software was used for image collection. Neutrophils within the skin were manually counted at each frame using the Spots module of the image analysis software IMARIS (version 9.2.1).

2.8.6 Analysis of Neutrophil Behaviour in *krtt1c19e*:IκBSR Background

Tg(krtt1c19e:KalTA4-ER^{T2}); Tg(lyz:DsRed2) adult zebrafish were out-crossed to *Tg(UAS:IκBSR)* adult zebrafish and fertilized eggs were injected with UAS:eGFP-HRas^{G12V} followed by induction as described previously. Larvae were screened at 20hpi for DsRed (neutrophils) and eGFP (PNCs) expression. The presence/absence of red-fluorescent marker “bleeding heart” (BH, cmlc2:mCherry) was used to differentiate *krtt1c19e*:IκBSR from WT larvae. A selected subset from each group were mounted as described above. Images were taken on a Leica TCS SP8 confocal laser scanning attached to an inverted, motorised DMi8 research microscope base with a HC PL APO 20x CS2 dry objective lens in 1 min 30 sec intervals for a duration of 3 hours (22-25 hpi) using the 488nm and 561nm lasers. Leica Application Suite Advance Fluorescence (LAS AF) software was used for image collection.

Time-lapse videos were analysed with the image analysis software IMARIS (version 9.2.1) as follow. Neutrophils were isolated using the Surfaces module based on absolute DsRed intensity and tracked using a Brownian movement

based algorithm. Cell tracking was manually checked and corrected when necessary. When more than one neutrophil converged into the same surface, the latter was cut at the appropriate intersection planes and tracks were rearranged accordingly. $HRas^{G12V}$ positive cells were isolated using the Surfaces module based on absolute eGFP intensity. The Distance Transformation XTension allowed for the generation of an additional channel where intensity translated the distance to $HRas^{G12V}$ generated Surfaces. Neutrophil tracks were only considered from the time-point they were first in contact with a $HRas^{G12V}$ positive cell forward. Neutrophil surfaces were analysed according to the following module featured parameters: Track Mean Speed, Track Distance Channel Mean Intensity corresponding to Track Distance to PNCs and Track Straightness. Retention Time was calculated manually as the maximum uninterrupted period of time spent "visiting" a specific PNC aggregate.

2.8.7 Analysis of *myd88* Gene Expression and Behaviour Diversity of Recruited Neutrophils

Tg(krtt1c19e:KalTA4-ER^{T2}); Tg(myd88:DsRed2) adult zebrafish were out-crossed to *Tg(krtt1c19e:KalTA4-ER^{T2}); Tg(lyz:lifeact-mTurquoise2a)* adult zebrafish and fertilized eggs were injected with UAS:eGFP-$HRas^{G12V}$ or UAS:eGFP-CAAX followed by induction as described previously. Larvae were screened at 22hpi for DsRed (*myd88* gene reporter), eGFP (PNCs/CAAX cells) and mTurquoise (neutrophils) expression. A selected subset from each group were mounted as described above. Images were taken on a Zeiss LSM-780 inverted confocal laser scanning microscope with a 20x dry objective lens in 2 min intervals for a duration of 2 hours (24-26 hpi) using the 405nm, 488nm and 561nm lasers. Zen 2011 software was used for image collection.

Time-lapse videos were analysed with the image analysis software IMARIS (version 9.2.1) as follow. Neutrophils were isolated using the Surfaces module based on absolute mTurquoise intensity or absolute DsRed intensity depending on which parameter allowed for a more accurate representation of

the full body of each individual neutrophil. Resulting surfaces were tracked using a Brownian movement based algorithm. Cell tracking was manually checked and corrected when necessary. When more than one neutrophil converged into the same surface, the latter was cut at the appropriate intersection planes and tracks were rearranged accordingly. Neutrophil surfaces were analysed according to mTurquoise mean intensity and DsRed mean intensity. To account for variation due to differences in transgene copy number, mean intensity values of each neutrophil were normalized to average intensity of all neutrophils within each larva. Relative DsRed average intensity (=1) was used as an arbitrary value to segregate the two neutrophil subsets compared in the subsequent analysis of migratory behaviour. Neutrophil Speed values were obtain through the Surfaces module inbuilt parameter measurements. Retention Time was calculated manually as the maximum uninterrupted period of time spent “visiting” a specific PNC aggregate and used to restrict Neutrophil Speed values to be considered.

2.9 Fluorescent Staining

2.9.1 EdU Labelling

Cell proliferation was assessed using the Click-iT™ Plus EdU Alexa Fluor™ 647 Imaging Kit (Life Technologies, C10640). Unless otherwise stated, all washes and incubation steps were carried out at room temperature with light shaking (60-65 rpm). Larvae were screened at appropriate time-points. Selected larvae were injected into the yolk with 0.5nL of 10mM EdU (5-ethynyl-2'-deoxyuridine, a nucleoside analogue of thymidine) and incubated for 2.5 hours at 28.5^{o}C. After a 30-min over the bench incubation in fixative solution, larvae were permeabilized in PBS containing 0.5% Triton X-100 (PBST) four times for 5 min and blocked with PBST containing 3% (w/v) Bovine Serum Albumin for 1 hour at room temperature. Larvae were then transferred to the Click-it Plus reaction cocktail (1xClick-iT Plus EdU reaction buffer, copper protectant, Alexa Fluor 647 picolyl azide dye, reaction buffer additive), made

as per manufacturer's instructions, incubated for 30 min protected from light and later subjected to whole-mount immunofluorescence staining as described below.

2.9.2 TUNEL Labelling

Cell death was assessed using the Click-iT™ Plus TUNEL Assay for In Situ Apoptosis Detection Alexa Fluor™ 647 Imaging Kit (Life Technologies, C10617). Unless otherwise stated, all washes and incubation steps were carried out at room temperature with light shaking (60-65 rpm). Larvae were transferred to fixative solution and incubated for 2 hours over the bench. Following extensive washing steps in PBST, larvae were permeabilized with 10 μg/mL Proteinase K in PBST. The duration of the treatment was dependent on their developmental stage: 3 min treatment for 3dpf (24hpi) larvae and 4 min treatment for 3.5dpf (36hpi) larvae. Larvae were then immediately rinsed twice in PBST and re-fixed for 20 min. After 4 consecutive 5-min washes with PBST, larvae were incubated in TdT reaction buffer for 10 min at 37°C. Larvae were, then, transferred to TdT reaction mix (TdT reaction buffer, EdUTP, TdT enzyme), made as per manufacturer's instructions, and incubated for 1h at 37°C. Following an 1-hour incubation in PBST containing 3% (w/v) Bovine Serum Albumin blocking solution, larvae were transferred to the Click-it Plus TUNEL reaction cocktail (1x Click-iT Plus TUNEL reaction buffer, copper protectant, Alexa Fluor 647 picolyl azide dye, Click-iT Plus TUNEL reaction buffer additive), made as per manufacturer's instructions, incubated for 30 min at 37°C protected from light and later subjected to whole-mount immunofluorescence staining as described below.

2.9.3 Whole Mount Immunofluorescence Staining

Unless otherwise stated, all washes and incubation steps were carried out at room temperature with light shaking (60-65 rpm). Larvae were washed in PBST 3 times for 15 min and blocked with PBST containing 10% (v/v) goat

serum, 3% (w/v) Bovine Serum Albumin for 2 hours at room temperature, before an over-night incubation at 4°C with primary antibody in blocking solution. Primary antibodies used through the course of this project include rabbit monoclonal anti-GFP (1:200) (Cell Signalling Technology, 2956) and mouse monoclonal anti-RAS (1:200) (BD Biosciences, 610001). After ten 15-min PBST washes, larvae were incubated with secondary antibody in blocking solution for 2 hours. Secondary antibodies used through the course of this project include Alexa Fluor 488 Goat anti-Rabbit IgG (H+L) (1:250) (A-11008, Invitrogen) and Alexa Fluor 488 Goat anti-Mouse IgG (H+L) (1:250) (A-11001, Invitrogen). Larvae were then washed in PBST 10 times and subjected to a gradient of decreasing concentrations of PBS and increasing concentrations of glycerol to be stored in a glycerol based antifading mounting medium (CitiFluor, AF1) at 4°C.

2.9.4 Confocal Image Acquisition and Analysis

Stained larvae were mounted, on lateral view, in the glycerol based antifading mounting medium on a slide and coverslip. Images were taken on a Leica TCS SP8 confocal laser scanning attached to an inverted, motorised DMi8 research microscope base with a HC PL APO 40x CS2 oil immersion objective lens using 488nm and 633nm lasers. Leica Application Suite Advance Fluorescence (LAS AF) software was used for image collection.

Images were analysed with the image analysis software IMARIS (version 9.2.1) as follow. Quantification of proliferating $HRas^{G12V}$/CAAX positive cells was performed manually by optical sectioning. For quantification of proliferating neighbouring cells, the remaining EdU positive nuclei, not within eGFP positive cells, were manually selected using the Spots module. $HRas^{G12V}$/CAAX positive cells were isolated using the Surfaces module based on absolute GFP intensity. The Spots Close To Surface XTension allowed segregation of the spots subset within 10 μm distance to the nearest point of the Surface objects. Proliferating neighbouring cells are shown as a proportion of the number of spots in that subset to the number of $HRas^{G12V}$/CAAX positive

cells. Quantification of dying cells $HRas^{G12V}$/CAAX positive cells was performed manually by optical sectioning from TUNEL labelling images.

2.10 Larvae Dissociation and Flow Cytometry Analysis

Larvae were screened at the appropriate time-point for eGFP (PNCs/CAAX cells) expression as well as the presence of the required reporter genes (neutrophil lineage specific transgenic line and either *myd88* or NF-κB reporter lines). Multiple larvae with the desired phenotype (35-40 larvae per group) were transferred to calcium-free Ringers solution and incubated at 4°C for 15 min. After two rinses in calcium-free Ringers solution, larvae were transferred to dissociation solution (Calcium-free Ringers solution, 2mM $CaCl_2$, 0.25% Collagenase D (Gibco)) and incubated at 28.5°C with shaking (100 rpm), during which additional mechanical dissociation was achieved with vigorous pipetting in 5-min intervals. Full dissociation was regularly achieved within 30 minutes and resulting cells were pelleted by centrifugation at 3000 rpm for 3 minutes at 4°C. Pellet was then washed twice with PBS and re-centrifuged each time with the same parameters. Pellet was resuspended in 750 µL PBS and filtered using a 40 µm Corning cell strainer to obtain a single cell suspension.

Flow cytometry was performed with a BD 5 laser LSR Fortessa cell analyser. mTurquoise positive cells were detected with V450/50-A laser. B525/50-A laser was used to detect eGFP positive cells.YG582/15-A laser was used to detect DsRed positive cells. B670/30-A laser was used to exclude autofluorescence. Single cell suspensions from WT and single transgenic larvae were equally obtained and analysed to establish appropriate compensation and gating strategy (Supplementary Figures 4 and 5). For compensation and gating strategy set up, a minimum of 100.000 total events were analysed per sample. For data acquisition, a minimum of 1000 events for the neutrophil population were analysed per sample.

2.11 Gene Expression Analysis

2.11.1 RNA Extraction and cDNA Synthesis

Larvae were screened at the appropriate time-point. Multiple larvae with the desired phenotype (40-50 larvae per group) were transferred to 500 µL TRIzol reagent (Invitrogen) to preserve RNA integrity. Following an over-night incubation at -80^{o}C, samples were thawed and homogenized by repeatedly passing through a 23 gauge needle (BD Microlance) with the help of a 1 mL syringe (BD Plastipak) and vigorous vortexing. Total RNA was isolated with chloroform extraction followed by isopropanol precipitation. After a 1-hour incubation at -20^{o}C to allow full RNA precipitation, RNA was pelleted by centrifugation at 4 °C, 14000rpm for 15 minutes. Pellet was then washed with 70% Ethanol and re-centrifuged with the same parameters. After removal of 70% Ethanol, pellet was air-dried for 5 minutes and resuspended in Nuclease-Free Water (Invitrogen, AM9930).

cDNA synthesis was achieved using the iScript™ Advanced cDNA synthesis Kit for RT-qPCR (Bio Rad, 1725037). As per manufacturer's instructions, 4 µL 5x iScript Advanced Reaction Mix and 1 µL iScript Advanced Reverse Transcriptase were added to 15 µL isolated RNA. Resulting reaction mixture was incubated at 46°C for 20 minutes and then at 95 °C for 1 minute, in a Mastercycler Nexus Gradient GSX1 Thermal Cycler (Eppendorf). cDNA was stored at -20°C.

2.11.2 Quantitative RT-PCR

For qRT-PCR reaction set up, cDNA was mixed with PowerUp™ SYBR™ Green Master Mix (Applied Biosystems, A25742) and loaded into a MicroAmp® EnduraPlate™ Optical 96-well Fast Clear Reaction Plate (Applied Biosciences, 4483485). The appropriate primers (Table 2.7) were also loaded into the plate at a final concentration of 500nM in a total reaction volume of 10 µL per well. qRT-PCR was performed using a StepOnePlus™ Real-Time PCR

System (Applied Biosystems) according to the protocol shown in Table 2.8 and results were analysed with StepOne Software (version 2.3).

Table 2.7 Primer sequences used for qRT-PCR

Gene	Primers
rps11	**Fw:** 5'-ACAGAAATGCCCCTTCACTG-3' **Rv:** 5'-GCCTCTTCTCAAAACGGTTG-3'
gapdh	**Fw:** 5'-GTGGAGTCTACTGGTGTCTTC-3' **Rv:** 5'-GTGCAGGAGGCATTGCTTACA-3'
mmp9	**Fw:** 5'-CATTAAAGATGCCCTGATGTATCCC-3' **Rv:** 5'-AGTGGTGGTCCGTGGTTGAG-3'
il-1	**Fw:** 5'-GAACAGAATGAAGCACATCAAACC-3' **Rv:** 5'-ACGGCACTGAATCCACCAC-3'
cxcl8	**Fw:** 5'-TGTGTTATTGTTTTCCTGGCATTTC-3' **Rv:** 5'-GCGACAGCGTGGATCTACAG-3'
cxcl18b	**Fw:** 5'-GGCATTCACACCCAAAGCG-3' **Rv:** 5'-GCGAGCACGATTCACGAGAG-3'

Table 2.8 qRT-PCR cycling conditions for analysis of gene expression

Step	Temperature	Duration	Cycles
UDG activation	50°C	2 min	Hold
Dual-Lock™ DNA polymerase	95°C	2 min	Hold
Denature	95°C	3 sec	40
Anneal/extend	60°C	30 sec	

2.12 Statistical Analysis

All graphs were generated using GraphPad Prism 8 for macOS (version 8.0.0). Graphs are shown as the mean +/- standard error of the mean (SEM) of all the individual data from repeated experiments as indicated in the figure legend. Statistical analysis was done using GraphPad Prism 8 for macOS (version 8.0.0) as described in the corresponding figures. Significance values: *p≤ 0.05, **p≤ 0.01, ***p≤ 0.001, ****p≤0.0001

3 Overexpression of the HRas^{G12V} Oncogene Promotes the Emergence of Pre-Neoplastic Cells

3.1 Introduction

Tumorigenesis consists of a stepwise process by which somatic cells acquire an increasing number of mutations in oncogenes or tumour suppressor genes, giving them an uncontrolled proliferative capacity and invasive properties. Despite the well characterised mechanisms whereby mutations in these genes potentiate tumour malignancy, only a few oncogenes are capable of unleashing clonal expansion of pre-neoplastic lesions, an important step in the process of tumour initiation. In fact, cancer related genetic and epigenetic alterations are often found in single cells and clonal patches of normal skin [209,210] and mammary epithelial tissue [211,212].

Ras proteins are ubiquitous small GTPases which control regulatory pathways important for cell proliferation, differentiation and survival. Gain-of-function mutations in the Ras gene family are often found in human cancers. Four different isoforms, HRas, NRas KRas4A and KRas4B, compose the Ras protein family. Active mutations in each isoform are more frequently found in distinct types of malignancies [24]. Amongst these, HRas mutations, particularly HRas^{G12V}, even though less frequent in cancer overall, are particularly found in skin squamous cell carcinoma and cancer of the urinary bladder [24,213,214]. Considering Val-12 has the lowest GTPase activity amongst possible amino acid substitutions at codon 12, HRas^{G12V} has the highest transformation potential [215,216]. The association between mutated HRas and tumour initiation *in vivo* was first established by Quintanilla et al., in 1986. In a ground-breaking study, these researchers showed nearly 100% of tumours produced by chemical DMBA/TPA two stage skin carcinogenesis exhibited the same mutation in the HRAS gene [217]. They further demonstrated that the nature of the activating mutation was specific to the initiating agent used [218]. In agreement with this study, other chemical carcinogens were also found to consistently induce tumours with recurrent

activating mutations in RAS genes [219–221]. Ras mutations have also been frequently found in spontaneously arisen benign lesions, placing oncogenic Ras as an early event of tumorigenesis [222–225]. Additionally, overexpression of oncogenic HRas and KRas in transgenic mice promotes hyperplasia and tumour formation, further confirming the potential role of Ras oncogenes as initiators of tumorigenesis [213,226–231].

In addition to the inherent proliferative capacity of pre-neoplastic lesions, a permissive microenvironment is a determinant of tumour development. Recent studies have revealed that an organized epithelial structure constitutes a suppressive environment for tumorigenesis. In these *in vitro* studies, the interaction of transformed cells with neighbouring *wildtype* (WT) epithelial cells triggered mechanisms of cell competition, whereby activation of distinct signalling pathways in this interface led to inhibition of clonal expansion or elimination of the transformed cells [232–235]. Considering the typical setting of the first stages of tumorigenesis, where transformation occurs in one cell or group of cells within an epithelial layer, and given the several lines of defence developed by complex multicellular organisms to eliminate aberrant cells, it is important to understand the mechanisms whereby certain oncogenic mutations can capacitate those cells to evade elimination and expand into self-sustained tumours.

Most of our knowledge of tumour initiation is gathered from transformed cell culture experiments, from which little can be inferred about the role of the microenvironment. The use of mouse models to study tumour formation driven by oncogene overexpression or tumour suppressor knockdown can give a more comprehensive analysis of the mechanisms involved in tumour progression. Murine studies are usually executed after a long latency period, when neoplastic lesions have already established dominance over their wildtype neighbouring cells, consequently missing key stages of tumour initiation. Given the shortage of available tools in this field, we embarked on the task of developing a new model to allow the study of interactions between pre-neoplastic cells and their microenvironment, and the role of these interactions in tumour initiation.

3.2 Using a KalTA4-ER^{T2}/UAS Mediated Inducible System to Generate Mosaic Expression of an Oncogene in the Skin

To better understand the events that lead to tumour initiation, an inducible, tissue specific, zebrafish model was developed in collaboration with Thomas Ramezani, a post-doctoral fellow in the laboratory. This will allow the temporal control of oncogene expression to generate pre-neoplastic cells (PNCs) and enable the detection of the first cues that initiate the process of tumour development. Zebrafish larval skin, a bilayer of translucent keratinocytes, is a relatively simple structure that allows a non-invasive approach for the study of epithelial tumour initiation in a controlled microenvironment in the context of a complex multicellular organism. Taking advantage of the GAL4/UAS genetic system developed in *Drosophila* and, since then, optimized for use in zebrafish model systems [236], we drive the expression of the HRas^{G12V} oncogene using the basal skin layer specific promoter *krtt1c19e* [177]. This system relies on the combinatorial effect of two separate elements: the zebrafish optimized version of the transcription factor Gal4, KalTA4, expressed in a tissue-specific manner, and the Upstream Activating Sequence (UAS) controlling the expression of the fluorescent protein fused HRas^{G12V} oncogene (Figure 3.2.1A). To conditionally induce oncogene expression, KalTA4 has been fused to the modified ligand-binding domain of human estrogen receptor α, ER^{T2}, which specifically binds to synthetic 4-Hydroxytamoxifen (4-OHT). In the absence of 4-OHT the KalTA4-ER^{T2} is retained in the cytoplasm by heat-shock proteins, blocking its transcriptional activity. Upon 4-OHT binding the heat-shock protein-ER^{T2} complex dissociates, allowing nuclear translocation of KalTA4-ER^{T2} and subsequent activation of the UAS controlled gene of interest [237,238].

When both components are stably integrated into the zebrafish genome, nearly 100% efficiency of expression is achieved [237,238]. The high efficiency of this system, however, introduces an obstacle for the study of tumour initiation. According to the clonal evolution of cancer theory [15], confining

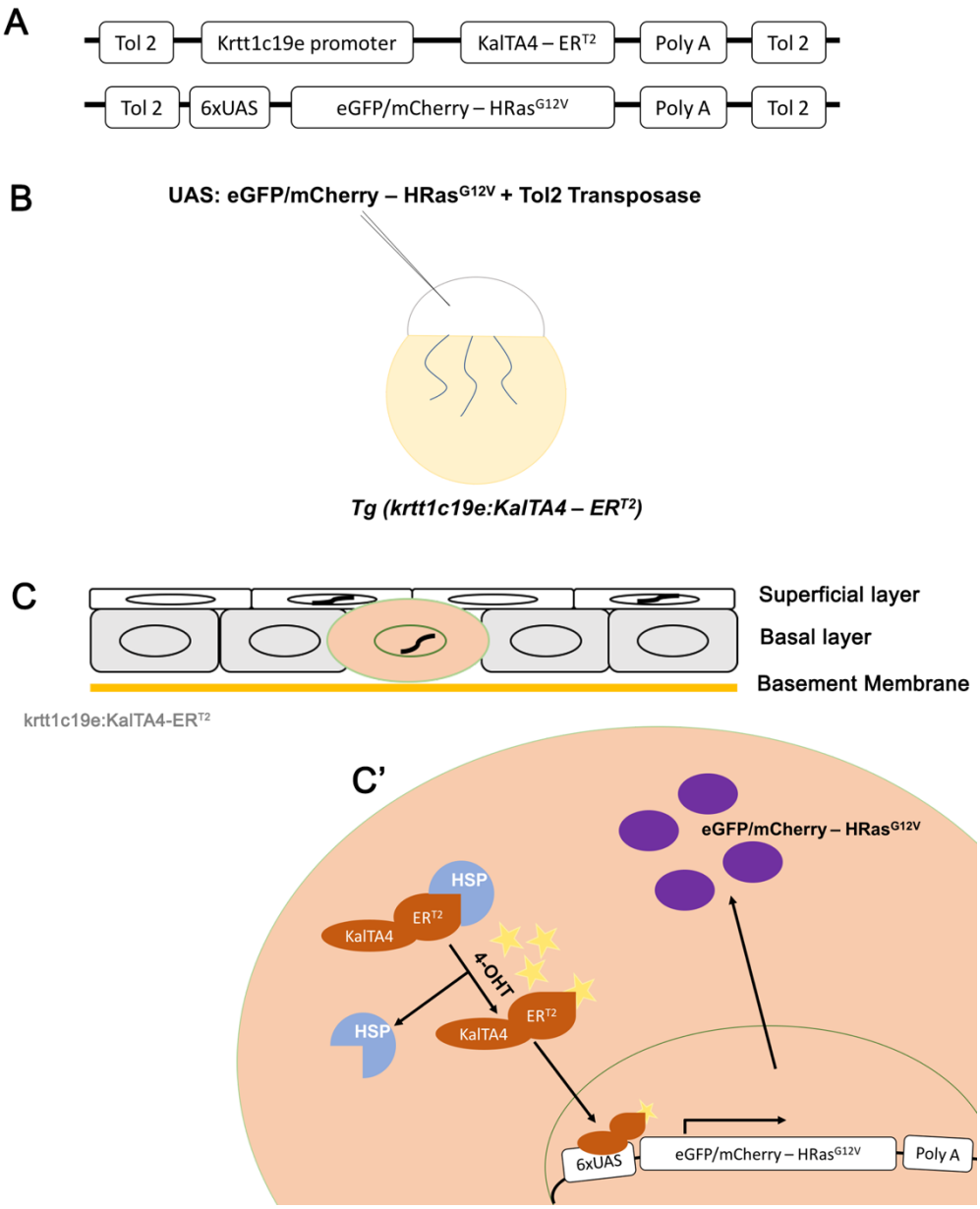

Figure 3.2.1 Schematic of the mechanism for conditional PNC generation in the basal skin layer. A) Tol2 flanked *krtt1c19e:*KalTA4-ER^{T2} and UAS:eGFP/mCherry-HRas^{G12V} expression vectors. B) Mosaic oncogene expression is achieved by transient co-injection of the UAS effector DNA construct and transposase mRNA into one-cell stage eggs from the *krtt1c19e:*KalTA4-ER^{T2} stable transgenic line. C) Profile of zebrafish larval skin where, following transient injection, only cells in the basal skin layer that successfully integrate the UAS effector construct have the potential to express the oncogene. C') For conditional oncogene expression KalTA4 has been fused to ERT2, which binds specifically 4-OHT. In the absence of 4-OHT the KalTA4-ERT2 is bound in the cytoplasm by heat-shock proteins. Upon 4-OHT binding the heat-shock proteins-ERT2 complex dissociates, allowing the nuclear translocation of KalTA4-ERT2 and subsequent activation of the UAS controlled oncogene.

oncogene expression to isolated cells/group of cells within a normal epithelium would more realistically mimic the microenvironment of a pre-neoplastic lesion. The transformation of single cells in a mosaic manner can be achieved by the combinatory use of the stable transgenic line of one component together with the microinjection of a DNA construct carrying the other component. We used Tol2-transposase-mediated transgenesis [202] to generate a stable zebrafish line carrying *krtt1c19e:*KalTA4-ER^{T2} (Supplementary Figure 1) into which we transiently co-inject the UAS:mCherry/eGFP-HRas^{G12V} construct (Supplementary Figure 3) and Tol2 transposase mRNA at the one-cell stage (Figure 3.2.1A,B).

The injected construct is randomly inserted into the genome of the developing embryo in a mosaic manner but only the cells within the basal skin layer have the potential to express the oncogene upon the introduction and continuous administration of 4-OHT (Figure 3.1 C-C').

Injected embryos are raised to larval stage and oncogene expression is induced at 2dpf (Figure 3.2.2 A). The KalTA4-ER^{T2}/UAS system has been previously shown to induce detectable eGFP expression within 3 hours of treatment [237,238]. Our HRas model follows comparable activation kinetics with the first fluorescent cells detectable 4 hours after addition of 4-OHT using both a UAS:eGFP-HRas^{G12V} or a UAS:eGFP-CAAX (membrane targeted eGFP) control plasmid. Within an hour, eGFP expression was detectable in isolated cells throughout the skin epithelia (Figure 3.2.2 B-B''). The transient nature of the UAS component in the system and the increased length of the fusion protein may be the cause for the small delay in eGFP detection and observably reduced fluorescent intensity of eGFP-HRas^{G12V} cells compared to eGFP-CAAX cells.

It is important to verify correct subcellular localization of these proteins to assure proper interaction with their binding partners and consequent high fidelity signal transduction [239]. Both conditions display membrane bound eGFP. In each condition, the fluorescent protein seems to distinctly disperse within the membrane, despite having the same lipid anchor domain. In contrast

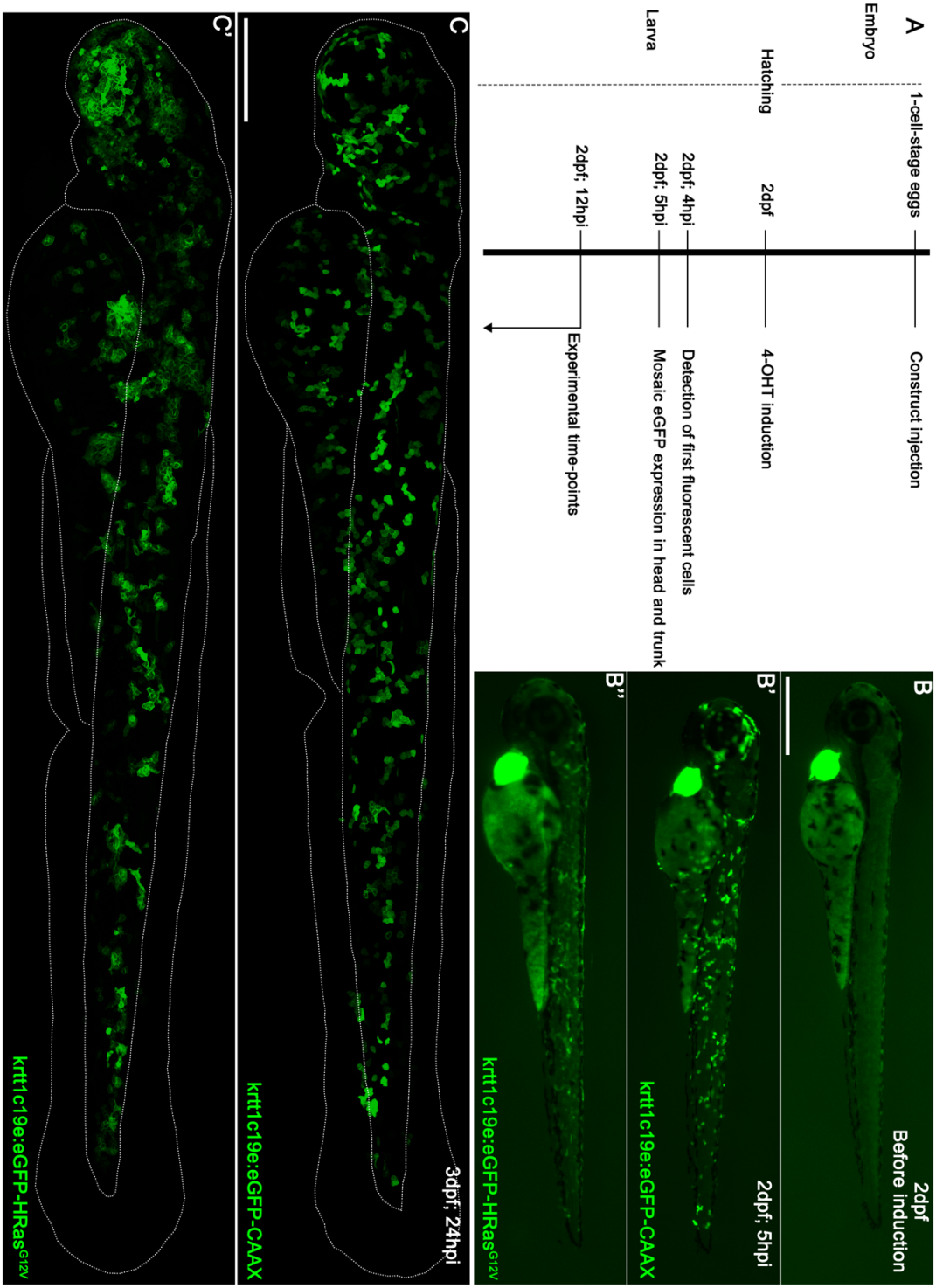

Figure 3.2.2 Transient injection of an oncogene expression plasmid allows mosaic generation of PNCs. A) Timeline of the experimental design B) Before induction no eGFP is detected other than cmcl2:eGFP transgenic selection marker in the heart. UAS driven expression of eGFP-CAAX control plasmid (B') or eGFP-HRas^{G12V} oncogene (B'') is detected 5 hours after induction in scattered cells in the skin. C-C') mosaic transgene expression remains 24hpi. Scale bar = 200μm

to the even distribution of eGFP-CAAX throughout the plasma membrane, $HRas^{G12V}$ proteins, in agreement to previous data [240,241], preferentially aggregated in clusters potentially near specific membrane microdomains (Figure 3.2.2 B-B''). The segregation of HRas could be a consequence of the repulsive force generated by the catalytic domain, lacking in our control plasmid [242].

As oncogene expression continues and eGFP fluorescence grows stronger the mosaic nature of this model remains (Figure 3.2.2 C, C'), revealing it to be a consequence of the transient injection rather than an irregular 4-OHT induction. To better understand the behaviour of these PNCs and their interaction with the microenvironment, I proceeded to characterise the model in more detail.

3.3 Characterization of the PNCs Morphology and Behaviour

The basal skin layer of the zebrafish larva is composed of polygonal shaped keratinocytes. These keratinocytes display the first signs of polarity at 3dpf when cytokeratin filaments localize the basal side of the cell [243]. Desmosomes maintain epithelial integrity and hemidesmosomes anchor them to the basement membrane laying underneath [175,243].

Cell motility and organization of the actin cytoskeleton are some of the mechanisms under Ras signalling regulation. Important mechanisms for the establishment and maintenance of oncogenic Ras transformation include cortical actin rearrangement, downregulation of cell adhesion molecules and degradation of extracellular matrix which can drastically change cell polarity and morphology [66]. Analysis of the cell morphology and behaviour can then be indicative of the mechanisms involved in the oncogenic Ras transformation of PNCs in our model for tumour initiation.

Observation of the polygonal shaped control eGFP-CAAX expressing cells at different time-points allowed the confirmation that membrane targeting of a fluorescent protein should not affect polarization and integrity of epithelial cells.

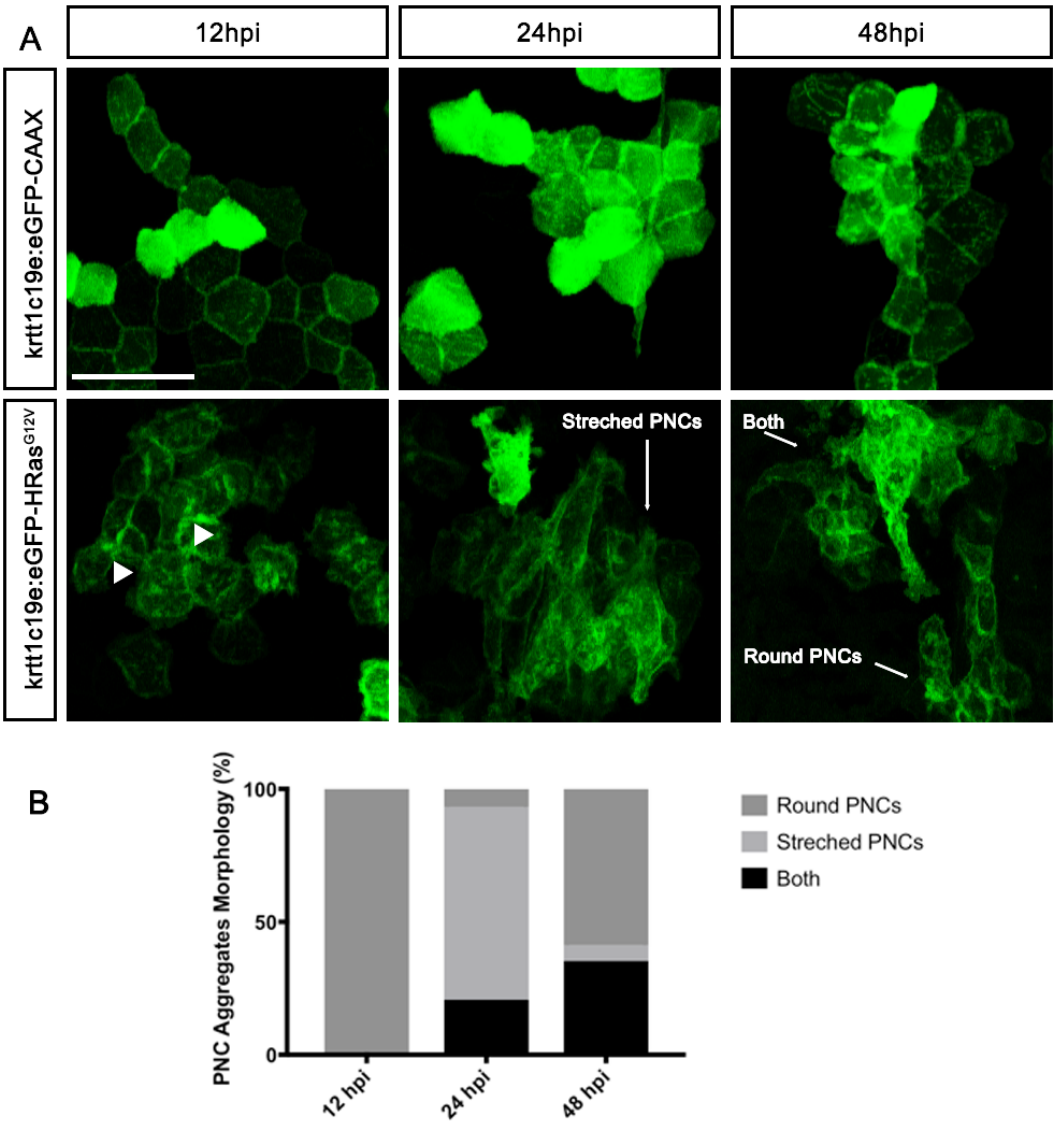

Figure 3.3.1 Characterization of cell morphology over time. A) Maximum intensity projection of eGFP-CAAX expressing cells (top panel) and PNCs (lower panel) at 12, 24 and 48 hpi. Control cells exhibit consistent epithelial morphology at all time-points. In contrast, PNCs develop a distinct morphology since early time-points. Arrowheads point to membrane domains of high eGFP intensity as an indication of eGFP-HRas^{G12V} protein accumulation. B) Frequency of the morphology of different types of PNC aggregates at different time-points. Examples of the three different types of PNC aggregates can be seen in (A). Data acquired from 3 independent experiments; n≥ 10 per time-point. Scale bar = 50 μm.

These cells exhibited consistent epithelial morphology at all time-points. Conversely, PNCs, displayed a very dynamic architecture (Figure 3.3.1 A, B). At 12hpi, PNCs had developed a slightly rounder morphology than the control cells. The eGFP-HRas^{G12V} protein aggregates accumulated preferentially in membrane domains in contact with other PNCs (Figure 3.3.1 A, arrowheads), suggesting these cells were capable of recognising each other and establishing a cross-talk.

At 24hpi, cell morphology diversifies with most PNCs acquiring a more stretched and elongated shape. At this stage, some PNC aggregates were no longer part of an organised monolayer epithelial sheet as seen in earlier time-points, and seem to have lost their polarity and aggregated into three-dimensional disorganised masses. At 48hpi, there was a decrease in the proportion of stretched cells and aggregates of round cells were found more frequently (Figure 3.3.1 A, B).

Live time-lapse imaging revealed cell elongation and epithelial disorganization to be a result of what appeared to be partial epithelial-to-mesenchymal transitions (EMTs) characterized by the formation of cellular protrusions (Figure 3.3.2 A, supplementary video 1), increasingly dynamic interaction between PNCs with rapid association and dissociation of cells and, ultimately, cell movement (Figure 3.3.2 B, supplementary video 2). Isolated PNCs often exhibited more static behaviour suggesting the importance of the crosstalk between cells to potentiate oncogene signalling activity and, consequently, EMT induction (Figure 3.3.2 A). Occasionally, PNC extrusion is also observed (Supplementary Figure 6), although not often enough for the mechanisms behind it to be properly understood without the appropriate studies. To better understand the mechanisms that mediate this highly dynamic PNC behaviour I performed qRT-PCR analysis of whole larvae for the EMT associated gene *mmp9* and found it is upregulated in PNC-bearing larvae (Figure 3.3.2 C).

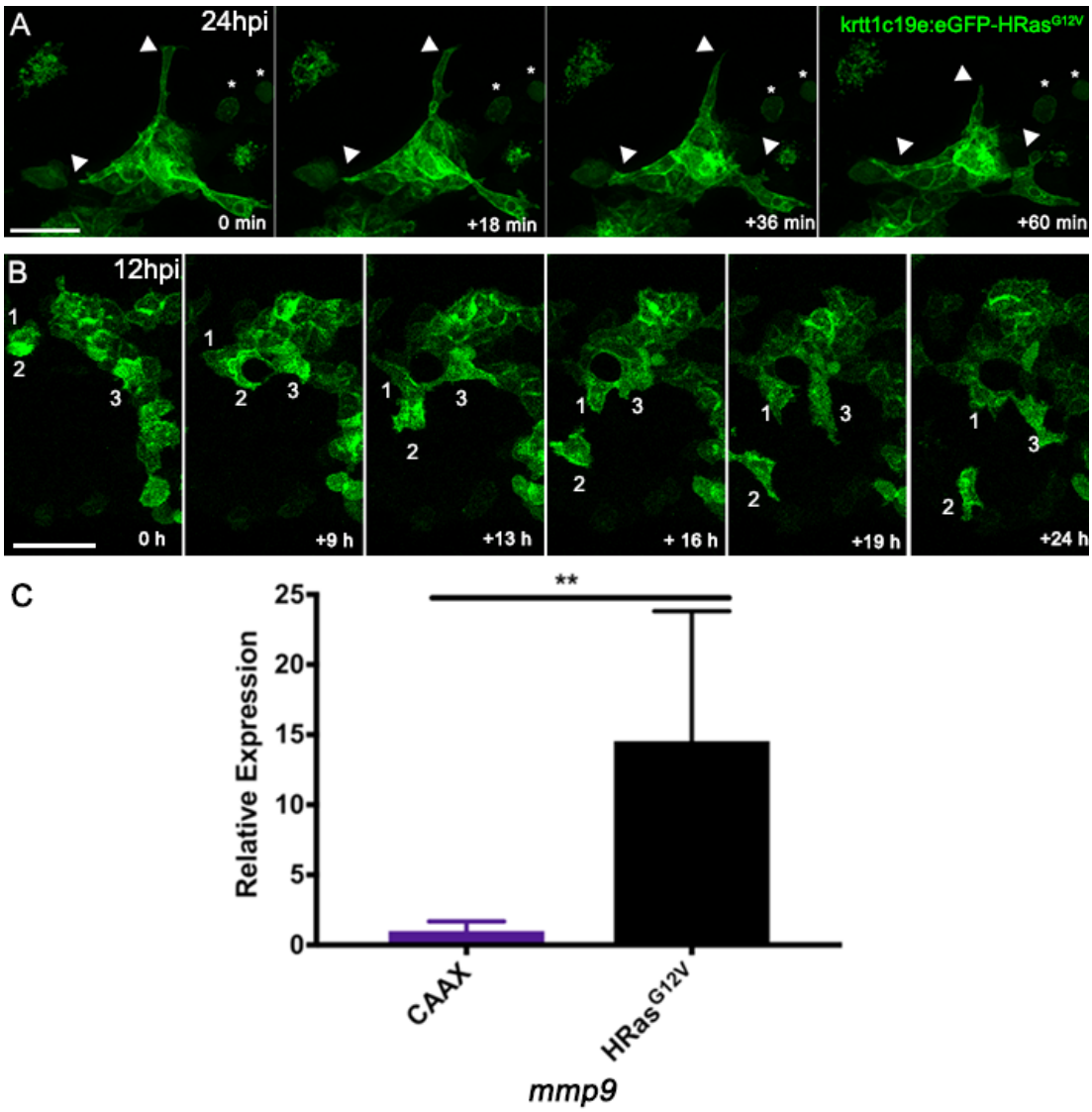

Figure 3.3.2 PNCs exhibit dynamic behaviour which resembles partial EMT. A) Still images of a 1 hour long time lapse movie from 24hpi showing the dynamic behaviour of PNCs with active rearrangement of PNCs, formation of protrusions (arrowheads) occasionally with interaction with other distant PNCs. Isolated PNCs (asterisks) retain a more static behaviour. B) Still images of a 24 hour long time lapse movie from 12hpi showing active rearrangement of PNCs and the movement of a PNC across the flank of the larva (cell 2) C) qRT-PCR was performed on pooled whole larvae at 24hpi for the EMT related gene *mmp9*.

Mean Ct of three technical replicates were normalized to housekeeping genes, *rps11* and *gapdh* (ΔCt), and then normalized to a CAAX control (ΔΔCt). Graph reads relative expression calculated as $2^{-(Mean\Delta\Delta Ct \pm SEM\Delta\Delta Ct)}$. n= 6 per group. Multiple Student t test with Holm-Sidak post-test were performed on ΔCt values. **p=0.0011. Scale bar = 50 μm.

3.4 Characterization of PNC Proliferative Capacity

Uncontrolled PNC proliferative capacity which overpowers normal epithelial expansion is a key determinant for PNCs to establish dominance over neighbouring cells and expand into tumours. Being a key regulator of cell cycle and cell proliferation, the continuous activation of the HRas signalling pathway through the expression of the $HRas^{G12V}$ oncogene, has the potential to promote PNC over-proliferation.

Considering the stochasticity of the number and distribution of PNCs, a characteristic of the transient injection used for their generation, coupled with their high motile nature, the quantification of number of cells or size/area of PNC clones, used by others [154,244], would not be an accurate measurement of proliferation. Instead, cell proliferative capacity was quantified as the proportion of PNCs which had incorporated a detectable nucleoside analogue of thymidine, 5-ethynyl-2'-deoxyuridine (EdU), into their DNA over a 2.5-hour period. EdU incorporation was thus used as an indication that a cell had gone through DNA replication.

Initially, at 12hpi, 10.7±0.7 % of the PNCs exhibited proliferative capacity, however, this was not significantly higher than the control CAAX cells with 6.88±1.12 % proliferating cells (Figure 3.4.1 B). This is likely to be a result of a high basal level of skin proliferation in 2-3 dpf embryos due to their rapid growth and development rather than a consequence of low HRAS signalling [178,245]. This hypothesis was supported by the analysis of later time-points, when proliferation of PNCs was significantly and progressively higher, reaching 43.2±2.5 % at 36hpi (Figure 3.4.1 A, B). In contrast, CAAX control cells exhibited a decreasing proliferative capacity, lower than 1% at 36hpi, as skin cell proliferation and larva growth slowed.

Interestingly, cells immediately surrounding the PNC clones had also become more proliferative (Figure 3.4.1 C). With no additional tissue specific marker, it was not possible to determine which cell types were proliferating. Nevertheless, the observation of EdU positive nuclei in proximity with all

surfaces of the PNC clones suggests proliferation was not restricted to the skin basal layer.

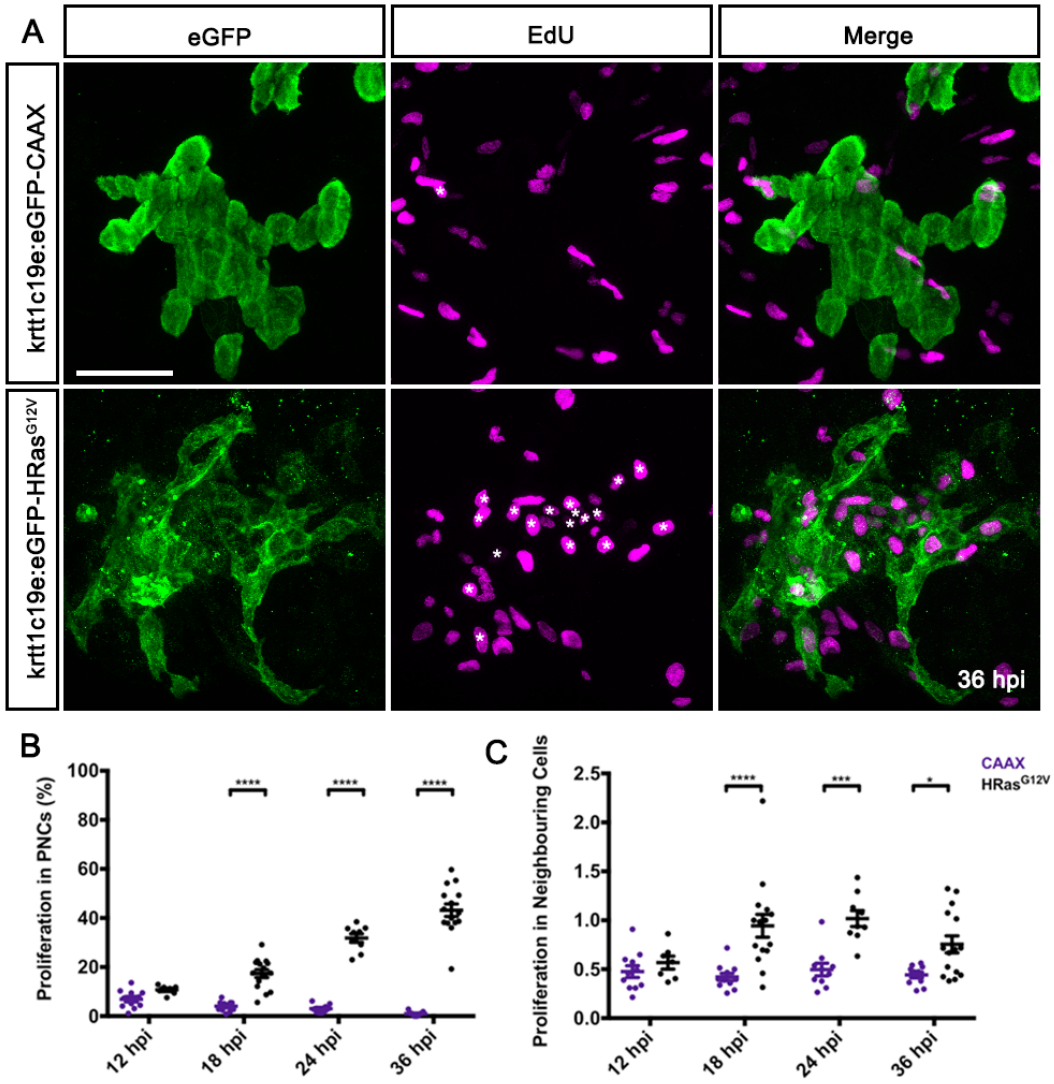

Figure 3.4.1 PNCs acquire increasing proliferative capacity and induce proliferation of neighbouring cells. A) Maximum intensity projection of confocal images of CAAX control cells (top panel) and PNCs (lower panel) following EdU detection and eGFP/HRas immunostaining of 36hpi larvae. Asterisks indicate eGFP/EdU double positive cells. B) Quantification of double positive cells at different time-points was performed by optical sectioning. C) Proliferation in neighbouring cells was measured as the number of EdU positive nuclei within 10 μm distance from the boundaries of eGFP positive cells normalized to the total number of eGFP expressing cells. Data acquired from 3 independent experiments; n≥ 7 per time-point, per group. Mean±SEM. 2 Way ANOVA with Sidak's post-test. * p= 0.0209; *** p=0.0004; **** p<0.0001. Scale bar = 50 μm.

3.5 Detection of Pre-Neoplastic Cell Death

Pre-cancerous lesions are often associated with a high incidence of apoptosis. This was shown to be consequence genomic instability caused by oncogene activation [246]. Activated oncogenes induce the collapse of replication forks causing double strand DNA breaks (DSBs) which will consequently induce a DNA damage response and p53-dependent cell cycle arrest, apoptosis or senescence [247,248]. Continuous observation of PNCs shows that, from 24hpi onwards, PNC clones tend to decrease in area, suggesting cell death is a characteristic of our model. Live time lapse imaging has allowed me to confirm this assumption by the observation of cells bursting into several vesicles and disappearing, in an undetermined type of cell death (cell on top left corner of Figure 3.3.2 A).

Given that only the final stage of apoptosis is morphological distinct and can be quickly cleared by phagocytes, an appropriate staining protocol was performed to detect the proportion of PNCs going through apoptosis at any given time-point. The Terminal deoxynucleotidyl Transferase-dUTP Nick End Labelling (TUNEL) assay is based on the incorporation of modified dUTPs by the enzyme terminal deoxynucleotidyl transferase (TdT) at the 3'-OH ends of DNA strand breaks. Since DNA damage is considered the main cause for oncogene-induced apoptosis at a pre-neoplastic stage, TUNEL staining was chosen to assay apoptosis.

Successful staining revealed PNCs sustained DNA damage which is indicative of apoptosis (Figure 3.5.1 A). Contrary to larvae with CAAX control cells, which showed minimal TUNEL staining, larvae with skin pre-neoplastic lesions exhibited a progressively higher proportion of eGFP/TUNEL double positive cells (Figure 3.5.1 B). There were also high levels of TUNEL staining in what appeared to be the superficial skin cell layer above some of the larger PNC clones, which suggests that the presence of PNCs on the basal skin layer promotes cell death in the superficial skin layer (Figure 3.5.1 A, A').

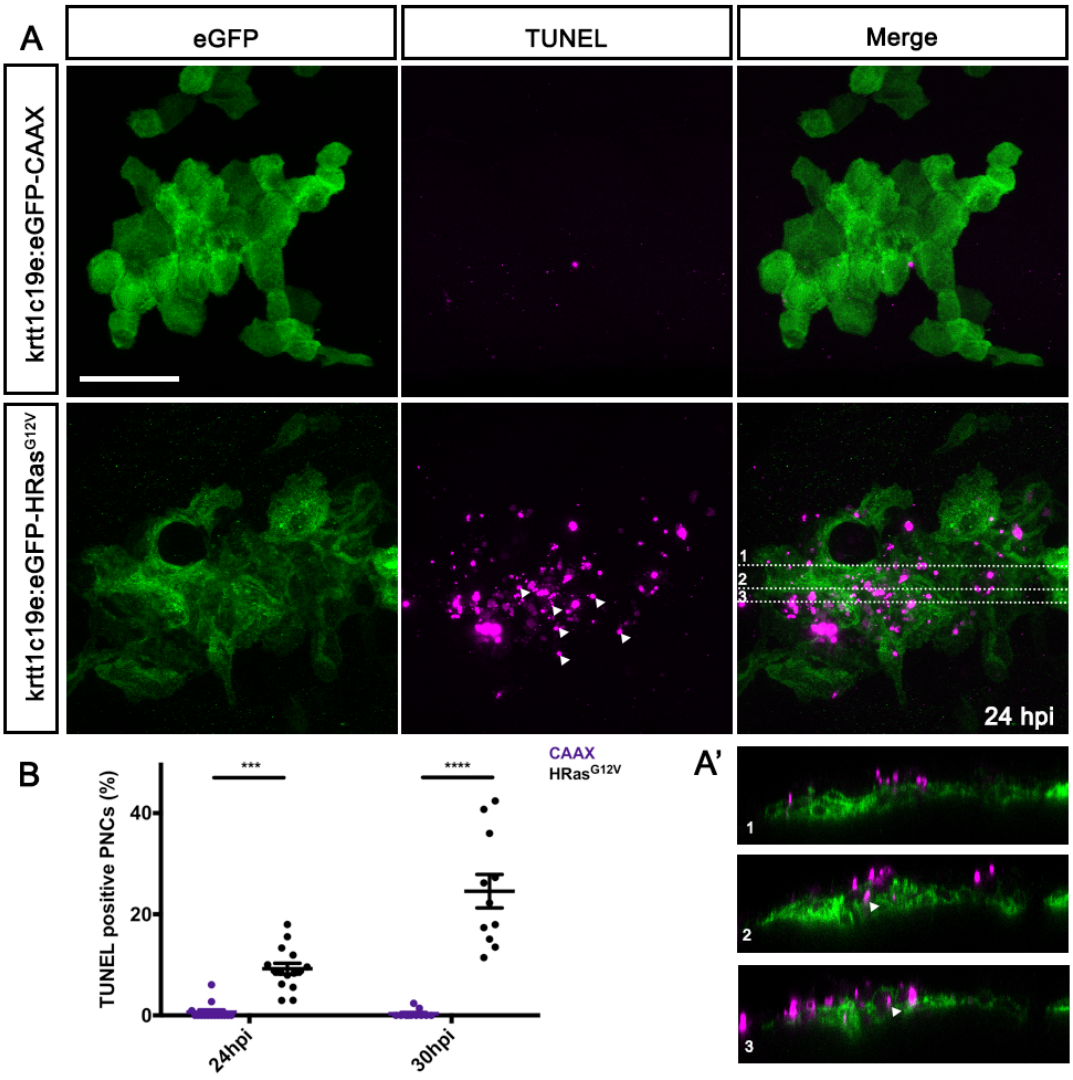

Figure 3.5.1 TUNEL staining showed increased cell death in PNCs and in the superficial cells immediately above them. A) Maximum intensity projection of confocal images of CAAX control cells (top panel) and PNCs (lower panel) following TUNEL staining and eGFP/HRas immunostaining of 24hpi larvae. A') Orthogonal views of 3 different XZ planes of the composite image in the PNC condition in (A) showing positive staining above the basal keratinocyte layer. Arrowheads in (A) and (A') indicate eGFP/EdU double positive cells. B) Quantification of double positive cells at different time-points was performed by optical sectioning. Data acquired from 2 independent experiments; n≥ 11 per time-point, per group. Mean±SEM. 2 Way ANOVA with Sidak's post-test**.** *** p=0.0002: **** p<0.0001. Scale bar = 50 μm.

3.6 PNCs Induce an Inflammatory Response

Several studies have shown that oncogenic Ras signalling induces the expression of several inflammatory mediators and initiates the establishment of an inflammatory milieu that promotes the survival of transformed cells. The ability of PNCs to elicit an inflammatory response could then be determinant for the progression of these cells into tumour masses. Neutrophils, specifically, are very sensitive to the smallest inflammatory cues and often the first cell type to be recruited to an inflammation site [249,250], therefore they may be interesting players in oncogene induced inflammation.

We, and others, have previously established that the presence of PNCs from a variety of cell lineages in the skin of larval zebrafish leads to an inflammatory response with recruitment of neutrophils and macrophages [149,150,154,160,206]. To explore whether our inducible basal skin layer model initiates a comparable inflammatory response, we crossed the *krtt1c19e:KalTA4-ER^{T2}* zebrafish driver line with the neutrophil specific *lyz:DsRed* transgenic zebrafish line [199]. Typically, at 2-3 dpf, unchallenged/inactivated neutrophils remain in the caudal hematopoietic tissue (CHT), head mesenchyme and over the yolk [198]. The presence of PNCs in the keratinocyte lineage of the basal skin layer promotes the recruitment of neutrophils to the skin near these lesions. The inflammatory insult occurs almost immediately after the appearance of the PNCs as neutrophils were observed being recruited to eGFP-HRas^{G12V} expressing cells in the skin as early as 5hpi (Figure 3.6.1 A-B).

Live, time-lapse imaging of these larvae for 24 hours allowed me to monitor the progression of the inflammation over time. An increasing number of recruited neutrophils could be seen near the PNCs, opposed to the CAAX control cells which did not generate any inflammatory response from neutrophils (Figure 3.6.1 C-E, supplementary video 3). After reaching a peak recruitment capacity, at 24-25hpi, the number of recruited neutrophils remains elevated, suggesting a chronic inflammation setting [154]. To determine which pathways might be involved in neutrophil recruitment to the PNCs, I performed

qRT-PCR for inflammatory cytokines and chemokines which are known neutrophil chemo-attractants. I found the presence of PNCs in the skin leads to the upregulation of the pro-inflammatory cytokine Il-1 and the chemokines Cxcl8 and Cxcl18b (Figure 3.6.1 F).

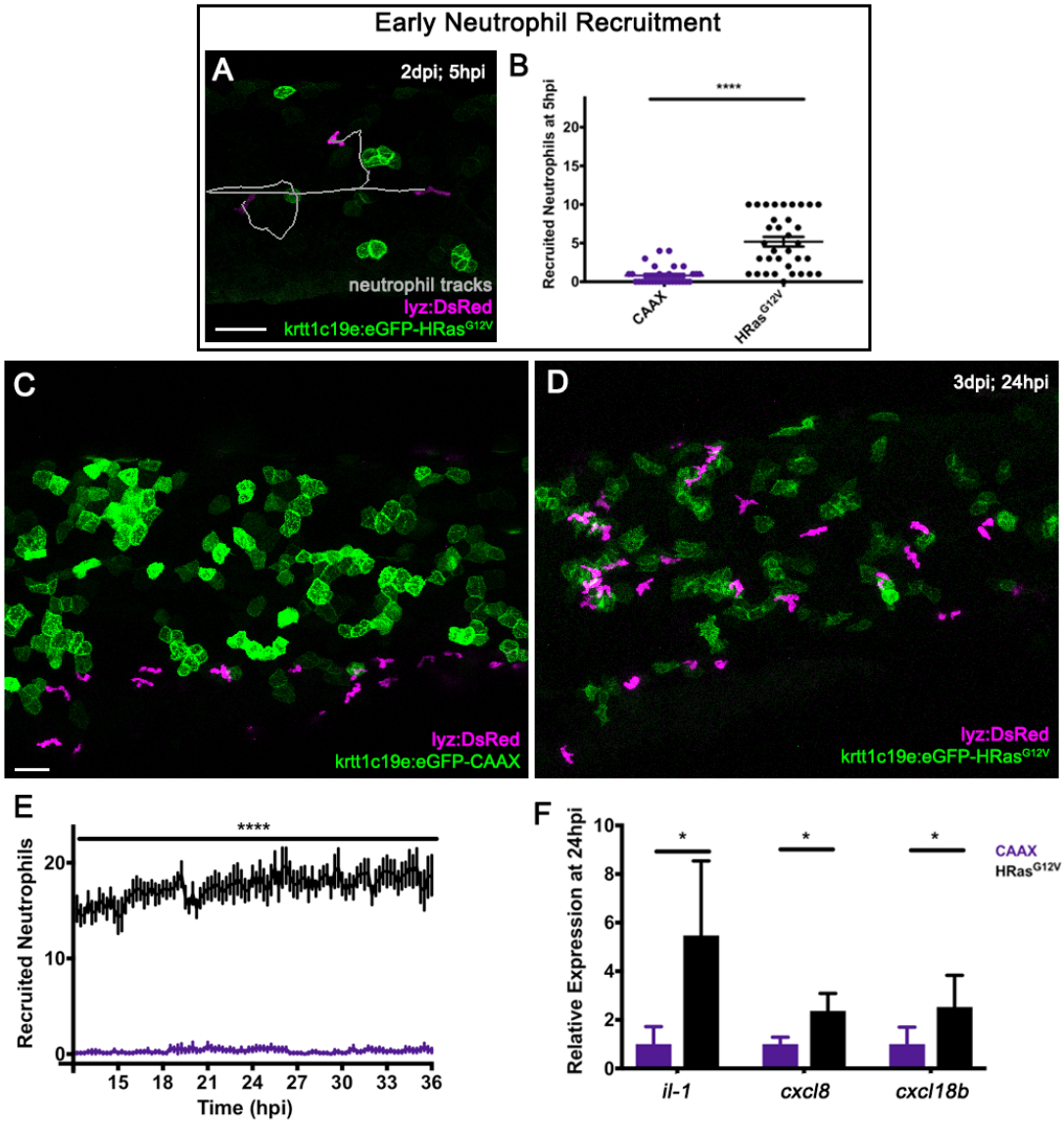

Figure 3.6.1 PNCs induce an inflammatory response from very early stages which evolve into a chronic inflammatory microenvironment. A) Still image from a time lapse movie showing the recruitment of neutrophils to the skin at 5hpi and their movement tracks in the following 45 minutes towards the PNCs. B) Number of neutrophils recruited to the skin within a 6-somite-wide area at 5hpi. Data acquired from 2 independent experiments; n≥ 30 per group. Mean±SEM. Mann-Whitney test. C) Still image from a time lapse movie showing

Figure 3.6.1 (continued) neutrophils remain in the CHT in the CAAX control condition D) Still image of equivalent time-point from a larva with PNCs showing active neutrophil recruitment. E) Number of neutrophils recruited to the skin through the course of a 24-hour time lapse movie. Data acquired from 2 independent experiments; n≥ 8 per group. Mean±SEM. 2 Way ANOVA with Sidak's post-test**.** F) qRT-PCR was performed on pooled whole larvae at 24hpi for the pro-inflammatory genes *il-1*, *cxcl8* and *cxcl18b* and analysed as in Fig 3.3.2. n= 6 per group, *p<0.05. **** p<0.0001. Scale bar = 50 μm.

3.7 Discussion

For a long time, cancer research was restricted to the study of late stage tumour development. The inability to detect pre-neoplastic lesions and follow their interactions with the surrounding tissues *in vivo* have made it difficult to establish the chronology and signalling events of tumour initiation. Here I present an in vivo model taking advantage of the genetic tractability and optical transparency of the zebrafish to overcome those issues. This new system for temporal control of the mosaic expression of the $HRas^{G12V}$ oncogene in the translucent zebrafish larval skin epithelia allows a non-invasive approach for the early detection of PNCs *in vivo* and the study of the mechanisms that initiate tumour formation. Considering the considerable morphological and functional similarities between the zebrafish larval skin and mammalian epithelial tissues such as lung, prostate, mammary gland, colon and kidney [176,178,182,183], the relevance of this study is not limited to the keratinocyte derived cutaneous squamous cell carcinogenesis and parallels can be drawn with tumour initiation in epithelial tissues coating mammalian internal organs which are inaccessible to high resolution *in vivo* studies.

Transformation of keratinocytes in the superficial skin layer of the zebrafish larva had been previously achieved by us and others [150,206]. The basal skin layer, however, containing the epidermal stem cell compartment which contributes to all layers of the adult epidermis [177], may be of greater biological relevance for cancer studies.

This model allowed the generation of detectable isolated pre-neoplastic lesions in a keratinocyte lineage which exhibited progressive signs of

oncogene transformation, namely their increasing proliferative capacity, epithelial cell plasticity, DNA damage, increasing cell death and release of pro-inflammatory signals.

Previous studies have demonstrated transformed cells fail to proliferate within a normal epithelium and cell competition mechanisms promote their elimination [232–235]. The observation of cell extrusion and apoptotic cell death in our model suggests similar mechanisms are in place but the increased proliferative capacity of the PNCs makes me believe they are capable of initiating processes to counteract this suppressive environment. In previous in vitro studies, the extension of basal protrusions and consequent translocation to the underlying collagen or apical extrusion have been shown to allow clonal expansion [232,235]. The activity of MMPs seem to be important for this translocation [235]. Disruption of cell-cell junctions via gene downregulation or displacement of E-cadherin or β-catenin proteins in the neighbouring cells could also counteract suppression of proliferation [235]. The observation of similar behaviours, such as apical extrusion and basal protrusions coupled with upregulation of *mmp9*, suggests active re-structure of the extracellular matrix may enable dynamic PNC interactions and movement facilitating evasion of the suppressive epithelium. Despite the evident dynamic morphology of PNCs, the mechanisms behind the cellular plasticity and mobility seen in this model are yet to be fully characterized. Whether disruption of epithelial integrity of neighbouring cells occurs also remains to be confirmed.

A more detailed analysis of the cell structure would greatly complement this study. Assessment of subcellular localization of the keratin filaments and cell junctions is required to determine PNC loss of polarity. The study of other EMT associated genes expression, such as vimentin, would help understand the mechanisms behind the increasing PNC plasticity.

A recent study on oncogene transformed keratinocytes in the zebrafish superficial skin layer showed that Cxcr2 dependent neutrophil recruitment is required for pre-neoplastic cell dynamic behaviour and EMT-related genes upregulation [150]. Our results, showing coincidence of a peak neutrophil recruitment time-point and the highly dynamic behaviour of the PNCs around

24hpi agree with this finding. However, it does not explain why, at 48hpi, when neutrophils are still actively recruited, this EMT like behaviour is less frequently detected.

It remains unclear whether the decrease in elongated, highly dynamic pre-neoplastic lesions overtime is a result of alteration of these cells to a rounder stem-like morphology, or the positive selection of originally less differentiated transformed cells and elimination of elongated cells. Several studies have shown that the clonogenic potential of an oncogene-transformed cell is determinant in its ability to respond to tumorigenic stimuli and that transformed stem cells are more likely to develop into tumours *in vivo* [228,251,252]. On the other hand, it is possible that the constitutive active Ras signalling coupled with extrinsic factors, such as, the inflammatory microenvironment are promoting the phenotypic changes of these PNCs. Many inflammatory mediators can regulate the transcriptional signature of cancer cells and facilitate tumorigenic features such as self-renewal and migration [253]. A more comprehensive study of the heterogeneity of these cells is required.

The increasing amount of DNA damage and cell death detected with TUNEL staining indicates PNCs suffer genomic instability which can trigger DNA damage responses (DDR) that induce apoptosis. The overexpression of $HRas^{G12V}$ could be directly responsible for that genomic instability through the induction of DNA replication stress [254–256]. The activation of different oncogenes has been associated with loss of heterozygosity and genomic instability [12,248]. Oncogenic Ras was found to cause chromosomal anomalies within one cell cycle in murine fibroblasts [257]. This oncogene-induced replicative stress seems to preferentially affect common fragile sites which are also often found compromised in naturally occurring pre-neoplastic lesions [258,259]. Oxidative stress induced in a chronic inflammatory environment can also cause genomic instability in a pre-cancerous stage [81]. The recruited neutrophils, which are present from very early stages in this model, could release reactive oxygen species into the environment causing additional DNA damage [260].

Given the potential for genomic instability, one cannot disregard the possibility that PNCs may acquire additional mutations. Mutations in genes that regulate DDR and cell proliferation would confer a survival advantage to PNCs making them more capable of surviving and evolving into neoplastic lesions [12,15]. This is consistent with our observations of surviving PNCs at later time-points with higher proliferative capacity.

Dying cells could also be triggering a form of compensatory proliferation in neighbouring living PNCs. Research on tumour re-incidence after cytotoxic therapy have uncovered some of the mechanisms involved. Namely, apoptotic tumour cells have been shown to stimulate proliferation of living tumour cells via caspase3-iPLA$_2$ dependent induction of PGE2 secretion [261,262], activation of the caspase3/7-PKCδ-AKT/p38 MAPK pathway [263] and activation of the caspase3/PKCδ/p38/MNK1 pathway [264]. The release of HMGB1 following necrosis was also found to induce proliferation through RAGE ligand binding dependent activation of ERK and p38 signalling pathways [265]. However, these mechanisms have not yet been shown in a pre-cancerous stage.

Considering the low specificity of TUNEL staining, in the sense that free 3'-OH termini can arise from mechanisms other than apoptosis, these results must be interpreted with caution [266,267]. TUNEL staining has been shown to be equally sensitive to other types of cell death, such as necrosis and autolysis [268]. It can also falsely label cells undergoing DNA repair or undergoing active gene transcription [269]. Some studies have also addressed how the method and duration of tissue fixation [270] as well as post-fixation processing of the tissue [271] can damage DNA. Nevertheless, the little staining detected in the CAAX control samples which went through the same fixation and proteinase K treatment method assures us this is not likely to have happened here. Given the susceptibility for TUNEL staining to give false positive results, it should only be considered as a method for DNA damage. Even though time lapse imaging gave irrefutable evidence of PNC death, the proportion of cells in which it occurs may have been overestimated. A secondary apoptosis-specific

staining, such as cleaved-caspase 3 immunofluorescent staining, should be performed to confirm that cell death occurs through apoptosis.

The high levels of TUNEL positive staining above wider areas of PNC aggregates, presumably in the superficial cell layer, suggest these cells suffer a great incidence of DNA damage and potential cell death. Scanning electron microscopy images of these pre-neoplastic lesions taken by our collaborators in Paul Martin's Laboratory, University of Bristol, show the loss of superficial cells immediately above basal layer PNCs, corroborating our TUNEL staining [van den Berg et al, unpublished]. The lesion overgrowth coupled with the highly dynamic PNC movement and rearrangement of extracellular matrix by metalloproteinases in the basal skin layer may be responsible for local loss of integrity of the superficial skin layer.

Another interesting consequence of the presence of PNCs is the high proliferation in neighbouring cells. This observation exposes the possibility of a non-cell-autonomous mechanism for overgrowth which has been extensively explored in Drosophila studies [272,273]. For instance, a Drosophila model for tumour-stroma interaction has highlighted the importance of the cross-talk between epithelial and mesenchymal cells via Wg/WNT and Dpp/TGF-β signals from the tumour epithelial cells to support expansion of both compartments [274]. Recently, it was also shown that oncogene induced senescence caused by $HRas^{G12V}$ activation and mitochondrial dysfunction in Drosophila imaginal epithelium promotes hyperplasia of *wild type* neighbouring cells through JNK-Yki dependent release of Upd/IL-6 [275]. Work done by a fellow colleague, Lisa Kelly, has revealed that PNCs in the superficial skin layer have impaired respiratory capacity due to mitochondrial dysfunction. However, whether that effect is replicated in the PNCs from the basal layer and whether it promotes oncogene-induced senescence it is not yet known.

Finally, I was able to demonstrate $HRas^{G12V}$ overexpression in keratinocytes can induce an inflammatory response comparable to previous models [149,150,154,160,206]. The upregulation of the pleiotropic pro-inflammatory cytokine Il-1 and the continuous recruitment of neutrophils indicate this

oncogene can initiate a chronic inflammatory environment in pre-neoplastic lesions. The very early detection of PNCs by neutrophils suggests the PNCs themselves, directly or indirectly, release signals for this effect. Several studies have shown oncogene-induced release of pro-inflammatory cytokines and chemokines into the microenvironment [67,69,73,77,154]. Amongst them, CXCL8 is of great interest for its role in neutrophil chemotaxis. Acute inflammation studies have shown this function is conserved in zebrafish larvae [249,276–280]. Cxcl18b was also associated to neutrophil recruitment in a zebrafish inflammation model [281]. The upregulation of these chemokines seen in larvae carrying a PNC burden suggests Cxcl8 and Cxcl18b are responsible for the neutrophil recruitment to PNCs. This is consistent with recent reports which demonstrated the involvement of these chemokines receptors in neutrophil recruitment in early tumorigenesis. Treatment with Cxcr2 and Cxcr1 inhibitors was found to block neutrophil recruitment to transformed epithelial cells and astrocytes, respectively [149,150].

In summary, we were able to establish a tissue specific inducible model to generate pre-neoplastic lesions and study the mechanisms that initiate tumour formation. The observation of behaviours similar to naturally occurring pre-cancerous lesions, such as increasing proliferative capacity, epithelial cell plasticity, DNA damage and increasing cell death, confirms this model mimics the mechanisms involved in epithelial tumour initiation. The early onset of an inflammatory response points to inflammation as a potential mediator of the mechanisms discussed here and the consequent progression of these cells into tumour masses. The following chapters will explore the role of an inflammatory signalling pathway in the progression of pre-neoplastic lesions.

4 NF-κB Pathway Activation in PNCs Modulates Neutrophil Recruitment and PNC Proliferation

4.1 Introduction

Inflammation has long been considered an enabling characteristic of the cancer microenvironment [5,282]. As a result of its role as a pivotal regulator of inflammation, NF-κB activity has been implicated in a variety of cancers [85]. Constitutive activation of this signalling pathway promotes the release of growth and survival factors, extracellular matrix-modifying enzymes and other bioactive molecules by tumour and stromal cells into the tumour microenvironment contributing to the acquisition of cancer hallmark capabilities [85].

However, due to the wide scope of mechanisms regulated by NF-κB transcriptional activity, its role in tumorigenesis is quite complex, exhibiting both tumour promoting and tumour suppressive effects. The investigation of the role NF-κB in development of skin cancer has particularly met contradictory results. It is well documented that squamous cell carcinomas constitutively activate NF-κB, which contributes to their survival, growth and pro-inflammatory microenvironment [283–285]. However, downregulation of NF-κB activity in normal epithelia allows for spontaneous generation of squamous cell carcinoma through TNF mediated inflammation [128,141,143,144]. These results indicate NF-κB could play conflicting roles in tumour development depending on the stage of progression. In line with its importance in the regulation of differentiation and immune homeostasis of normal skin, NF-κB is thought to suppress tumour initiation [286,287]. In the event of an oncogenic insult, NF-κB signalling switches to favour the activation of tumour promoting mechanisms [129,288]. With regards to oncogenic Ras driven tumour initiation, NF-κB signalling has been suggested to play a pro-tumorigenic role from a very early stage. Several *in vitro* studies have suggested NF-κB to be a downstream target of oncogenic Ras signalling. Activation of the

transcriptional function of the NF-κB RelA/p65 subunit by oncogenic Ras signalling was shown to be required for cellular transformation [69,117–124].

In a study using the DMBA/TPA two stage chemical skin carcinogenesis model, which is often associated with oncogenic Ras mutations, researchers were able to mechanistically separate the initiation and promotion stages of tumour development and evaluate the role of NF-κB in each stage [129]. In this study, during tumour initiation, NF-κB prevents cell death induced by DMBA mediated DNA damage. Following DMBA treatment, NF-κB is important for TPA induced release of cytokines and chemokines that promote skin inflammation and epidermal hyperplasia [129].

Further analysis into the mechanisms activating NF-κB signalling in transformed keratinocytes have shown sustained activation of NF-κB requires the establishment of an autocrine loop through IL-1α-IL-1R-MyD88 signalling [130]. Production of IL-1α is downstream of EGFR, and both MAPK and PKCα pathways have been implicated in this autocrine loop [130,289]. The importance of NF-κB signalling in tumour development is not limited to its direct role in the expression of pro-inflammatory, survival and mitogenic factors and has been implicated in the amplification of other positive autocrine loops of Ras signalling. For instance, NF-κB dependent expression of CXCR2 ligands potentiates activation of ERK and AKT pathways [290].

Furthermore, NF-κB has been suggested to promote early tumour development by suppressing immune cell surveillance. NF-κB activation in tumour cells allows them to evade macrophage cytotoxicity by upregulating anti-apoptotic genes and releasing soluble factors, such as GDF-15, which block macrophage synthesis of TNF and NO [288,291]. Conversely, the role for NF-κB activation in the modulation of neutrophil cytotoxicity in tumour initiation is less well known.

In this Chapter, I demonstrate that the activation of NF-κB signalling is a very early event of tumour development. I then analyse how the suppression of this signalling pathway affects PNC proliferation and neutrophil behaviour.

4.2 Detection of NF-κB Activity in PNCs

Following the detection of a persistent inflammatory microenvironment from very early stages of PNC emergence, I pursued a characterization of the signalling pathways involved in its regulation. The upregulation of known NF-κB target genes (*mmp9*, *il-1*, *cxcl8*, *cxcl18b*) (see Chapter 3) observed in this model directed me to NF-κB as a likely regulator of PNC induced inflammation. I characterized NF-κB activity in the PNC environment by crossing the superficial skin layer specific *krt4*:KalTA4-ER^{T2} zebrafish driver line [206] with a previously published NF-κB activity reporter zebrafish line [207]. In this *Tg(NFκB:eGFP)* reporter line, eGFP is under the transcriptional control of 6 concatenated NF-κB recognition sequences which drive eGFP expression upon the activation and translocation of NF-κB transcription factors to the nucleus, allowing temporal and spatial detection of NF-κB activity [207].

In vivo, time-lapse imaging of PNC bearing larvae revealed increasing eGFP expression over time, indicative of continuously high levels of NF-κB activity (Figure 4.2.1 A-B, Supplementary video 4). EGFP intensity in the PNCs revealed an increasing slope and reached a 10.6±1.6 fold change by 24hpi, with 59.5±3.0% double positive cells (Figure 4.2.1B-D). CAAX control cells showed little variation of eGFP intensity over time, reaching 2.1±0.2 fold increase within 14 hours (Figure 4.2.1 A-B). These results are consistent with the current knowledge of the critical role of a finely regulated NF-κB activity in the maintenance of keratinocyte homeostasis [286,287,292] and point to this signalling pathway as a potential key regulator of the inflammatory response induced by the oncogenic Ras overexpression.

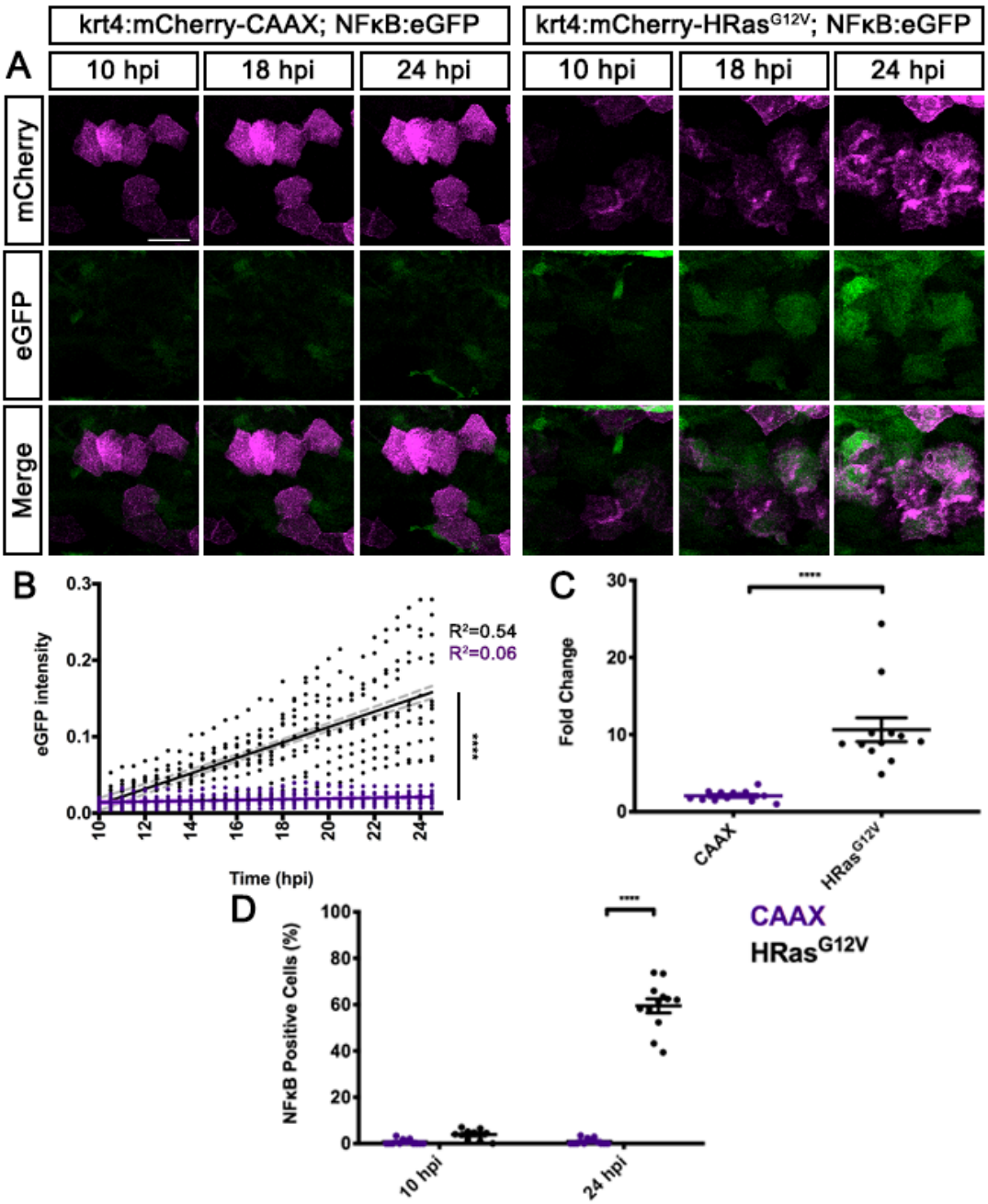

Figure 4.2.1 PNCs show high levels of NF-κB activity. A) Still images from 14 hour time-lapse movies (10-24 hpi) showing activation of the NF-κB:eGFP reporter in PNCs. B) Quantification of mean eGFP intensity in mCherry expressing cells from 10-24 hpi. C) Fold change of eGFP intensity in mCherry expressing cells between 10hpi and 24hpi. To account for variation due to differences in transgene copy number mean intensity values within each larva were normalized to eGFP expression level in the lateral line at 10hpi. D) Quantification of eGFP/mCherry double positive cells at 10hpi and 24hpi was performed by optical sectioning. Data acquired from 3 independent experiments; n=12 per group. Mean±SEM. (B) Correlation with Squared Pearson's Coefficient. (D) 2 Way ANOVA with Sidak's post-test.

Figure 4.2.1 (continued) (C) Mann-Whitney test. * p= 0.0242; **p<0.01; *** p=0.0005; **** p<0.0001. Scale bar = 50 μm.

4.3 Characterization of *myd88* Gene Upregulation in the PNC Niche

As an extremely important intermediate of NF-κB dependent signalling, the MyD88 adaptor protein has also been associated with the mechanisms involved in the pro-tumorigenic inflammatory response. The importance of this protein in tumour formation is not limited to the maintenance of the autocrine/paracrine production of NF-κB mediated factors and has also been shown to exert a cell intrinsic role in the amplification of the Ras canonical signalling pathway [130,132,293–295]. Upregulation of *MYD88* gene expression has been detected in a variety of human primary cancer tissues and is often associated with poor prognosis [296–298]. Following the initial observation that emerging preneoplastic cells induce an inflammatory response, I wanted to determine if *myd88* expression changed in the early stages of tumour initiation.

To study *myd88* gene expression I crossed the basal skin layer specific *krtt1c19e*:KalTA4-ER^{T2} zebrafish driver line to a previously published *myd88* gene expression reporter zebrafish line [208]. In this *Tg(myd88:DsRed2*) reporter line, DsRed2 is under the control of the ≈3.7 kb long genomic sequence immediately upstream of the *myd88* initiation codon.

Observation of PNCs over time showed *myd88* gene upregulation from 36hpi onwards and by 48hpi nearly 30% of PNCs had detectable DsRed expression (Figure 4.3.1 A-C). *myd88* upregulation was also detected in neighbouring cells (Figure 4.3.1 A,D).

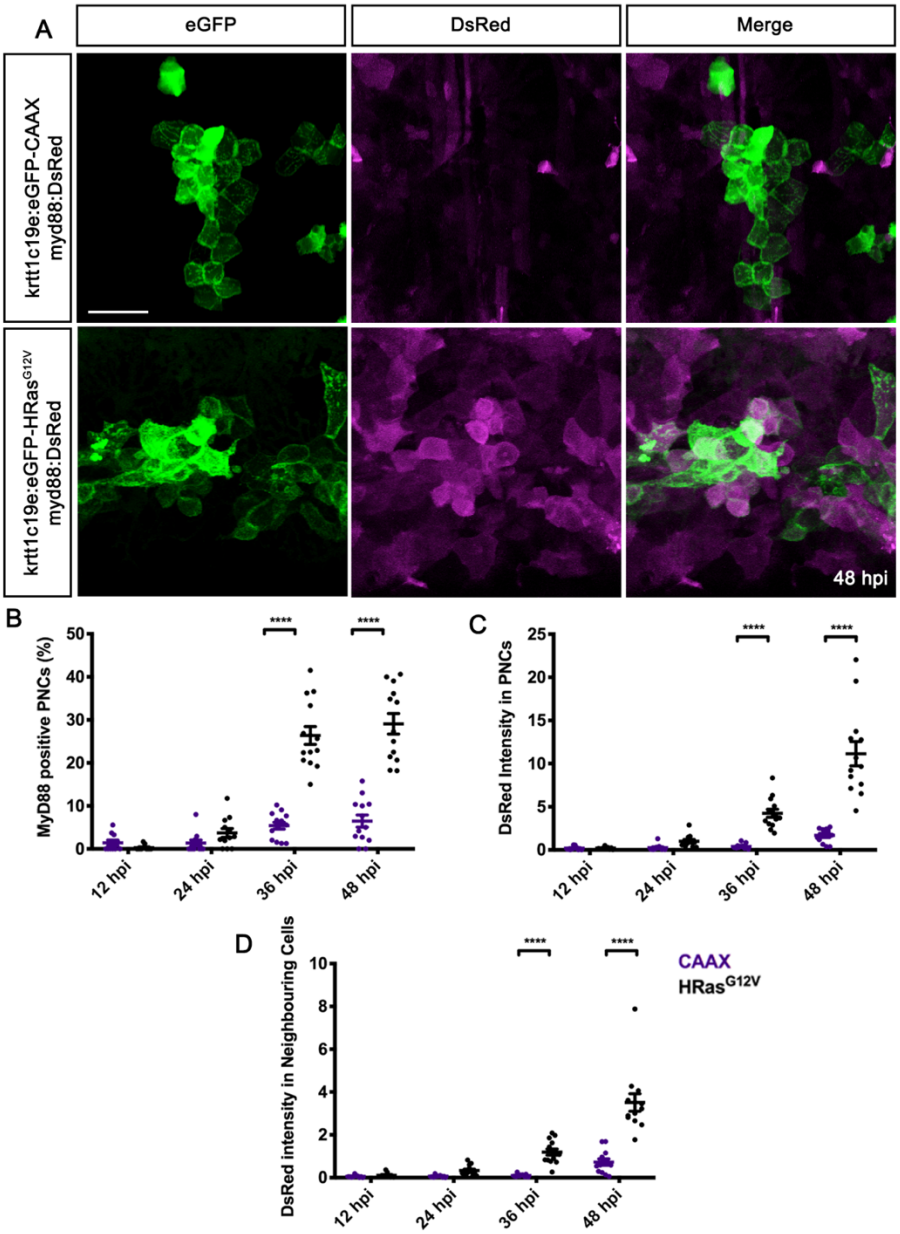

Figure 4.3.1 *myd88* expression is induced in PNCs and neighbouring cells. A) Maximum intensity projection of live confocal images of CAAX control cells (top panel) and eGFP-HRas^{G12V} PNCs (lower panel) showing expression of DsRed as a reporter of *myd88* gene upregulation in a subset of PNCs and in the surrounding cells at 48hpi. B) Quantification of eGFP/DsRed double positive cells at different time-points performed by optical sectioning. C-D) Quantification of DsRed mean intensity in aggregates of eGFP expressing cells (C) and neighbouring cells within 25 μm distance from of eGFP positive cells (D). Data acquired from 3 independent experiments; n≥10 per group, per time-point. Mean±SEM. 2 Way ANOVA with Sidak's post-test**.** **** p<0.0001. Scale bar = 50 μm.

4.4 Inhibition of MAPK Signalling Does Not Affect NF-κB Activity in PNCs

NF-κB activation can be induced by over 150 stimuli [84]. Following oncogenic Ras transformation several downstream effector targets have been shown to activate NF-κB signalling and consequently promote oncogene induced inflammation [123,124,126,299]. Murine studies identified the MAPK pathway and, more specifically, Erk1/2 phosphorylation to be upstream of NF-κB dependent upregulation of Il-1, Mmp9 and Cox2 expression [118,289,300]. The upregulation of pro-inflammatory genes detected in this model suggests that similar mechanisms may be responsible for NF-κB activation in PNCs.

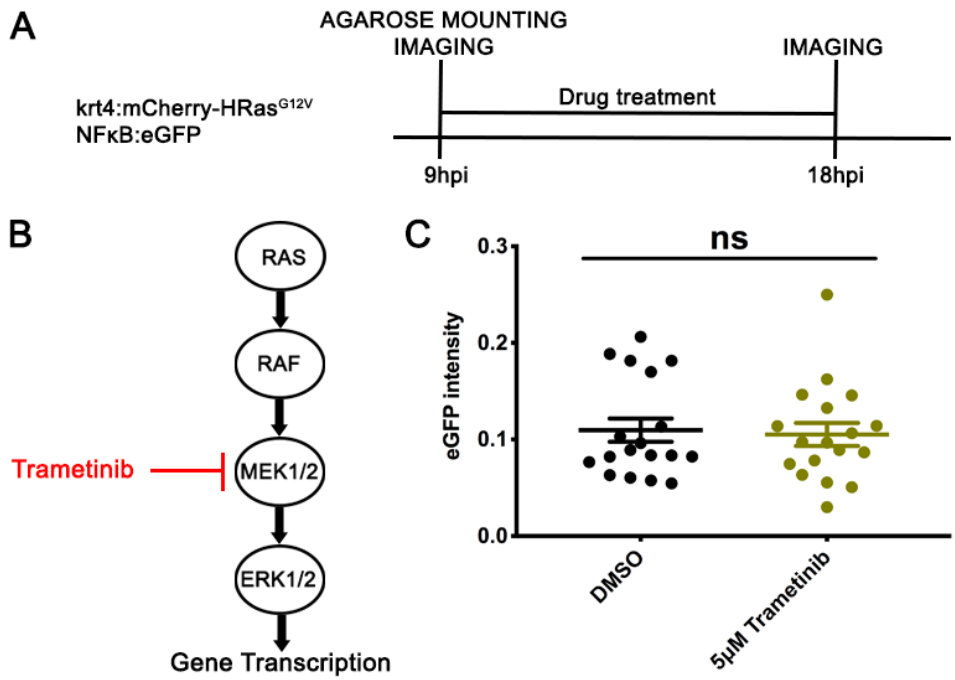

Figure 4.4.1 NF-κB activity in PNCs is not affected by MEK inhibition. A) Schematic figure of experimental procedure showing time points and duration of treatment. B) Schematic figure of MAPK signalling pathway showing at which level Trametinib exerts its inhibitory effect. C) Quantification of eGFP mean intensity in aggregates of mCherry expressing cells at 18hpi following 0.5% (v/v) DMSO or 5μM Trametinib treatment. To account for variation due to differences in transgene copy number mean intensity values within each larva were normalized to eGFP expression level in the lateral line at 9hpi. Data acquired from 2 independent experiments; n=18 per group. Mean±SEM. Mann-Whitney test. ns $p>0.9999$

To test this hypothesis PNC bearing, NF-κB reporter larvae were treated with the MEK inhibitor Trametinib, which has been reported to successfully abrogate Erk phosphorylation in zebrafish [301]. To allow for effective MEK inhibition larvae were treated for 8-9 hours from the detection of PNCs (Figure 4.4.1 A-B). Image analysis of Trametinib treated and DMSO treated control larvae showed no difference in eGFP expression suggesting NF-κB activity was not Erk dependent (Figure 4.4.1C).

4.5 The Intrinsic Role of NF-κB in the PNC Proliferation

A major pro-tumorigenic role of NF-κB signalling is its effect on the regulation of proliferation. By promoting the release of regeneration enhancing cytokines and the expression of growth factors, NF-κB activation has the potential to promote the proliferation of tumour cells.

A transgenic line previously established in the laboratory that allows for cell lineage specific suppression of NF-κB activity was used to assess the role of NF-κB activation in PNC proliferation. In this model, NF-κB suppression is achieved through the overexpression of a constitutively active dominant negative mutant form of the murine IκBα, IκBSR. This mutant IκBα is resistant to phosphorylation and consequent proteasome degradation, thus, retaining NF-κB in the cytoplasm and preventing its translocation to the nucleus [302,303]. Well described and used extensively in mammalian systems, IκBSR has also been shown to inhibit NF-κB signalling in zebrafish embryos [304,305]. To determine the effect of diminished NF-κB signalling in PNCs, I crossed *Tg(UAS:IκBSR)* with *Tg(krtt1c19e:KalTA4-ER^{T2})* enabling KalTA4/UAS mediated expression of IκBSR specifically in keratinocytes of the larval basal skin layer upon 4-OHT treatment (Figure 4.5.1, A). As explained in the previous chapter, EdU incorporation was used as an indication of PNC proliferative capacity. As expected, PNCs with induced suppression of NF-κB signalling displayed a significantly lower proliferative capacity at 24hpi. In comparison to the ≈31% proliferation rate of WT PNCs at this time-point, only

≈22% of PNCs exhibited proliferative capacity in an IκBSR background (Figure 4.5.1, B). This result suggests an intrinsic role for NF-κB signalling in promoting PNC proliferation.

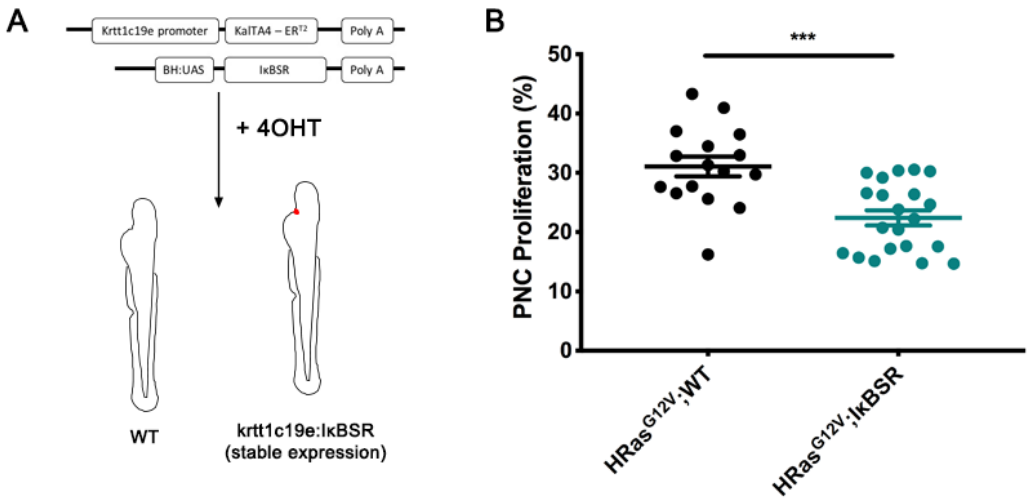

Figure 4.5.1 NF-κB activity promotes PNC proliferation. A) Schematics of how basal skin layer specific suppression of NF-κB activity is achieved in this model of tumour initiation. B) Percentage of proliferating PNCs in *krtt1c19e*:IκBSR transgenic larvae and their WT siblings at 24hpi. Quantification of double positive cells following EdU detection and eGFP/HRas immunostaining was performed by optical sectioning. Data acquired from 2 independent experiments; n≥ 16 per group. Mean±SEM. Mann-Whitney test. *** p=0.0004.

4.6 NF-κB Signalling in PNCs Affects Neutrophil Retention but Not Recruitment

Several chemokines are amongst the proinflammatory factors downstream of MyD88-NF-κB signalling in oncogenic Ras transformed keratinocytes. It is well established that chemokines expressed by cancer cells, are major chemoattractants of neutrophil recruitment and infiltration within tumour microenvironment . As a potential upstream regulator of these chemokines expression, NF-κB signalling may be one of the mechanisms promoting neutrophil recruitment to PNCs. However, contrary to expectations, live time lapse imaging of PNCs in *krtt1c19e*:IκBSR transgenic larvae revealed only a slightly lower number of recruited *lyz*:DsRed positive neutrophils, when

compared to their WT siblings (Figure 4.6.1). While the results shown here display no statistical significance, conclusions should be drawn cautiously, considering the small size of the sample. As such, this experiment, should be repeated a few more times to generate more powerful statistics.

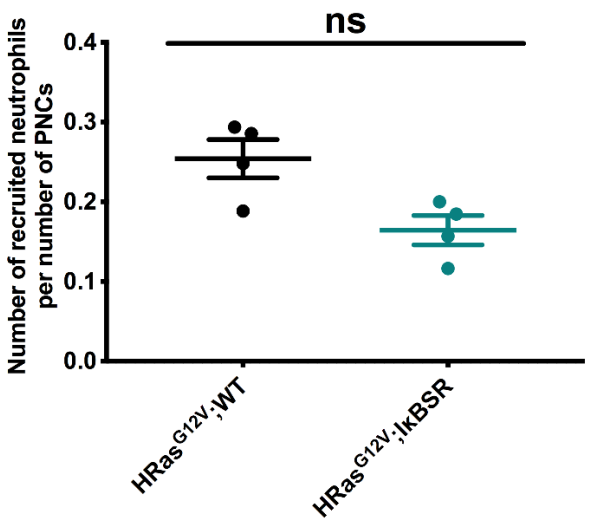

Figure 4.6.1 Inhibition of NF-κB signalling in the PNCs has little effect on recruitment of neutrophils to PNCs. Number of *lyz*:DsRed positive neutrophils recruited to PNCs in *krtt1c19e*:IκBSR transgenic larvae and their WT siblings through the course of a 3-hour long time lapse movie at 24hpi. Data acquired from 3 independent experiments; n=4 per group. Mean±SEM. Mann-Whitney test. ns p=0.0571.

Despite suppression of NF-κB activity having no significant effect on the recruitment of neutrophils to the PNC niche, close analysis of the behaviour of recruited neutrophils suggests short range recruitment mechanisms may be compromised. To inspect neutrophil migratory behaviour in detail, the acquired time lapse videos were further analysed using IMARIS software. This software allowed the tracking of individual neutrophils and provided a variety of measurements that captured neutrophil behaviour (Figure 4.6.2). Observation of the neutrophil tracks revealed recruited neutrophils often move between isolated PNC aggregates, but not all PNCs are persistently “visited” by these leucocytes. In fact, neutrophils are often attracted to a subset of PNCs where they exhibit a persistent concentrical migratory behaviour, such that, when they establish contact with a PNC aggregate, neutrophils repeatedly surround

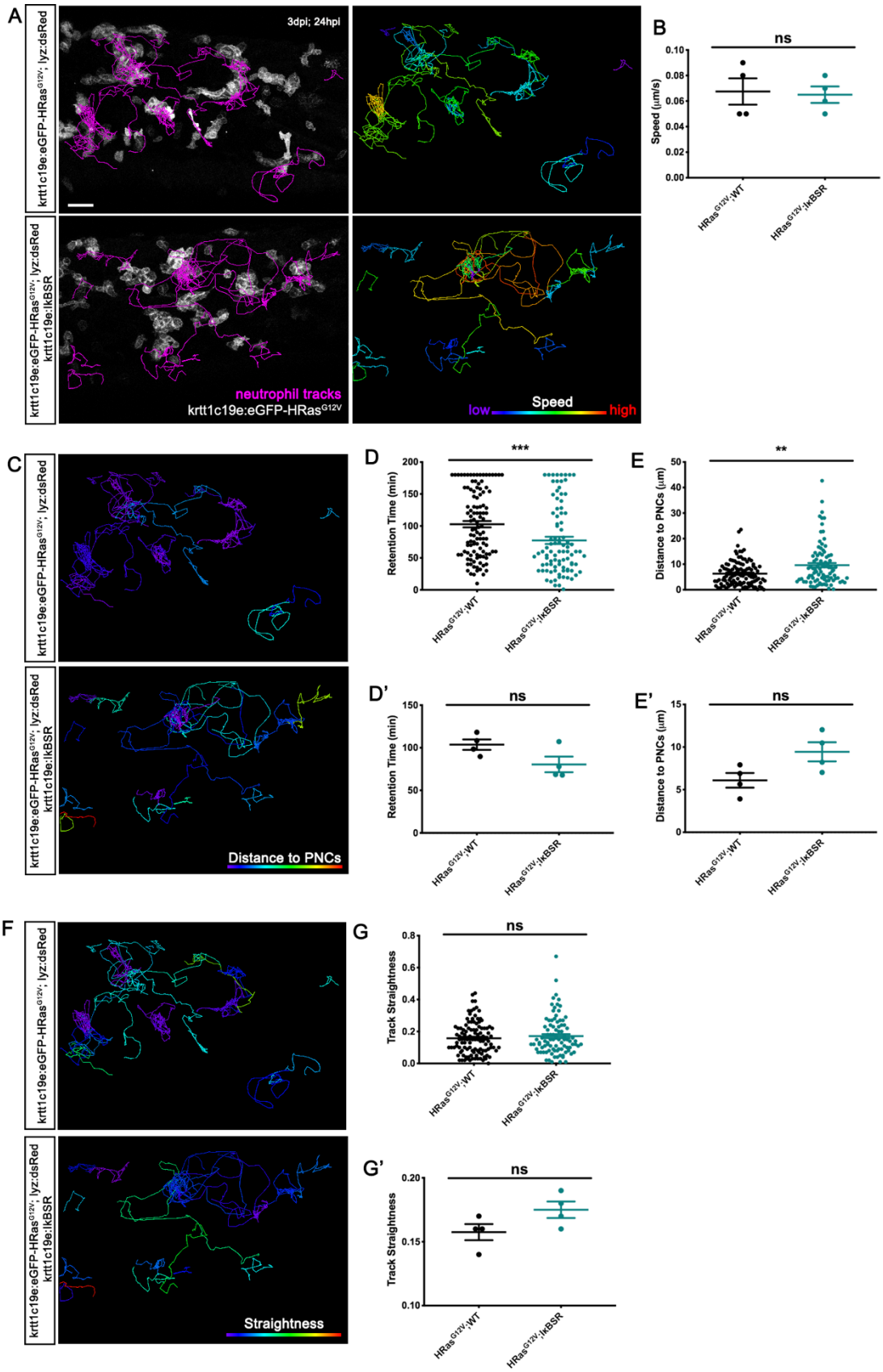
A
krtt1c19e:eGFP-HRasG12V; lyz:dsRed
krtt1c19e:eGFP-HRasG12V; lyz:dsRed krtt1c19e:lkBSR
3dpi; 24hpi
neutrophil tracks
krtt1c19e:eGFP-HRasG12V
Speed
low
high
B
ns
Speed (μm/s)
HRasG12V;WT
HRasG12V;lkBSR
C
Distance to PNCs
D
***
Retention Time (min)
D'
ns
E
**
Distance to PNCs (μm)
E'
ns
F
Straightness
G
ns
Track Straightness
G'
ns

Figure 4.6.2 Neutrophil track analysis reveals that inhibition of NF-κB signalling in the PNCs affects migratory behaviour of recruited neutrophils. A) Still image from a 3-hour long time lapse movie at 24hpi showing movement tracks of neutrophils recruited to PNCs in *krtt1c19e*:IκBSR transgenic larvae (bottom panel) and their WT siblings (top panel). The same tracks are then statistically coded according to (A right panel) mean speed, (C) mean distance to PNCs and (F) straightness index. Semi-automated analysis of neutrophil tracks with IMARIS software allowed quantification of distinct parameters such as: (B) neutrophil mean speed, (D,D') neutrophil retention time, (E,E') track mean distance to PNCs and (G,G') track straightness index. Data acquired from 3 independent experiment; n=4 larvae per group ($HRas^{G12V}$;WT= 110 tracks; $HRas^{G12V}$; IκBSR= 91 tracks). (D) (E) (G) display neutrophil specific analysis. (B) (D') (E') (G') display mean values per larva. Mean±SEM. Mann-Whitney test. (B) p>0.9999; (D) ***p=0.0003; (D') p=0.1143; (E) **p=0.0035; (E') p=0.0571; (G) p=0.6017; (G') p=0.2000. Scale bar = 50 μm.

it from multiple angles in interactions that can last several hours. During these interactions physical contact with the one PNC aggregate is not constant and neutrophils can momentarily move away from the PNCs but are almost immediately pulled back. (Figure 4.6.2 A, supplementary video 5).

Suppression of NF-κB activity in PNCs seem to have attenuated this concentric behaviour. It is generally accepted that chemotactic gradients guide leukocytes to sites of their highest concentration by increasing their velocity and directionality [278,281]. Decreases in chemokine expression levels due to the suppression of NF-κB activity could affect the speed at which neutrophils were recruited to PNCs. However, no statistical difference was found (Figure 4.6.2 A,B). Further analysis revealed, in a larval background with basal skin layer specific inhibition of NF-κB, that neutrophils displayed a lower retention time (maximum uninterrupted period of time spent "visiting" a specific PNC aggregate). Consequently, in this group, neutrophils exhibited shorter persistent tracks and were more often found moving from one PNC aggregate to the other as it is evident from the higher track mean distance to PNCs (Figure 4.6.2 C-E'). Considering the traits just mentioned, one would expect the neutrophil track straightness index, calculated as the ratio of track displacement length to track length, to be higher in larvae with a basal skin layer specific inhibition of NF-κB. However, no statistical difference was found

between the two conditions (Figure 4.6.2 F-G'). Nevertheless, one should remember that the inherently random nature of neutrophil movement, both in the presence and absence of chemoattractants, often described as Brownian random walk [278], will introduce a high degree of variation within each group. Therefore, great mechanistic changes in short range neutrophil recruitment often cause apparent small changes in neutrophil behaviour.

4.7 Discussion

The role of NF-κB in tumour development is extremely complex. Depending on the type of tissue studied and the nature of the mechanism used to induce tumour formation, NF-κB was found to have both tumour promoting and tumour supressing effects. The study of this signalling pathway in skin carcinoma has resulted in especially contradictory findings, mainly due to its well-established role in the regulation of skin immune homeostasis [286,287]. The model here established presents a unique opportunity to follow, in real time, the early stages of tumour initiation and how the NF-κB signalling machinery is engaged to potentiate tumour promotion. Here, I show that overexpression of $HRas^{G12V}$ promotes rapid activation of NF-κB signalling in PNCs which enables rapid PNC turnover and mediates close neutrophil-PNC interaction.

Using the NF-κB reporter transgenic line, where eGFP expression reads out NF-κB activity, NF-κB activity seems to be constitutively active from very early stages of preneoplastic cell emergence. The slow maturation time of eGFP, which could take a minimum of 2 hours, limits the temporal accuracy of this measurement. Nevertheless, given the cumulative nature of this reporter, the increasing trend from as early as the first timepoint analysed at 10hpi indicates the signalling pathway is already active. The early activation of NF-κB suggests it to be a direct downstream target of $HRas^{G12V}$ signalling. As a downstream effector of Ras signalling, the role of MAPK signalling in NF-κB activation was tested. However, suppression of this pathway through the treatment with the MEK inhibitor, Trametinib, showed no effect on NF-κB

activity. Nevertheless, other downstream effectors of Ras signalling have also been implicated in the activation of NF-κB. Ras was shown to promote direct IκBα phosphorylation and subsequent degradation via activation of PI3K-AKT signalling [117]. Other mechanisms include activation of RalGEF/RalB/Sec5 and recruitment of the noncanonical kinase TANK-binding kinase 1 (TBK1) [121] and activation of PKCα and subsequent assembly of the CARMA1/3-Bcl10-MALT1 complex [119]. Interestingly, PKCα was also shown to be upstream of IL-1α cytokine release contributing to the establishment of the autocrine loop through IL-1R-MyD88 pathway [130]. It should be noted, for the purposes of this study, zebrafish genome has only an ancestral version of the *IL-1* gene, before expansion of the *IL-1* locus into *IL-1α*, *IL-1β* and other members of *IL-1* gene family. This zebrafish ancestral version contains higher homology to the mammalian *IL-1β* [306]. Nevertheless, zebrafish Il-1, which is also found upregulated from very early stages of PNC emergence (preliminary data by Nikolay Ogryzko, not shown), could be a plausible alternative in the establishment of this autocrine loop in our zebrafish model. However, it should be considered that the inactive pro-Il-1 requires a secondary stimulus, such as ATP, to be processed by the inflammasome and released [307]. Further activation of the NF-κB canonical pathway can be achieved via TLRs. In fact, carcinogen initiated inflammation in skin has been shown to depend on TLR4 activation by the release of HMGB1 [308]. HMGB1 is a nuclear protein which is passively released during cell necrosis, but can also be actively secreted by inflammatory cells and cells under stress [309]. The observation of the upregulation of *myd88* gene expression at a later stage of PNC development can also be indicative and sufficient for amplification of NF-κB signalling via its canonical pathway without requirement for external stimuli [100]. In agreement with these results, several studies with epithelial specific MyD88 knockout mice have demonstrated the requirement of MyD88 dependent signalling in intestinal, breast and skin tumour development [130,295]. However, the requirement for a long latency period before one can detect these lesions in murine models makes it impossible to attribute the requirement of MyD88 dependent signalling to tumour initiation. Furthermore, MyD88 downstream

effects are not necessarily dependent on NF-κB transcriptional activity. MyD88 was shown to amplify MAPK signalling by maintaining Erk in its active, phosphorylated form [293]. While MyD88 is also mechanistically involved in activation of AP1 transcription factor, in skin cancer its role in AP1 activation does not seem to be relevant [5]. Taking all this into consideration, the complexity with which RAS and NF-κB signalling are linked and the multitude of external signals that can further stimulate NF-κB activity indicate a more comprehensive study is required to understand the signals activating NF-κB in PNCs.

Despite not being able to identify the main signal upstream of NF-κB activation, so far, the use of a basal layer keratinocyte specific IκBSR zebrafish transgenic line has allowed the study of how the suppression of the NF-κB signalling pathway affects PNC proliferation and neutrophil behaviour. The impaired PNC proliferative capacity observed in *krtt1c19e*:IκBSR larvae suggests that NF-κB has a pro-tumorigenic role in tumour initiation by promoting PNC proliferation, similar to what has been shown in a mouse model [129]. Several mechanisms can contribute to this effect. NF-κB can directly promote cell cycle progression via expression of CyclinD1 [310–312]. Furthermore, NF-κB stimulates the expression of c-Myc which can also promote cell proliferation [84].

Additionally, NF-κB can promote proliferation by initiating a dedifferentiation program and promoting stemness. Oncogenic Ras transformed murine keratinocytes have been shown to escape terminal differentiation and consequent cell cycle arrest [313]. NF-κB signalling has been implicated in this mechanism by promoting downregulation of the gene expression of differentiation associated keratins as well as other genes characteristic of keratinocyte differentiation [130]. It is not yet known if this could be consequence of a direct effect of NF-κB mediated gene silencing or an autocrine effect of the pro-inflammatory phenotype. This ability to dedifferentiate and initiate a stem cell like signature expression profile is especially relevant during tumour initiation as it has been demonstrated in a

study of intestinal tumorigenesis. The study in question provided evidence that $KRas^{G12D}$ dependent activation of NF-κB signalling enhances β-catenin/Tcf-mediated transcriptional activity leading to dedifferentiation of non-stem intestinal epithelial cells that acquire tumour-initiating abilities [314]. The consistent observation of a progressive decrease in PNC fluorescence from 24hpi onwards (observational detail, data not shown) could be indicative of downregulation of keratinocyte specific genes driven by the initiation of a dedifferentiation program. However, a more comprehensive analysis of PNCs expression profile and its dependence on NF-κB activity is required.

By promoting a pro-inflammatory environment with expression of pro-tumorigenic cytokines, such as Il-1, NF-κB initiates an autocrine loop maintaining its activated state. Other inflammatory mediators, such as IL-6 and CXCL8, can also amplify other signalling pathways which also promote proliferation, such as STAT3 and MAPK [85,290].

The induction of a pro-inflammatory microenvironment through the activation of NF-κB signalling could also be a source of chemoattractants that promote the early neutrophil response seen in this model. Another model of skin early tumorigenesis has shown diminished neutrophil infiltration when NF-κB signalling is compromised [129]. However, this study revealed the basal layer keratinocyte specific suppression of NF-κB activity did not significantly affect neutrophil recruitment to the PNCs. Despite the small decrease (not statistically significant trend) in neutrophil infiltration, the observation that recruitment is still active suggests the existence of alternative alarmin signals which are not dependent on NF-κB activity. Several studies in zebrafish larvae point to hydrogen peroxide as a likely important signal for early neutrophil recruitment. Acute injury has been shown to generate a tissue-scale gradient of hydrogen peroxide by dual oxidase (Duox) [315]. Similarly, in a tumour initiation setting, $HRas^{G12V}$ transformed mucous secreting cells have been shown to generate Duox-mediated extracellular bursts of hydrogen peroxide [154]. Neutrophils are equipped with a redox sensor, Lyn, which, when activated by exposure to reactive oxygen species (ROS), drives neutrophil polarization and migration along hydrogen peroxide gradient [316,317].

Consequently, abrogation of hydrogen peroxide production is often met with reduced neutrophil recruitment to wound and $HRas^{G12V}$ transformed cells [154,315]. Lipid mediators, such as Leukotriene B_4 (LTB_4), have also been implicated in neutrophil chemotaxis [318]. This leukotriene is often found elevated in $HRas^{G12V}$ transformed cells *in vitro* and blockage of its receptor, BLT2, suppresses tumour formation *in vivo* [319,320]. These signals, hydrogen peroxide and LTB_4, can be rapidly produced and released in a NF-κB independent manner, whereas chemokine release is usually slower due to regulation at the transcriptional and translational levels [318]. As such, if present in this model, they are likely to initiate the earliest neutrophil recruitments and promote subsequent release of chemokines which have longer half-life and the ability to act at longer distances. While the PNCs' ability to produce chemokines may be compromised due to inhibition of NF-κB signalling activity in *krtt1c19e*:IκBSR transgenic larvae, recruited neutrophils maintain their ability to activate NF-κB signalling and downstream targets. These early signals can activate neutrophils to release cytokines and chemokines and, thus, amplify the inflammatory response [318].

Nevertheless, as evident in the more detailed analysis of neutrophil behaviour, NF-κB dependent signals derived from PNCs are important for short range neutrophil recruitment. In a wild type background neutrophils often exhibit a low directional persistent migration resembling neutrophil behaviour in other models of chronic inflammation [154,321]. This behaviour is consistent with the 2-fold manner Cxcl8 directs neutrophil migration. It has been shown that this chemokine establishes tissue-bound gradients by binding to heparan sulphate proteoglycans and modulates neutrophil recruitment by imposing a directional bias and triggering orthotaxis towards the source where it restricts neutrophil movement [278]. It is, then, very likely that Cxcl8 is the primary PNC-derived chemokine promoting persistent neutrophil-PNC interaction. The loss of this persistent neutrophil-PNC interaction in the *krtt1c19e*:IκBSR larvae as it is evident by the lower retention time and higher mean distance to PNCs suggests NF-κB signalling is required for PNC retention signal. Considering the dichotomy with which Cxcl8 influences neutrophil migration, one can

understand why, despite these distinct behaviours, track straightness index remained unaffected. While qRT-PCR analysis (Chapter 3) confirms this chemokine expression is upregulated in PNC bearing larvae, further studies are required to verify its origin. Techniques such as *cxcl8 in situ* hybridization and qRT-PCR on FAC sorted PNCs from both, WT and *krtt1c19e*:IκBSR larvae, will greatly elucidate if Cxcl8 is the NF-κB dependent signal mediating persistent neutrophil-PNC interaction.

Another mechanism that could be responsible for this less persistent neutrophil migration in *krtt1c19e*:IκBSR larvae is the release of DAMPs by dying cells. While the role of NF-κB signalling in cell death was not assessed in this model, it is generally understood that NF-κB can prevent DNA damage induced cell death with the expression of anti-apoptotic genes [129]. It is also known that in the face of two conflicting chemotactic signals, neutrophils prioritize newly arising or newly encountered attractants [322]. Therefore, in the absence of a retention force that keeps neutrophils interacting with a certain PNC aggregate, the death of a cell nearby can easily divert neutrophils from their original course.

While these observations fit nicely with the possible importance of NF-κB-Cxcl8 axis in neutrophil-PNC interaction, one cannot ignore that other chemokines may be involved. In fact, *cxcl18b* gene expression, which is also regulated by the MyD88-NF-κB pathway, was found to be upregulated in this model (Chapter 3). Cxcl18b can induce Cxcr2 dependent neutrophil recruitment, similarly to Cxcl8 [281]. However, whether these chemokines share other features, such as the mechanism of retention at the source, is not yet known.

Moreover, the potential involvement of other inflammatory signalling pathways in the release of chemotactic signals cannot be ignored. A previous report established a connection between hydrogen peroxide and *cxcl8* expression via AP1 transcriptional regulation in zebrafish wound response [323]. Even though it is likely this requires a persistent influx of hydrogen peroxide supplied by the wound gradient, which is not met in the stochastic and short-lived bursts transformed cells generate, it highlights the fact that the same pro-

inflammatory genes can be regulated by several signalling pathways. Therefore, despite the well documented contribution of NF-κB signalling to the expression of these cytokines and chemokines, confirmation that their expression is compromised in *krtt1c19e*:IκBSR larvae is required.

While this study allows for tissue specific suppression of NF-κB activity, a few limitations must be considered. The use of a UAS-regulated transgene as a stable transgenic line is susceptible to gene silencing due to methylation of the UAS promoter sequence. This gene silencing seems to be progressively more frequent from generation to generation [324,325]. Moreover, considering NF-κB signalling regulates skin immune homeostasis, general suppression of its activity in both, PNCs and neighbouring cells, could potentially allow for a TNF mediated inflammatory response in PNC neighbours [142,144,287]. To overcome these limitations, a post-doctoral fellow in the laboratory, Nikolay Ogryzko, has generated a DNA construct in which a bidirectional UAS sequence controls both eGFP-HRas^{G12V} and IκBSR transgenes (Supplementary Figure 7). Using this construct transiently, as per nature of this model, will allow us to avoid UAS silencing and restrict inhibition of NF-κB activity to PNCs.

5 Characterization of MyD88-NF-κB Signalling in Recruited Neutrophils and Its Trophic Role

5.1 Introduction

Neutrophils constitute a great part of the inflammatory cells in the tumour microenvironment. However, until recently, their contribution to carcinogenesis and tumour development had been overlooked [146,147].

Today, it is known that tumour associated neutrophils (TANs) can greatly influence several events of tumour development. With that influence dependent on their N1 or N2 polarization, they can have anti-tumorigenic or pro-tumorigenic functions, respectively [155]. Considering neutrophil phenotype is dependent on environmental factors, it has been suggested their polarization bias is correlated with the stage of tumorigenesis. TANs from early tumours were found to be more cytotoxic and produce higher levels of TNF, NO and H_2O_2. This effect was progressively reduced with tumour progression [157]. However, recent studies have shown a pro-tumorigenic role of neutrophils from an early neoplastic stage [149,150,154,160,161].

As inflammatory cells, neutrophils influence the tumour microenvironment by releasing cytokines to promote tumour associated inflammation [326], a process mainly dependent on the activation of NF-κB and selective MAPK pathways [327].

However, contradictory results have arisen in the study of the role of NF-κB signalling in myeloid cells during tumorigenesis, suggesting it's action to be organ and context dependent. While some studies demonstrated decreased tumour growth following abrogation of myeloid specific NF-κB signalling [135,328,329], others suggest NF-κB activity in these cells potentiate their anti-tumorigenic phenotype [330–332]. It should be noted that these studies abrogate NF-κB signalling in the entire myeloid lineage, rather than specifically in neutrophils. It has been suggested the whole leucocyte population behaves in a similar manner as the neutrophil population, exhibiting comparable

expression of NF-κB responsive genes when activated with LPS [333]. However, the complexity of factors present in a tumour microenvironment and the heterogeneity of phenotypes observed within the same cell population indicate this approach in cancer studies may be overly simplistic.

In this Chapter, I demonstrate that neutrophils exhibit an NF-κB dependent trophic role in PNCs and show evidence of heterogeneity within the neutrophil population.

5.2 Detection of NF-κB Activity in Recruited Neutrophils

Activated neutrophils can trigger the expression of many genes, including cytokines and chemokines, which contribute to the establishment of an inflammatory microenvironment. Many of these genes depend on the activation of the NF-κB pathway [327].

Using the NF-κB activity reporter zebrafish line previously introduced in Chapter 4, I tested whether neutrophils recruited to PNCs activated NF-κB signalling. However, the analysis of eGFP expression level in *lyz*:DsRed positive recruited neutrophils using live imaging was inconclusive. Live imaging of recruited neutrophils revealed that neutrophils maintained low levels of eGFP expression. When in close contact with PNCs, neutrophil eGFP intensity widely fluctuated, the high rate of which suggested that this was unlikely to be caused by NF-κB signalling activation (Figure 5.2.1). Similar occurrences were observed when neutrophils were in close contact with neuromasts or the lateral line, structures within the larval skin which display constitutive activation of NF-κB signalling, and therefore high EGFP intensity, throughout embryo development (not shown) [207].

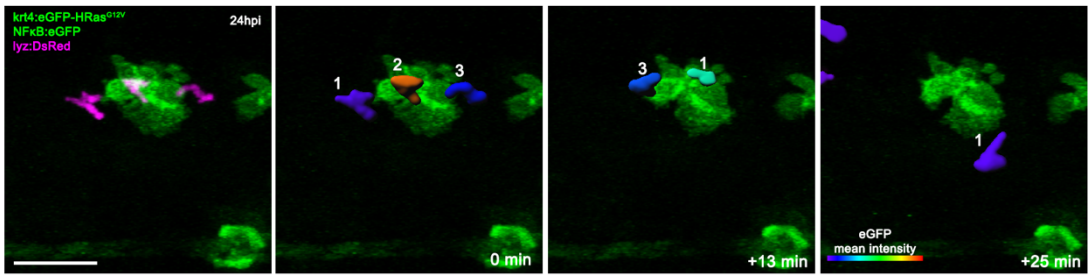

Figure 5.2.1 Live imaging of PNC recruited neutrophils in an NF-κB reporter background is an inaccurate approach for the analysis of their NF-κB activation state. Still images of a time-lapse movie in a *Tg(NFκB:eGFP)* background with eGFP as a reporter of NF-κB activity. Neutrophils represented by surfaces, generated with IMARIS software, statistically coded for mean eGFP intensity showing that the neutrophil (follow neutrophil 1) GFP intensity fluctuates when in close contact with eGFP-HRas^{G12V} PNCs due to automated neutrophil fluorescent intensity based segmentation defining PNC GFP fluorescence as within a neutrophil. Scale bar = 50 μm.

Considering the automated neutrophil segmentation is based on DsRed fluorescence intensity, the image analysis software, IMARIS, may include some of the neighbouring eGFP fluorescence as within the neutrophils. As such, it is possible, while in close contact with cells exhibiting high levels of eGFP expression, the neutrophils eGFP intensity variation was an artefact caused by the inclusion of some of these cells fluorescence as within the neutrophil. Given the low basal levels of NF-κB activity in the neutrophils compared to other cells within the skin, with which recruited neutrophils often closely interact, live imaging was an impractical approach for proper analysis of NF-κB activity in neutrophils.

As it seemed that proximity to PNCs and high levels of eGFP intensity in other cell types within the larval skin were an impediment to analysis of neutrophil NF-κB activity, the isolation and analysis of *lyz*:DsRed positive neutrophils by flow cytometry was a potential alternative.

Triple transgenic (*krt4*:eGFP-CAAX/HRas^{G12V}; NFκB:eGFP; *lyz*:DsRed) larvae were dissociated at 24hpi and the GFP intensity of DsRed positive neutrophils was assessed as a read-out of NF-κB activation (Figure 5.2.2 A, gating strategy in Supplementary Figure 4). Larvae with CAAX control cells displayed

only 0.5% eGFP positive neutrophils with a low level of mean intensity. PNC bearing larvae displayed a slightly higher, but not statistically significant, proportion of neutrophils with NF-κB activity. In the $HRas^{G12V}$ condition 1.5% of *lyz*:DsRed positive neutrophils were eGFP positive with higher levels of mean intensity (Figure 5.2.2 B, C).

Considering the evident trend, the lack of statistical significance may be due to the small size of the sample. This experiment, should, then, be repeated a few more times to generate more powerful statistics.

Considering the cumulative nature of this reporter, low levels of eGFP intensity, observed in the CAAX condition, could indicate that the NF-κB signalling pathway hadn't been activated for long. Therefore, this small population of presumably recently activated neutrophils could be a result of the dissociation process. Note that the entire process of sample preparation takes nearly 2 hours, in which larvae dissociation is achieved with the combination of both enzymatic and mechanical forces and lasts for nearly 30 minutes at 28.5ºC. In PNC bearing larvae, the higher levels of mean eGFP intensity detected in eGFP/DsRed double positive neutrophils could then be the result of longer activation period (Figure 5.2.2 B,C). These results could also indicate a difference in the level of NF-κB activation, with PNC bearing larvae having a stronger NF-κB signalling in activated neutrophils.

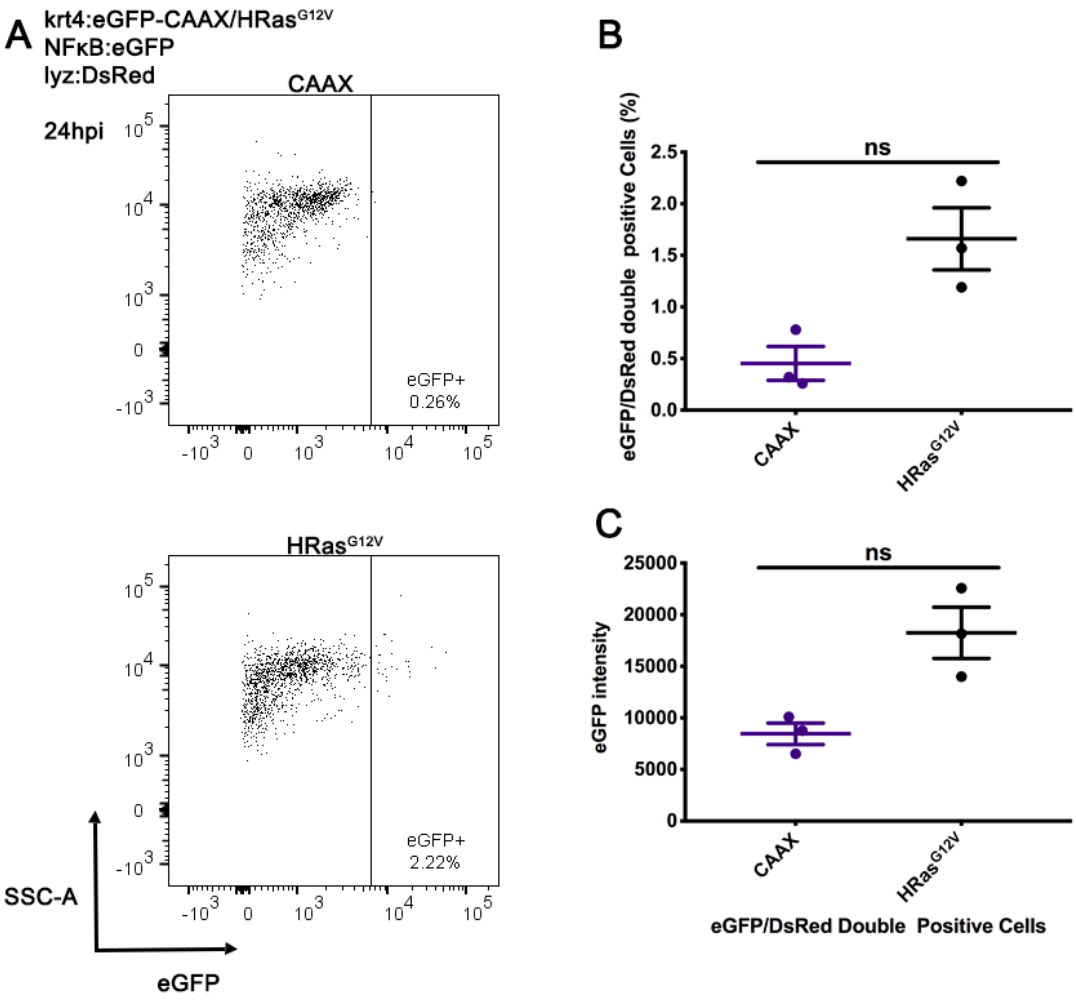

Figure 5.2.2 Flow cytometry analysis of *lyz:*DsRed^{+} neutrophils showed a small population of neutrophils with NF-κB activity A) Representative Scatter dot plots from flow cytometry analysis of DsRed positive neutrophils in CAAX control and PNCs bearing larvae in an NF-κB reporter background at 24hpi. The vertical line across the plot denotes the threshold used to distinguish between NF-κB positive and NF-κB negative cells. B) Proportion of DsRed positive cells which are eGFP positive. C) eGFP mean intensity of eGFP/DsRed double positive cells. Data acquired from 3 independent experiments (n=3). Mean±SEM. Mann-Whitney test. ns p=0.1000

5.3 NF-κB Activity Inhibition in Neutrophils Affects PNC Proliferation

Neutrophils have been shown to promote tumour growth and studies of tumour initiation have suggested the pro-tumorigenic effect of recruited neutrophils is relevant from early stages of tumour development [149,150,154,160,161]. As a pathway promoting the inflammatory response from activated neutrophils, NF-κB transcription factors could potentially regulate the mechanisms through which neutrophils promote proliferation of tumour cells.

To assess the effect of neutrophil specific NF-κB signalling in PNC progression, I used a transgenic line that allows for neutrophil specific suppression of this signalling pathway. Lineage specific suppression of NF-κB activity was achieved with expression of the constitutively active dominant negative mutant form of the murine IκBα, IκBSR, now under the control of the neutrophil specific promoter *lyz* [199]. This mutant IκBα is resistant to phosphorylation and consequent proteasome degradation [302,303]. It should be noted that while in most cell types NF-κB activation is regulated by the nuclear translocation of its subunits, in neutrophils, IκBα is present in both, cytoplasm and nucleus, and NF-κB activation correlates with a substantial reduction of this protein in both cell compartments [334]. As IκBα has great functional and structural similarities between teleosts and mammals, IκBSR has also been shown to inhibit NF-κB signalling in zebrafish embryos [304,305].

The *Tg(lyz:IκBSR)* zebrafish transgenic line was made using Tol2-transposase-mediated transgenesis [202] by another member of the Feng Laboratory. The active expression of the transgene was confirmed by RT-PCR on total RNA extracted from whole larvae. Comparison of larvae carrying the *cry*:CFP (blue retina) selection marker with WT siblings showed successful integration and expression of both, the selection marker and transgene (Figure 5.3.1 A).

To determine the effect of neutrophil-specific inhibition of NF-κB signalling on PNC proliferation, I crossed *Tg(lyz:IκBSR)* with *Tg(krtt1c19e:KalTA4-ER^{T2})*

and used EdU incorporation to study PNC proliferative capacity. Suppression of NF-κB signalling in neutrophils is associated with a significantly lower PNC proliferative capacity at 24hpi. While in a WT background ≈37% of PNCs were detected as actively dividing at 24hpi, only ≈19% of PNCs exhibited proliferative capacity when NF-κB signalling in neutrophils was suppressed (Figure 5.3.1 B). Therefore, NF-κB signalling is likely to be, at least in part, a positive regulator of neutrophil derived mechanisms promoting PNC proliferation.

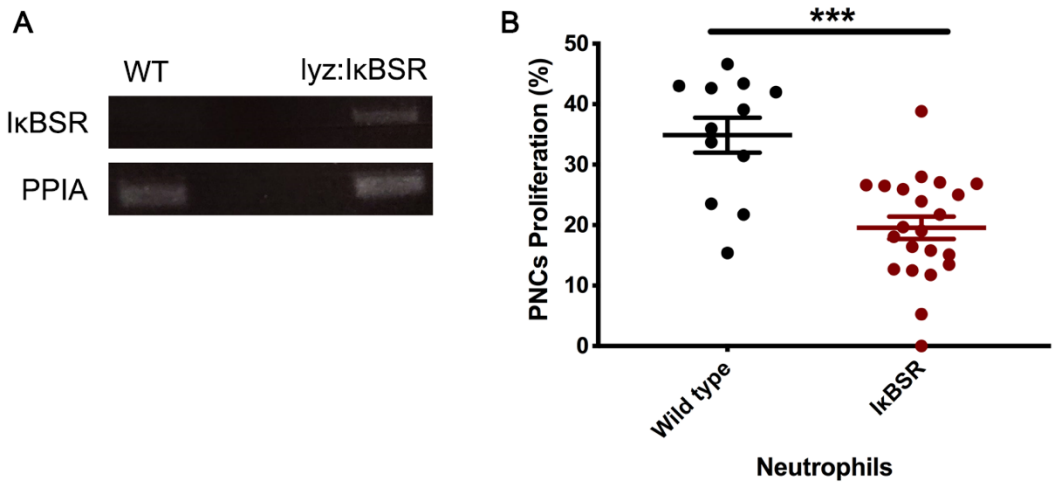

Figure 5.3.1 Neutrophil specific NF-κB activity inhibition affects PNC proliferative capacity A) RT-PCR on total RNA extracted from whole larvae showing larvae positive for the *cry*:CFP (blue retina) selection marker from the *lyz*:IκBSR zebrafish transgenic line efficiently express the transgene in comparison to their WT siblings with no selection marker. Peptidylprolyl isomerase A (PPIA) is used as a housekeeping gene to assure comparable overall gene expression levels (performed by Nikolay Ogryzko). B) Percentage of proliferating PNCs in *lyz*:IκBSR transgenic larvae and their WT siblings at 24hpi. Quantification of double positive cells following EdU detection and eGFP/HRas immunostaining was performed by optical sectioning. Data acquired from 2 independent experiments; n≥ 12 per group. Mean±SEM. Mann-Whitney test. *** p=0.0003.

5.4 Neutrophils with Different Levels of MyD88 Expression Exhibit Different Recruitment Behaviour

As it has been discussed previously, MyD88 is crucial for initiating signalling responses to IL-1β and other cytokines [99]. Therefore, leucocytes and tissues where these cells originate display a high basal level of *MYD88* gene expression [208,335]. Moreover, *MYD88* gene expression can be further upregulated in a variety of immune cells by several pro-inflammatory mediators such as, IL-6 [335], LTB_4 [336,337], IFN-α and IL-12 [338]. Following the initial observation that emerging preneoplastic cells induce an inflammatory response, I hypothesised that *myd88* expression in neutrophils changed in the early stages of tumour initiation.

Similarly to previous experiments, the *Tg(myd88:DsRed2)* reporter line [208] was used to study *myd88* expression levels in neutrophils. As the MyD88 reporter controls a DsRed transgene, using eGFP-$HRas^{G12V}$ necessitated the development of a neutrophil reporter line with a distinct fluorophore to enable this experiment. In the newly generated transgenic line, neutrophils express lifeact-mTurquoise2a under the control of the neutrophil specific *lyz* promoter [199]. Lifeact is a peptide, containing the first 17 amino acids of the actin-binding domain, Abp140, present in *Saccharomyces cerevisi*ae, which targets the fluorophore to bind F-actin filaments in the cytoskeleton [339]. Initially tested in mammalian cells, this peptide has been successfully used to label actin filaments in zebrafish larvae [340,341]. While particularly advantageous for studies of actin dynamics and cell polarity, this feature was not explored in the following studies.

Taking a whole embryo approach, with flow cytometry analysis, triple transgenic (*krtt1c19e*:eGFP-CAAX/$HRas^{G12V}$; *myd88*:DsRed; *lyz*:lifeact-mTurquoise2a) larvae were dissociated at 24hpi and mTurquoise2a positive neutrophils were assessed for their DsRed fluorescent level as a read-out of *myd88* gene expression level (gating strategy in Supplementary Figure 5). Both, CAAX control and $HRas^{G12V}$, conditions displayed a wide range of DsRed intensity levels within mTurquoise2a positive neutrophils (Figure 5.3.1

A). Similarly to what had been suggested in a previous report [208], approximately 80% of neutrophils displayed some level of DsRed expression, and consequently *myd88* promoter activity (Figure 5.3.1 A,B). This proportion was also found in PNC bearing larvae which showed no evidence of *myd88* gene upregulation in neutrophils, compared to CAAX control larvae (Figure 5.3.1 A,B).

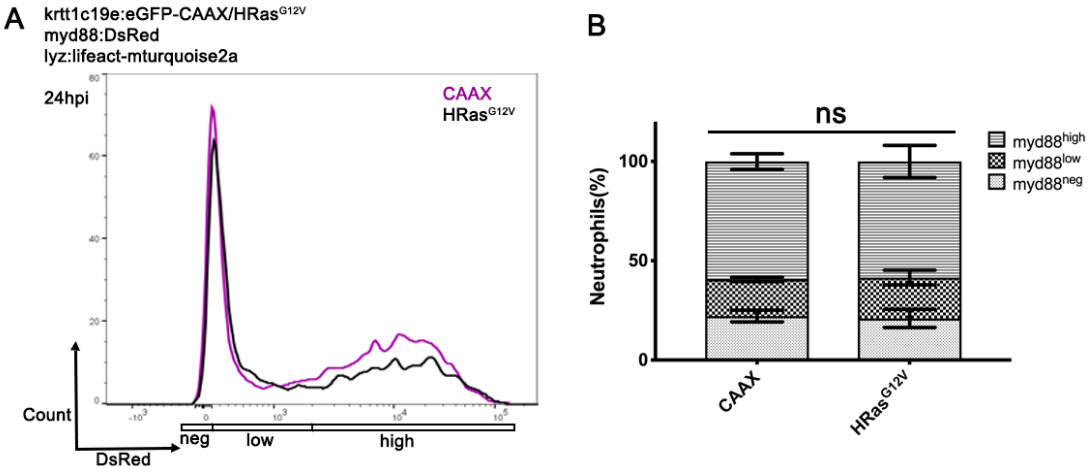

Figure 5.3.1 Flow cytometry of *lyz*:lifeact-mTurquoise2a^{+} neutrophils showed *myd88* gene expression is not affected in PNC bearing larvae A) Representative histogram from flow cytometry analysis of mTturquoise2a positive neutrophils according to DsRed intensity levels, in CAAX control and PNCs bearing larvae at 24hpi. Cell Count on the Y axis and DsRed fluorescence intensity on the X axis. B) Proportion of mTurquoise2a positive neutrophils with different levels of *myd88* gene expression categorised as depicted in (A). Data acquired from 3 independent experiments (n =3). Mean±SEM. 2 Way ANOVA with Sidak's post-test. ns $p \geq 0.9837$

Given the wide range of DsRed intensity levels within the neutrophil population, I decided to evaluate the potential of neutrophils with different levels of *myd88* promoter activity to contribute to the inflammatory response induced by the emergence of PNCs.

Live time-lapse imaging of triple transgenic larvae at 24hpi suggested all neutrophil subsets contribute to an inflammatory response as various levels of DsRed intensity are observed within neutrophils recruited to PNCs (Figure

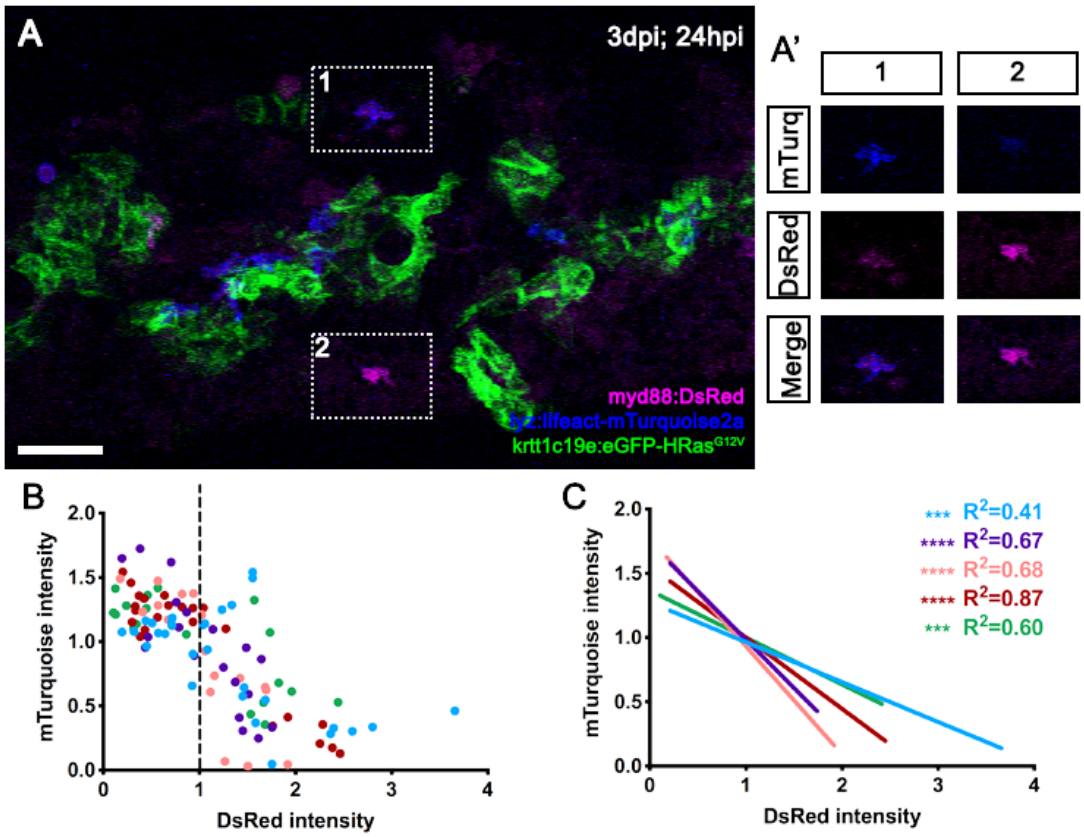

Figure 5.3.2 *myd88* and *lyz* expression levels seem to be negatively correlated. A) Still image of a time lapse movie showing recruited neutrophils displaying different levels of DsRed intensity as a readout for myd88 gene expression. A') Examples of neutrophils from (A) with separated colour channels for better visualization of negative correlation between mTurquoise and DsRed intensity. B-C) Neutrophils recruited within a 2-hour time lapse movie at 24hpi according to their mTurquoise (Y axis) and DsRed (X axis) mean intensity. Scatter plot of individual neutrophils (B) and linear regression estimate (C) where each colour represents an individual larvae. To account for variation due to differences in transgene copy number, mean intensity values of each neutrophil were normalized to average intensity of all neutrophils within each larva. Consequently, plotted values represent relative intensity where X/Y=1 represents the neutrophil average intensity within each larva. Dashed line at X=1 in (B) represents the value separating the two neutrophil subsets compared in the subsequent analysis of migratory behaviour. Data acquired from 3 independent experiments. n=5. Correlation with Squared Pearson's Coefficient. ***p=0.0002; ****p <0.0001. Scale bar = 50 μm.

5.3.2 A, A', Supplementary video 6). Interestingly, when intensity values for DsRed and mTurquoise are plotted for each individual neutrophil recruited to the skin, a negative correlation between them was evident. Neutrophils with high mTurquoise intensity levels, indicating high lyz promoter activity, would often show low DsRed intensity, indicating low *myd88* promoter activity. On the contrary, neutrophils with low mTurquoise intensity levels would preferentially display high DsRed intensity (Figure 5.3.2 B,C).

While these results show a strong negative correlation between mTurquoise and DsRed expression, the bias introduced by the approach used to identify leucocytes should be considered. Neutrophils were identified by *lyz* promoter activity and automated detection by the image analysis software, IMARIS, which is dependent on the fluorescent intensity of either, mTurquoise or DsRed. A few neutrophils with low intensity levels for both fluorophores were observed being recruited to PNCs, however as they fell below the detection threshold for IMARIS they are missing from the analysis, presenting a possible source of error.

Following the observation that the neutrophil population being recruited to the skin had highly heterogenous *myd88* gene expression. I wanted to study if these transcriptionally distinct neutrophils would also exhibit distinct behavioural patterns when interacting with PNCs.

Given the great variety of DsRed and mTurquoise intensity values of recruited neutrophils, there is no distinct separation of neutrophil subsets with regards to these parameters (Figure 5.3.2 B). With no other characteristic available, an arbitrary division at the average neutrophil DsRed intensity was used to separate the recruited neutrophils into two subsets. As such, neutrophils with relative DsRed intensity lower than 1 were grouped into the $MyD88^{low}$ neutrophil subset, and neutrophils with relative DsRed intensity higher than 1 were grouped into the $MyD88^{high}$ neutrophil subset (Figure 5.3.2 B).

Once again, time-lapse videos were analysed using the tools provided by the IMARIS software package. Using this image analysis software, individual neutrophils were tracked and their recruitment, persistence and close interactions with PNCs were assessed. Speed while in contact with PNCs and

retention time, measured as maximum uninterrupted period of time spent "visiting" a specific PNC aggregate (Figure 5.3.3) were analysed. When comparing the two neutrophil subsets, MyD88^{low} neutrophils behaved more similarly to what had been described in the previous chapter. These neutrophils remained in close proximity with PNCs for the majority of the time, exhibiting persistent tracks around distinct PNC aggregates where they exhibit low mobility range as depicted by their low speed. On the contrary, MyD88^{high} neutrophils displayed a wider array of tracks not restricted to PNC rich areas (Figure 5.3.3 A). This is likely to be consequence of their inability to be retained by and interact closely with PNCs, as suggested by their high speed and low retention time in comparison to MyD88^{low} neutrophils (Figure 5.3.3 B-C').

As mentioned before, while the differences in migratory behaviour are evident, the chosen method for the separation of the two population subsets may not be accurate. Considering that neutrophil MyD88-dependent signalling is unlikely to directly affect their migratory behaviour, the concurrence of consistent levels of *myd88* expression and behavioural pattern within each group may not be related. A more comprehensive characterization of these neutrophils, with regards to differences in expression of surface receptors, will greatly contribute to more accurately define population of cells and a better understanding of the mechanisms behind their distinct behaviours.

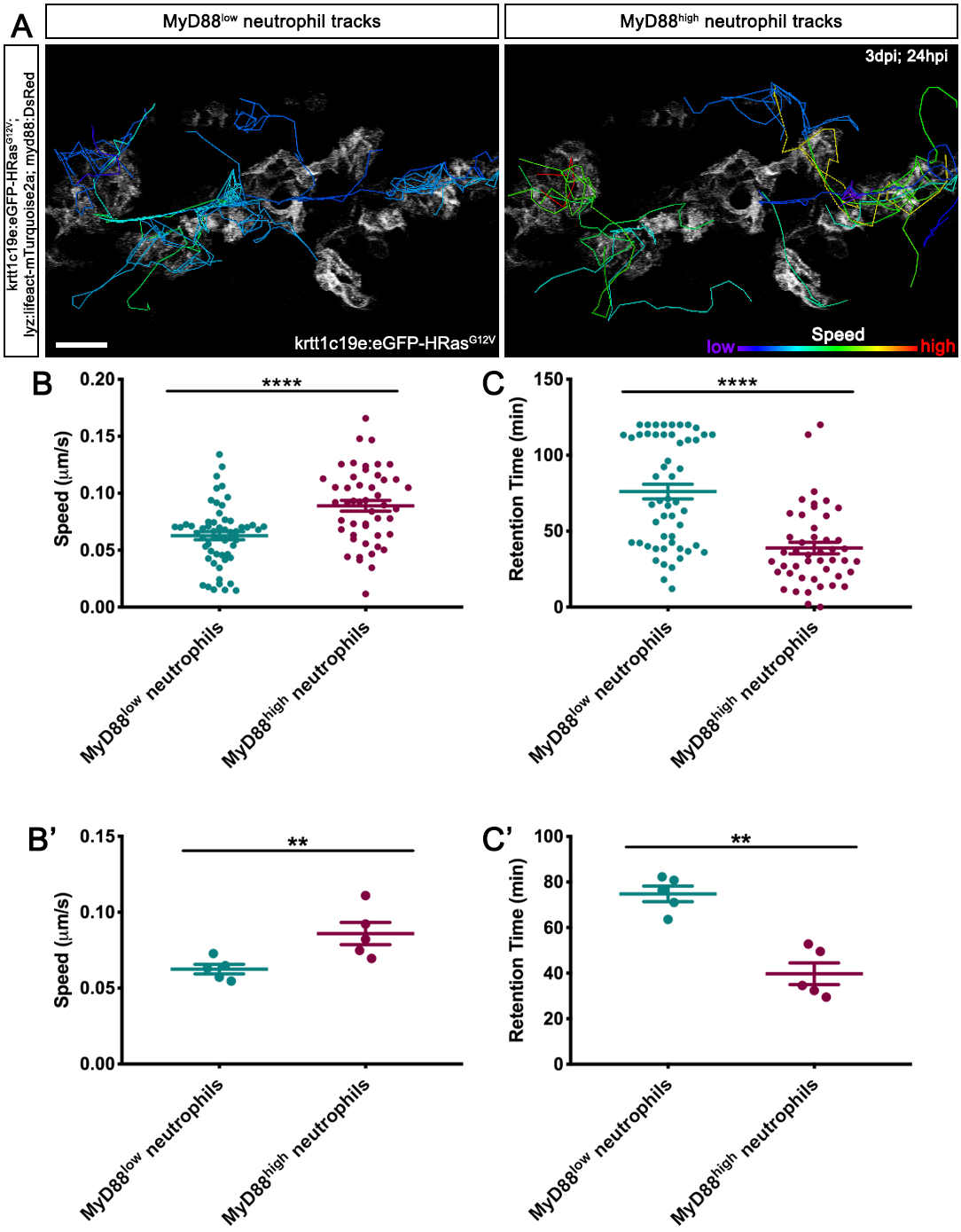

Figure 5.3.3 Neutrophils with different levels of *myd88* expression exhibit different recruitment behaviour. A) Still image from a 2-hour long time lapse movie at 24hpi showing movement tracks of MyD88^{low} neutrophils (left panel) and MyD88^{high} neutrophils (right panel) recruited to PNCs. Tracks are statistically coded according to track mean speed. Semi-automated analysis of neutrophil tracks with IMARIS software allowed comparison of the two neutrophil subsets according to distinct parameters such as: neutrophil speed (B,B') and retention time (C,C'). Data acquired from 3 independent experiment; n=5 larvae (MyD88^{low}

Figure 5.3.3 (continued) neutrophils= 57 tracks; MyD88^{high} neutrophils= 48 tracks). (B) (C) display neutrophil specific analysis. Mean±SEM. Unpaired Student t test. (B') (C') display group mean values per larva. Mean±SEM. Paired Student t test. (B,B') **p= 0.0097; ****p<0.0001. (C,C') **p= 0.0021; ****p<0.0001. Scale bar = 50 μm.

5.5 Discussion

Oncogene transformed cells have been shown to elicit a prompt neutrophilic inflammatory response [149,150,154,160,206]. Therefore, neutrophils have the potential to affect tumour development from the initiation stage. Identifying their effector mechanisms and how they influence tumour cells is of extreme importance for a better understanding of the events that drive tumour progression. Considering the central role of NF-κB activity in the regulation of inflammatory genes, here I studied the ability of PNC recruited neutrophils to activate NF-κB and explored the role of this signalling pathway in neutrophil mediated PNC proliferation.

While the NF-κB reporter transgenic line had been previously useful in the characterization of NF-κB activity in PNCs, detection of this signalling pathway activity in neutrophils faced some issues. Live imaging of recruited neutrophils was impractical due to the higher levels of eGFP expression in cells within the skin with which neutrophils would regularly and persistently interact. Trying to overcome this limitation, flow cytometry analysis of dissociated larvae allowed the assessment of NF-κB activity in individual neutrophils. However, this approach only detected of a very small population of neutrophils with NF-κB activity. Many studies have already demonstrated the central role NF-κB activity in the regulation of inflammatory genes in neutrophils [327,333,334,342]. Additionally, it has been previously suggested that continuously stimulated neutrophils, as it should be the case in this model of tumour initiation, maintain persistent NF-κB activity despite considerable levels of IκBα present in the nucleus [343]. Given the small proportion of eGFP positive neutrophils detected, one could argue that NF-κB activity is not biologically significant for neutrophil function in this model of tumour initiation.

Nevertheless, with NF-κB playing such a central role in neutrophil biology, one should first consider the possibility of poor sensitivity of the transgenic reporter in neutrophils. For instance, while all NF-κB subunits have the ability to bind the consensus recognition sequence, distinct NF-κB dimers do so with different affinities [90]. Moreover, activation of distinct dimers is the main factor allowing selective regulation of NF-κB target genes [90]. As such, depending on the dimers preferentially formed in recruited neutrophils this transgenic line may not be an accurate reporter for NF-κB activity in neutrophils.

Considering the high sensitivity of activated neutrophils to shear stress [344,345], it is also possible the mechanic forces in place during the process of cell dissociation induced some degree of neutrophil apoptosis, resulting on the loss of the cells of interest.

Despite not conclusively demonstrating NF-κB activation in recruited neutrophils, the use of a neutrophil specific IκBSR zebrafish transgenic line has confirmed that this signalling pathway is, in fact, active. The impaired PNC proliferative capacity observed in *Tg(lyz:IκBSR)* larvae suggests neutrophils exhibit a tumour promoting role in tumour initiation which is, at least in part, dependent on NF-κB activation. This is consistent with previous reports showing that myeloid specific IKKβ ablation causes decreased proliferation in early tumour development in both inflammation and oncogene induced carcinogenesis [328,329]. According to these studies, the main mechanism by which myeloid cells promote tumour growth in an NF-κB dependent manner is with transcriptional activation of pro-inflammatory cytokines and chemokines such as, IL-1β, IL-6 and CXCL8, which activate proliferation promoting signalling pathways within tumour cells [328,329]. COX2 expression level is also compromised in myeloid cells following IKKβ ablation [328]. This enzyme is required for prostaglandin E2 (PGE2) synthesis [320]. Neutrophils and other leucocytes have been shown to be the main sources of this eicosanoid, which promotes tumour cell proliferation [161,244,346]. Myeloid derived MMP9, another known NF-κB target, has also been implicated in proliferation of neoplastic lesions. In a murine transgenic model of skin tumorigenesis elicited

by a HPV16 oncogene, the reduced keratinocyte proliferation observed in *Mmp9* knockout mice was restored when irradiated mice were transplanted with bone-marrow from WT mice [163]. *mmp9* expression is also upregulated in our tumour initiation model (Chapter 3). But, while in this study it is not clear which cell types within the PNC microenvironment contribute to this effect, other studies suggest a predominant contribution from neutrophils [150,163,347].

Further studies are needed to elucidate the relevance of each of these factors in the NF-κB dependent, neutrophil trophic role observed in this model.

It is also evident, from these results, that recruited neutrophils comprise a heterogeneous population with distinct migratory behaviours. With the available tools, two populations were defined according to their *myd88* gene expression level. MyD88^{low} neutrophils with high levels of *lyz* promoter activity displayed a close and persistent interaction with PNCs, consistent with the previous neutrophil behaviour analysis in Chapter 4. Additionally, a distinct MyD88^{high} neutrophil subset with low levels of *lyz* promoter activity was identified having a less persistent, more widespread movement.

The results obtained here are not sufficient to identify, with certainty, the origin of this neutrophil subset. Nevertheless, the continuous high to low spectrum of mTurquoise intensity suggests that, rather than being a distinct population, these are immature neutrophils at various stages of development.

Previous studies have demonstrated the presence of a small population of immature granulocytes in the tumour microenvironment [348–350]. These cells are believed to originate from the activation of an emergency granulocytic differentiation program in circulating and bone marrow-derived hematopoietic stem and progenitor cells (HSPCs). This mechanism is driven by tumour derived cytokines and growth factors, such as, IL-6 and granulocyte-colony stimulating factor (G-CSF) [351–353]. Gene expression analysis showed immature granulocytes displayed low levels of chemokine receptors CXCR1 and CXCR2 when compared to fully matured neutrophils, and, consequently decreased chemotaxis towards the tumour signals [349,354]. Consequently, during early tumour progression, these cells are most commonly found

accumulated in the peripheral tissues but not within the primary tumour [349,352]. While the presence, or rather, the lack of these receptors in the MyD88^{high} neutrophils needs further analysis, that could explain their inability to form long lasting interactions with PNCs as it is evident by their track pattern and low retention time.

Given their immature myeloid characteristics these immature granulocytes are often considered as part of the heterogeneous population of myeloid derived suppressor cells (MDSCs). However, several independent studies showed that, contrary to what is observed in late stages of cancer, during early tumour progression, these cells do not exhibit immunosuppressive activity [350,354,355]. Additionally , these immature granulocytes displayed higher metabolic activity and ATP production, which were correlated with enhanced spontaneous migration [354]. Despite the role of immature granulocytes in early tumour development is still unclear, they have been suggested, due to their enhanced spontaneous migration, as mediators of early tumour cell dissemination [354]. Given the difference observed in the speed of the two populations, it would be interesting to test whether the high velocity of MyD88^{high} neutrophils is also regulated by an ATP mediated autocrine loop [354,356].

While these observations are correlative rather than causative, they provide a future direction of how to move forward to identify and better characterize this neutrophil subset. By understanding what defines this subset and how it is recruited to the PNCs I could potentially manipulate their effect in the PNC microenvironment to determine their mechanism of action in tumour initiation. Given their high level of *myd88* expression, it would also be interesting to know the role of MyD88 and, potentially, NF-κB signalling in these cells.

6 Final Discussion

Tumour development is a multi-stage process initiated by one or more somatic cells possessing genetic alterations which confer them proliferative advantage and invasive properties. These events are powered by both intrinsic mechanisms and by the microenvironment of the transformed cells.
Modelling such complex disease using experimental organisms provides an unprecedented opportunity to study tumour initiating events from the perspective of all responsible cells and signalling pathways to identify potential targets in preclinical studies for early detection and preventive therapies [357].

6.1 Establishment of a New Zebrafish Model for the Study of Tumour Initiation

As part of this project, a model of epithelial tumour initiation in zebrafish larval skin was developed. This model uses tissue specific, mosaic over-expression of the $HRas^{G12V}$ oncogene to drive tumour initiation. While one cannot identify, with certainty, the driving oncogene which initiated tumorigenesis in spontaneously developed tumours, increasing evidence places uncontrolled Ras signalling amongst the earliest events. Ras gene mutations are an early and frequently detected event in tumour lesions. Activating Ras mutations are amongst the most common tumour drivers, present in approximately one third of all human cancers [46]. Epigenetic alterations leading to constitutively active Ras signalling are even more frequent in skin cancer [130,358]. A great number of studies have previously shown the potential of oncogenic HRas and KRas to promote hyperplasia and tumour formation in transgenic mice and zebrafish models [160,172,174,213,228–231,357,359]. Therefore, understanding the consequences of the activation of Ras signalling is of extreme importance for understanding early tumorigenesis.
The inducible zebrafish PNC model with temporal and spatial control of oncogene expression allowed the early detection and study of PNC emergence and of the first events that initiate the process of tumour

development. Early work for this project comprised detailed observational studies of PNC phenotype progression and initial characterisation of the model. Analysis of PNC development allowed the observation of progressive cell morphology and behaviour alterations, vastly recognised as consequence of oncogene transformation. As such, PNCs exhibited increasing proliferation, epithelial cell plasticity and motility, DNA damage and cell death, in agreement with features of naturally occurring preneoplastic lesions.

Even though not immediately evident, PNCs developed into heterogeneous populations with distinct morphologies and behaviour. While some cells exhibited a round morphology, others developed a more elongated shape, presumably as a result of a more interactive behaviour. Given the multitude of downstream effectors of Ras signalling and their specific effect on distinct cellular mechanisms [24,66], it is possible that different cells exhibit distinct signalling networks, depending on the activation of a selective fraction of downstream effectors, which may be responsible for the heterogeneous PNC phenotype. However, the mechanisms whereby specific Ras effector pathways are preferentially activated are still poorly understood. Nevertheless, one cannot ignore the additional variability introduced by the transient approach for generating PNCs in this model, as cells can carry varying numbers of oncogene copies. Therefore, each larva often exhibits a PNC population with heterogeneous $HRas^{G12V}$ expression levels. Considering that Ras downstream signalling networks, the final signal output and, ultimately, the determination of a cell's fate can be greatly influenced by the intensity and duration of HRas signalling activity [24,31], it is likely that the variation in $HRas^{G12V}$ expression levels is partially driving PNC heterogeneity.

The possibility of inserting multiple copies of the HRas oncogene introduces an additional concern. As one would logically deduce, high oncogene copy number increases the aggressiveness of a transformed cell's phenotype [24,299,360]. Additionally, mutant allele copy gain is a well-documented required event for the progression to papilloma stage of tumour development [213,361]. Therefore, it is possible that some of the PNCs produced in this model develop a strong phenotype which does not mimic spontaneously arisen

preneoplastic lesions. Nevertheless, a stronger phenotype may speed up PNC progression allowing the succession of events which would naturally occur during the course of several years to be studied within an experimentally feasible timeline.

It should be noted that the very same features that allow for temporal and spatial resolution, limit the scope of this model to early stages of tumorigenesis. The design of this model requires constant treatment with 4-OHT for continuous expression of the oncogene. Given that long term treatment with 4-OHT is detrimental to normal zebrafish development and health, there is a limit as to how long it is possible to follow PNC progression without avoiding the adverse effects of this drug. Additionally, the oncogene is under the control of a keratinocyte specific promoter. Tumour progression is often associated with the alteration of cell fate decisions, as tumour cells develop plasticity and stemness [23,362]. As such, it is possible that oncogene expression is eventually silenced at later stages. In fact, progressive decrease in PNC fluorescence from 24hpi onwards was consistently observed throughout the project.

Taking all these limitations into account, a new improved mechanism for the generation of PNCs is currently under development in the Feng Laboratory. Nevertheless, the current model can be used to study many aspects of tumour initiation. As mentioned in this thesis, this model offers a platform for the study of cell competition, PNC plasticity, PNC survival and oncogene induced inflammation. Other aspects of tumour initiation, not mentioned here, but being explored by other members in the Feng Laboratory are mitochondrial and metabolic alterations, and oncogene-induced senescence.

6.2 Linking NF-κB with Tumour Promotion at Early Stages of Tumour Development

Following the observation of a strong inflammatory response to early stages of PNC emergence I set out to study the role of the NF-κB signalling pathway in the early stages of tumour development.

This model showed that PNCs promote a strong early activation of NF-κB signalling, however, the mechanisms for its activation are not yet fully elucidated.

From this study it is evident that NF-κB activity has an important role in PNC clonal expansion. Suppression of NF-κB activity in both PNCs and neutrophils, led to a lower proportion of proliferating cells. There are several mechanisms whereby NF-κB signalling can promote, either intrinsically or through paracrine effects, PNC proliferation and they have been discussed previously. To understand the importance of each of these mechanisms in this model, however, further studies blocking specific NF-κB dependent signals, are required. Nevertheless, globally, this effect strongly suggests that NF-κB activity is extremely important for the early stages of tumour promotion.

As it is evident in this study PNCs sustain increasing amounts of DNA damage. Previous studies have provided evidence that oncogene activation generates replicative stress, causing high incidence of DSBs [246]. DNA breaks often trigger a DNA damage response and p53-dependent cell cycle arrest, apoptosis or senescence, halting tumour progression [12,246,248]. Conversely, they also potentiate genomic instability and lead to deleterious mutations of critical tumour suppressor genes inactivating the DNA damage response and promoting tumour progression [12,248,258,259]. By stimulating DNA damaged cells to enter the cell cycle, NF-κB signalling can contribute to this effect by generating sequence rearrangements and point mutations which will be transmitted to daughter cells [80–82]. Therefore, NF-κB activation can increase the number of DNA damaged cells that accumulate oncogenic and tumour suppressor gene mutations, mediating progression of tumour development [85].

A related, well characterized, NF-κB mechanism of action, that is yet to be confirmed in this model, is its role in PNC survival [85,129,288], as well as the mutual antagonism of NF-κB and p53 activation [88,363]. As pre-cancerous lesions are often associated with a high incidence of apoptosis and senescence due to a p53-dependent response, it would be interesting to

evaluate the role of NF-κB in PNC survival and verify if its activation can contribute to PNC evasion of oncogene-induced senescence.

While the role of NF-κB in PNC proliferation is well established, the importance of this signalling pathway in establishing an inflammatory microenvironment is less evident. Analysis of neutrophil migratory behaviour allowed the finding that basal skin cell layer specific NF-κB inhibition affects neutrophil retention at the PNC areas but has little effect on its recruitment. This is inconsistent with a previous study showing considerably lower myeloid cell infiltration in mice with $p65^{-/-}$ tumour cells when compared to mice with WT tumour cells [129]. While the analysis shown here may be considerably underpowered, the different techniques used in the two studies may also be responsible for the contradictory results. Namely, the use of different model organisms and the mechanism for oncogenic Ras transformation: here I used oncogene transgenesis, contrary to the DMBA/TPA-induced carcinogenesis in the other report. A recent study has shown NF-κB signalling in different cell compartments of tumour microenvironment contribute differently for early tumour promotion. While tumour cell derived signalling enhanced epithelial turnover, myeloid cells contributed to production of tumour and stemness enhancing cytokines [135]. The report corroborates the findings described here. Nevertheless, further analysis of inflammatory cytokine and chemokine expression in both basal skin cell layer and neutrophil specific IκBSR needs to be done for a better understanding of these findings. With this analysis, identification of the PNC derived signal/s which promote close PNC-neutrophil interaction may also be possible.

As mentioned before, these issues will also be reassessed in a PNC specific IκBSR background for confirmation that the effects here observed are the consequence of PNC intrinsic NF-κB suppression.

Although not discussed here, the contribution of macrophages to tumour development is well established. Preliminary data have shown that PNCs also elicit a macrophage inflammatory response (data not shown), however the study of recruited macrophages in PNC progression has only recently been of interest in the Feng Laboratory. Considering previous reports, suggesting

tumour cells specific NF-κB activity is important for tumour evasion of immune surveillance by supressing macrophage cytotoxicity [288,291,364], it would be interesting to test if PNCs in this model exhibit a similar behaviour. Future directions will also involve the study of the effect of macrophage specific NF-κB suppression on PNC proliferation and ultimately early tumour development. The regulatory effect of NF-κB in PNC progression was evaluated using IκBSR as a suppressive mechanism. Even though IκBSR is widely used as a tool for inhibition of NF-κB activity, one has to consider the secondary consequences of over-expressing this protein. Since IκBα does not bind to all NF-κB subunits with the same affinity, IκBSR over-expression is likely to have an effect on the availability of different dimers and direct gene expression in an unclear way [365]. IκBSR could also mediate carcinogenesis in an NF-κB independent way. Several reports have shown IκBα can bind promoter sequences directly and regulate gene expression of Notch target genes [366] and Polycomb target genes [367] controlling differentiation and cancer in keratinocytes.

6.3 A Potential Model for the Study of Immature Granulocytes in Tumorigenesis

While studying neutrophil recruitment a new subset of neutrophils was observed being recruited to PNCs. These neutrophils exhibited a distinct behaviour from what had been observed previously, moving at a higher speed and lower capacity to be retained in contact with PNCs. The newly found subset of neutrophils had a characteristic decreased transcriptional activity of the neutrophil marker and was defined as $Myd88^{high}$ Lyz^{low}. Therefore, they were hypothesised to be immature granulocytes. While a more detailed characterization of this neutrophil subset is necessary, the analysis of their behaviour corroborates their presumed origin. Immature granulocytes are often found in circulation in tumour patients [348–350]. These cells are of particular interest as they are believed to support tumour dissemination by migrating to distant sites away from inflammation to mediate tumour spread [365]. They are also believed to mature at later stages of tumorigenesis into

MDSCs [349,350,352,354,355]. The study of the mechanisms that promote the premature release of immature granulocytes from the CHT and the chemotactic signals they respond to, as well as their effect on tumour promotion need to be addressed for a better understanding of the role of these cells in tumorigenesis.

6.4 Final Conclusion

Due to the limited availability of suitable platforms for the study of tumour initiation, the Feng Laboratory developed a new *in vivo* zebrafish model. The model, here characterized, allows for a non-invasive approach for the early detection of PNCs *in vivo* and the study of their interactions with the surrounding tissues. For the purposes of this project, I used this model to study the onset of an inflammatory microenvironment during PNC progression and the role of NF-κB as a potential regulator of inflammation. I was able to detect early activation of NF-κB signalling in PNCs and demonstrate its importance in PNC proliferation and promotion of an intimate interaction with recruited neutrophils. According to these results, recruited neutrophils also exhibit a trophic effect which is, at least partially, dependent on NF-κB signalling. While the mechanisms by which NF-κB activity promotes the effects here observed are not yet clear, these findings demonstrate the importance of this signalling pathway in the progression of this first stage of tumorigenesis. Finally, I provided evidence of heterogeneity within the recruited neutrophil population and the different behaviours they exhibit, setting the ground for future analysis of the specific role of different neutrophil subsets in tumour initiation.

7 Supplementary Figures

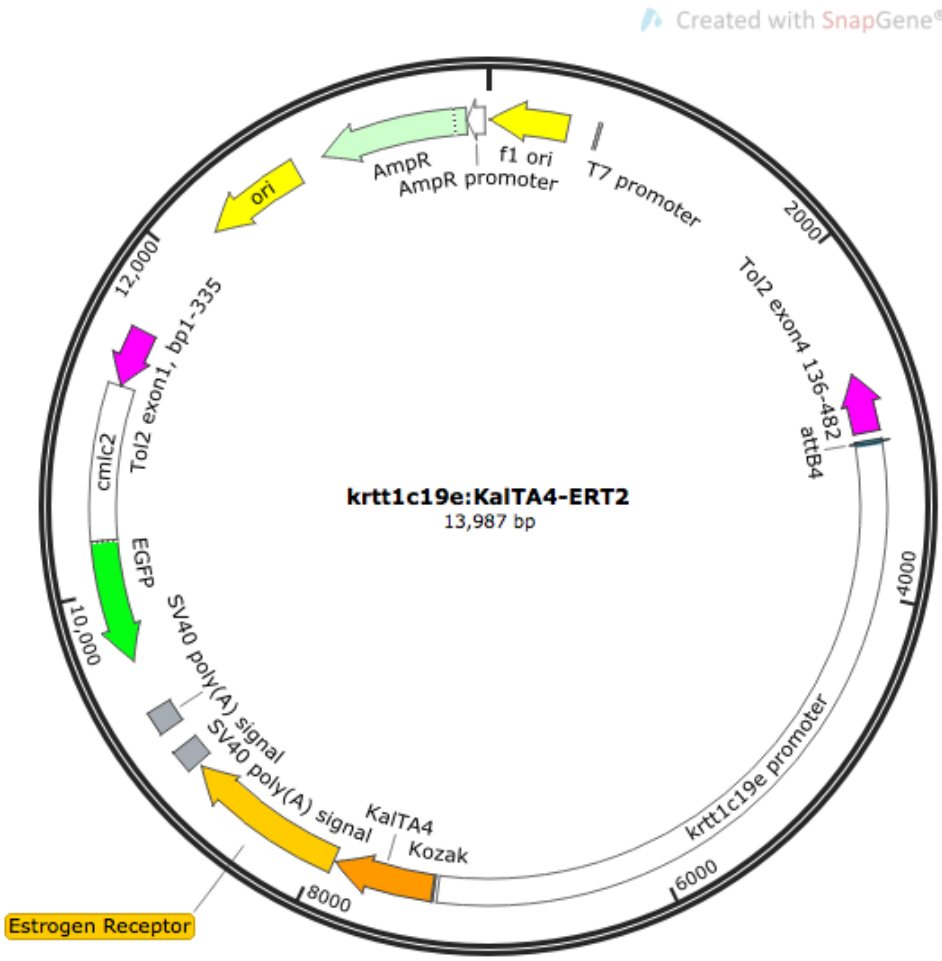

Supplementary Figure 1 Construct map for *krtt1c19e*:KalTA4-ER^{T2} used for generation of transgenic zebrafish line. Designed and generated by Thomas Ramezani (Yi Feng, The University of Edinburgh).

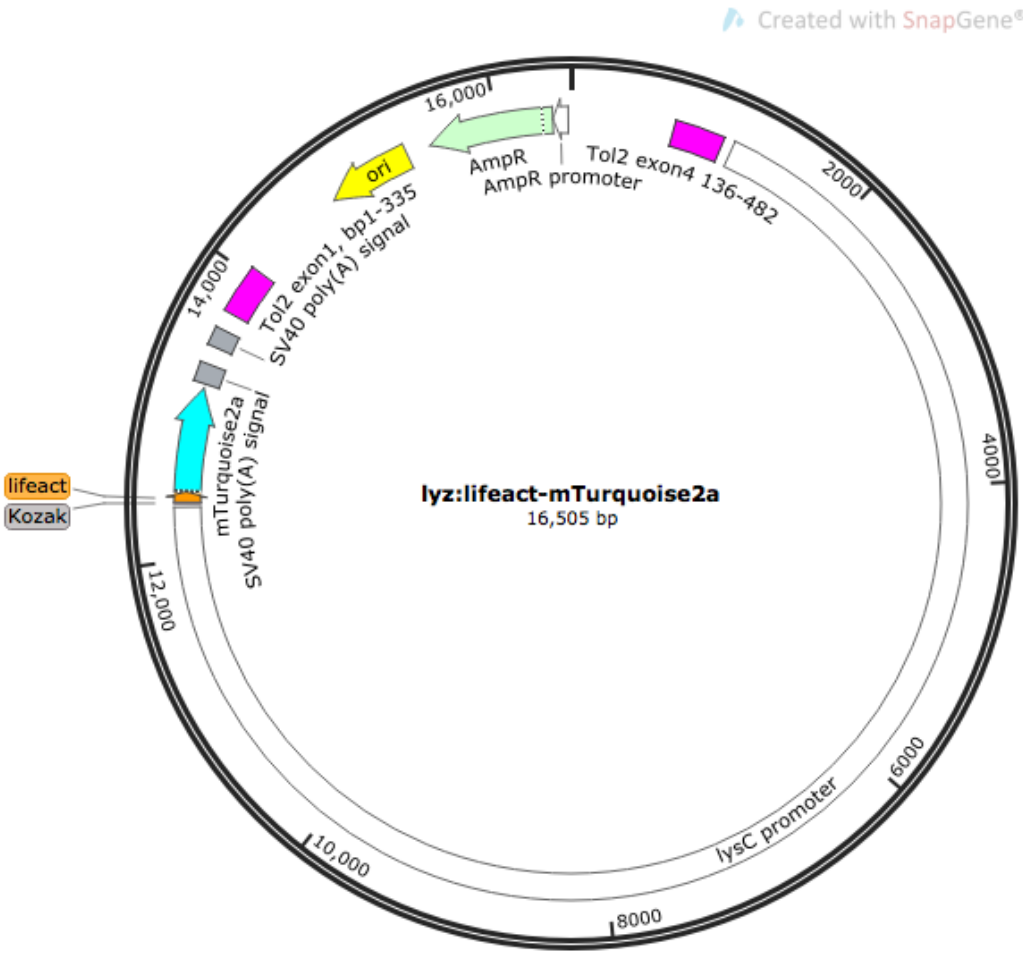

Supplementary Figure 2 Construct map for *lyz*:lifeact-mTurquoise2a used for generation of transgenic zebrafish line. Designed and generated by Thomas Ramezani (Yi Feng, The University of Edinburgh).

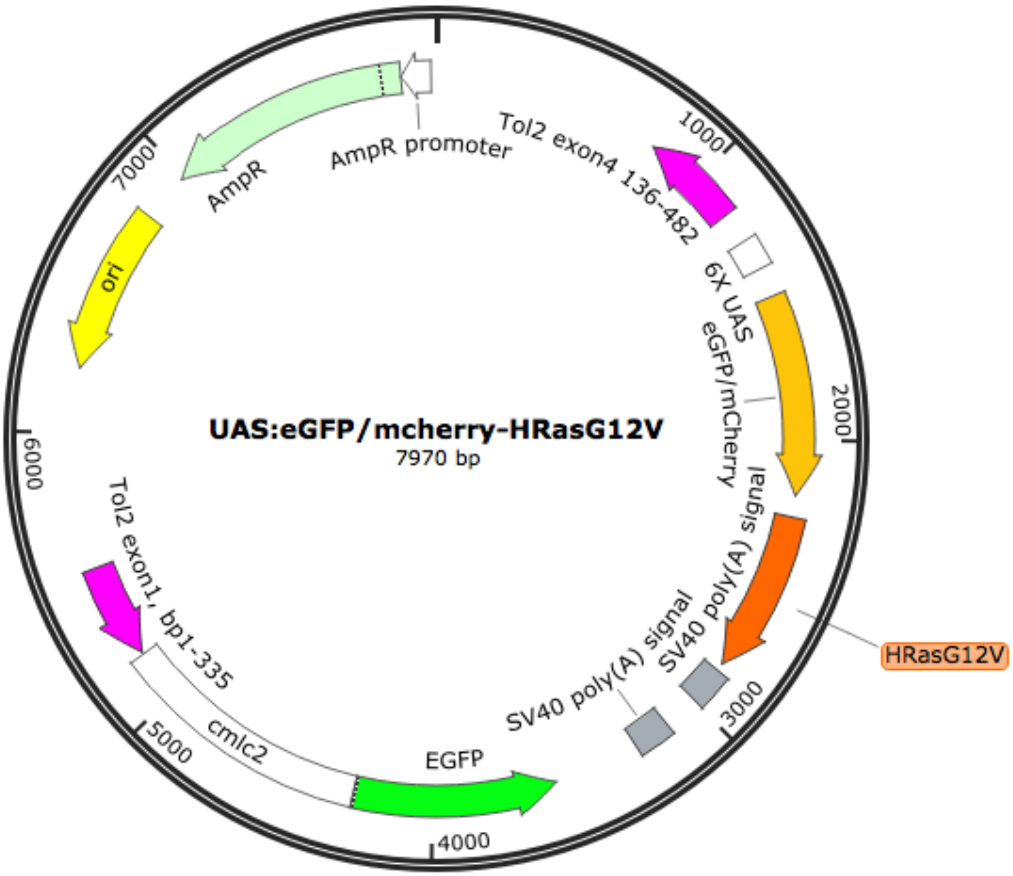

Supplementary Figure 3 Construct map for UAS:eGFP/mCherry-HRAS^{G12V} used for microinjection into one-cell-stage eggs of krtt1c19e:KalTA4-ER^{T2}. UAS:eGFP-HRAS^{G12V} designed and generated by Thomas Ramezani (Yi Feng, The University of Edinburgh).

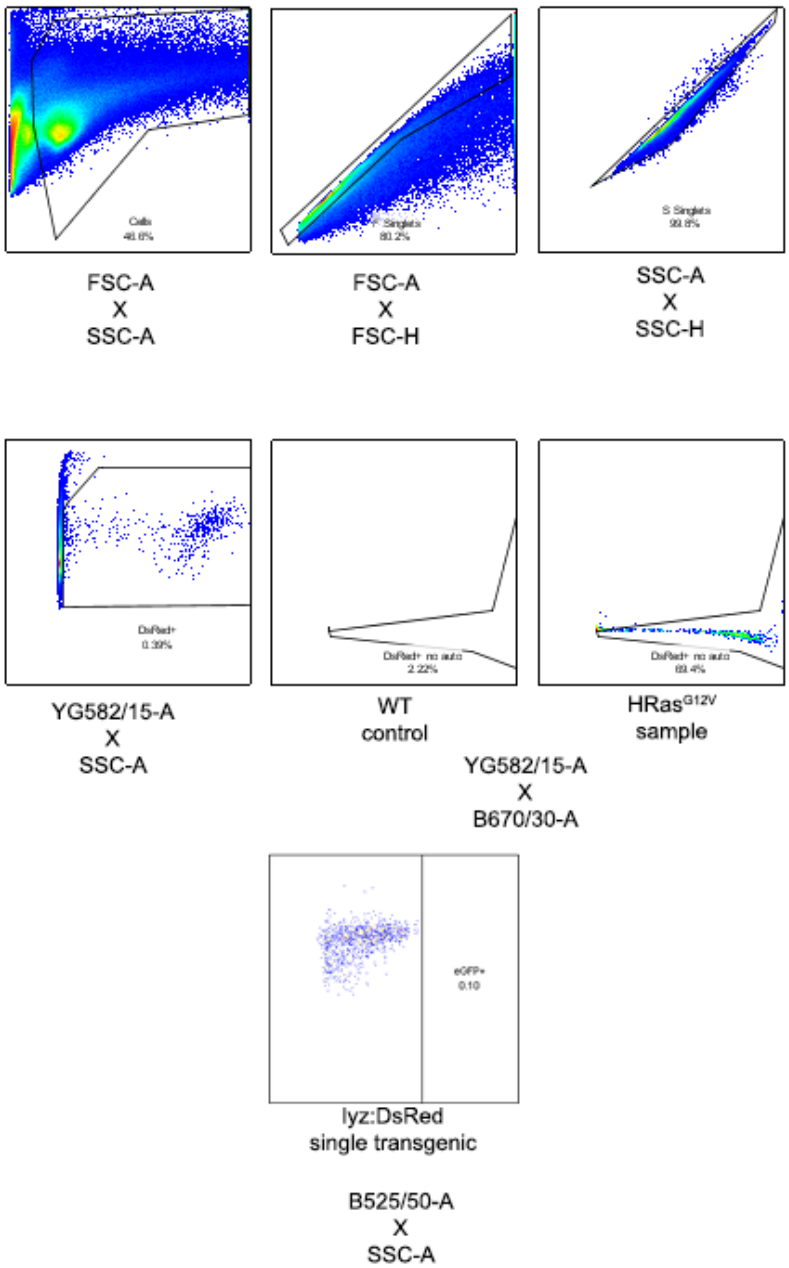

Supplementary Figure 4 Gating strategy for flow cytometry analysis of *lyz*:DsRed positive neutrophils in *Tg(NFκB:eGFP)* larvae. Following identification of fully dissociated single cells using FSC and SSC parameters in the detailed combinations, DsRed positive neutrophils were detected with YG582/15-A laser ($DsRed^{+}$). B670/30-A laser was used to exclude autofluorescence ($DsRed^{+}$ no auto). B525/50-A laser was used to detect eGFP positive cells.

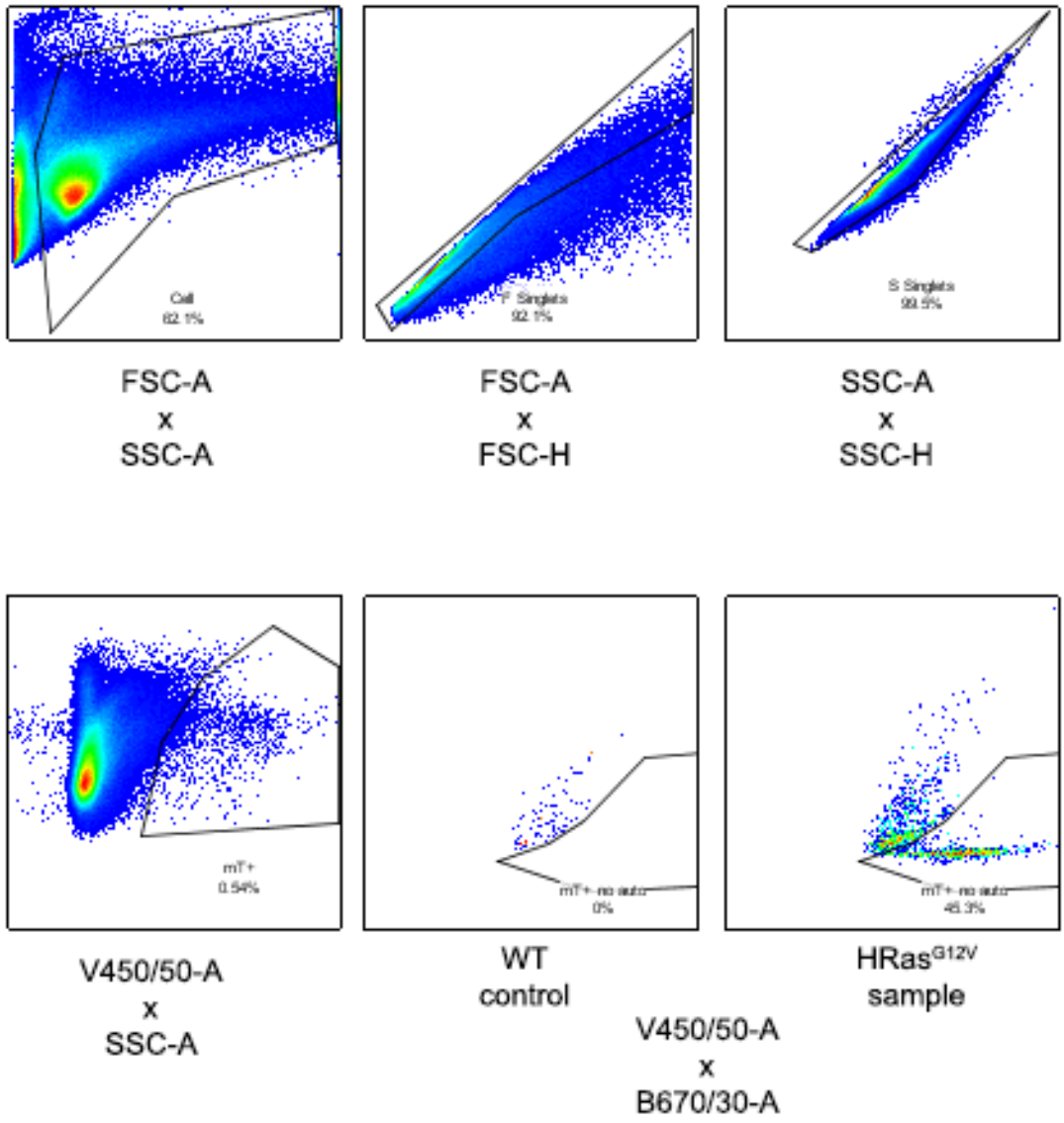

Supplementary Figure 5 Gating strategy for flow cytometry analysis of lyz:lifeact-mturquoise2a positive neutrophils in *Tg(myd88:DsRed2)* larvae. Following identification of fully dissociated single cells using FSC and SSC parameters in the detailed combinations, mTurquoise positive neutrophils were detected with V450/50-A laser (mT^+). B670/30-A laser was used to exclude autofluorescence (mT^+ no auto). YG582/15-A laser was used to detect DsRed positive cells.

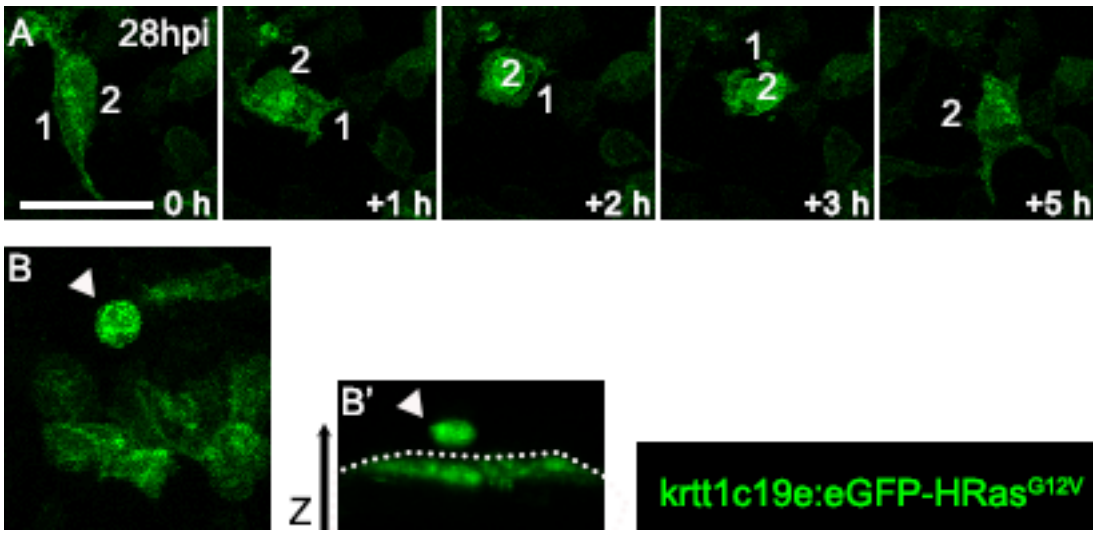

Supplementary Figure 6 PNC extrusion happens on rare occasions. A) Still images of a 5 hour long time-lapse video showing extensive interaction between two neighbouring PNCs. One PNC (2) is eventually extruded and sits on top of the other and eventually expands over the epithelium. B) Extruded cell (arrowhead) sits at the surface of the zebrafish larval skin (dotted line delineates basal skin layer) where it stays during a 3 hour long time-lapse video. Scale bar = 50 μm

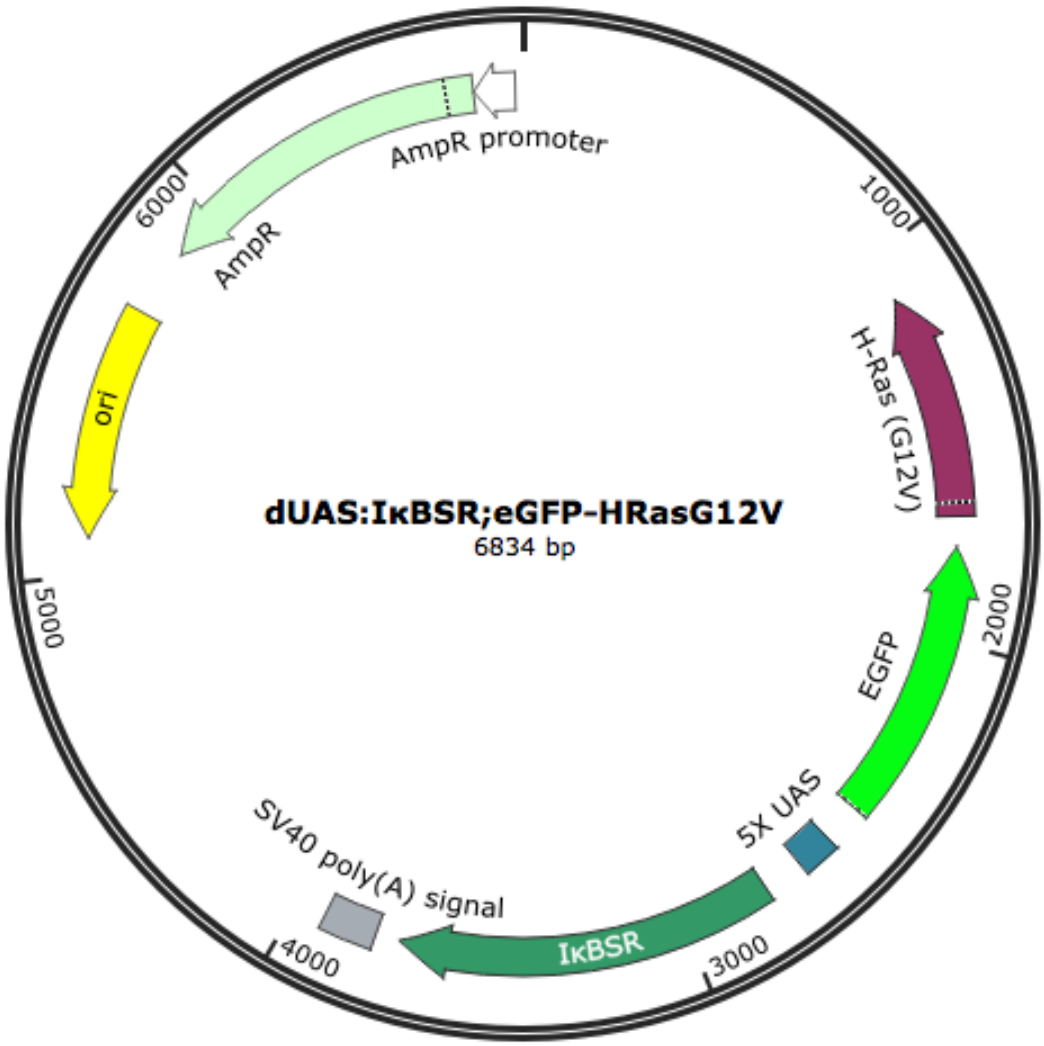

Supplementary Figure 7 Construct map for dUAS: IκBSR;eGFP-HRas^{G12V} to be used for microinjection into one-cell-stage eggs of krtt1c19e:KalTA4-ER^{T2}. Designed and generated by Nikolay Ogryzko (Yi Feng, The University of Edinburgh).

8 Bibliography

1. Cancer Research UK. Available at: https://www.cancerresearchuk.org/health-professional/cancer-statistics/worldwide-cancer/incidence [Accessed December 23, 2018].
2. Stratton, M.R., Campbell, P.J., and Futreal, P.A. (2009). The cancer genome. Nature *458*, 719–724.
3. American Cancer Society (2018). Cancer Facts & Figures 2018. Atlanta: American Cancer Society
4. Boveri, T. (1914). Zur Frage der Entstehung Maligner Tumoren (Gustav Fischer).
5. Grivennikov, S.I., Greten, F.R., and Karin, M. (2010). Immunity, Inflammation, and Cancer. Cell *140*, 883–899.
6. Ng, P.K.S., Li, J., Jeong, K.J., Shao, S., Chen, H., Tsang, Y.H., Sengupta, S., Wang, Z., Bhavana, V.H., Tran, R., *et al.* (2018). Systematic Functional Annotation of Somatic Mutations in Cancer. Cancer Cell *33*, 450-462.
7. Bailey, M.H., Tokheim, C., Porta-Pardo, E., Sengupta, S., Bertrand, D., Weerasinghe, A., Colaprico, A., Wendl, M.C., Kim, J., Reardon, B., *et al.* (2018). Comprehensive Characterization of Cancer Driver Genes and Mutations. Cell *173*, 371-385.
8. Sanchez-Vega, F., Mina, M., Armenia, J., Chatila, W.K., Luna, A., La, K.C., Dimitriadoy, S., Liu, D.L., Kantheti, H.S., Saghafinia, S., *et al.* (2018). Oncogenic Signaling Pathways in The Cancer Genome Atlas. Cell *173*, 321-337.
9. Cancer Research UK: New funding for early detection research. Available at: www.cancerresearchuk.org/funding-for-reseachers/research-features/2017-06-19-new-funding-for-early-detection-research [Accessed December 23, 2018].
10. National Cancer Institute: Early Detection Research Network. Available at: https://edrn.nci.nih.gov [Accessed December 23, 2018].
11. Loeb, L.A., Bielas, J.H., and Beckman, R.A. (2008). Cancers exhibit a

mutator phenotype: Clinical implications. Cancer Res. *68*, 3551–3557.

12. Negrini, S., Gorgoulis, V.G., and Halazonetis, T.D. (2010). Genomic instability an evolving hallmark of cancer. Nat. Rev. Mol. Cell Biol. *11*, 220–228.
13. Martincorena, I., and Campbell, P.J. (2015). Somatic mutation in cancer and normal cells. Science *349*, 1483–1489.
14. Cairns, J. (1975). Mutation selection and the natural history of cancer. Nature *255*, 197–200.
15. Nowell, P., and C., P. (1976). The clonal evolution of tumor cell populations. Science *194*, 23–28.
16. Lodish H, Berk A, Zipursky SL, et al. (2000) Molecular Cell Biology. 4th edition. New York: W. H. Freeman. Section 24.2, Proto-Oncogenes and Tumor-Suppressor Genes.
    Available at: https://www.ncbi.nlm.nih.gov/books/NBK21662/
17. Knijnenburg, T.A., Wang, L., Zimmermann, M.T., Chambwe, N., Gao, G.F., Cherniack, A.D., Fan, H., Shen, H., Way, G.P., Greene, C.S., *et al.* (2018). Genomic and Molecular Landscape of DNA Damage Repair Deficiency across The Cancer Genome Atlas. Cell Rep. *23*, 239-254.
18. Kandoth, C., McLellan, M.D., Vandin, F., Ye, K., Niu, B., Lu, C., Xie, M., Zhang, Q., McMichael, J.F., Wyczalkowski, M.A., *et al.* (2013). Mutational landscape and significance across 12 major cancer types. Nature *502*, 333–339.
19. Martincorena, I., Raine, K.M., Gerstung, M., Dawson, K.J., Haase, K., Van Loo, P., Davies, H., Stratton, M.R., and Campbell, P.J. (2017). Universal Patterns of Selection in Cancer and Somatic Tissues. Cell *171*, 1029-1041.
20. Hanahan, D., and Weinberg, R.A. (2000). The hallmarks of cancer. Cell *100*, 57–70.
21. Floor, S.L., Dumont, J.E., Maenhaut, C., and Raspe, E. (2012). Hallmarks of cancer: Of all cancer cells, all the time? Trends Mol. Med. *18*, 509–515.
22. Hanahan, D., and Coussens, L.M. (2012). Accessories to the Crime:

Functions of Cells Recruited to the Tumor Microenvironment. Cancer Cell *21*, 309–322.

23. Hanahan, D., and Weinberg, R.A. (2011). Hallmarks of Cancer: The Next Generation. Cell *144*, 646–674.
24. Schubbert, S., Shannon, K., and Bollag, G. (2007). Hyperactive Ras in developmental disorders and cancer. Nat. Rev. Cancer *7*, 295–308.
25. Hancock, J.F. (2003). Ras proteins: Different signals from different locations. Nat. Rev. Mol. Cell Biol. *4*, 373–384.
26. Simanshu, D.K., Nissley, D. V., and McCormick, F. (2017). RAS Proteins and Their Regulators in Human Disease. Cell *170*, 17–33.
27. Cherfils, J., and Zeghouf, M. (2013). Regulation of Small GTPases by GEFs, GAPs, and GDIs. Physiol. Rev. *93*, 269–309.
28. Boguski, M.S., and McCormick, F. (1993). Proteins regulating Ras and its relatives. Nature *366*, 643–654.
29. Boriack-Sjodin, P.A., Margarit, S.M., Bar-Sagi, D., and Kuriyan, J. (1998). The structural basis of the activation of Ras by Sos. Nature *394*, 337–343.
30. Ahmadian, M.R., Stege, P., Scheffzek, K., and Wittinghofer, A. (1997). Confirmation of the arginine-finger hypothesis for the GAP-stimulated GTP-hydrolysis reaction of Ras. Nat. Struct. Biol. *4*, 686–689.
31. Marshall, C.J. (1995). Specificity of receptor tyrosine kinase signaling: Transient versus sustained extracellular signal-regulated kinase activation. Cell *80*, 179–185.
32. Margolis, B., and Skolnik, E.Y. (1994). Activation of Ras by receptor tyrosine kinases. J. Am. Soc. Nephrol. *5*, 1288–99.
33. Kyriakis, J.M., App, H., Zhang, X., Banerjee, P., Brautigan, D.L., Rapp, U.R., and Avruch, J. (1992). Raf-1 activates MAP kinase-kinase. Nature *358*, 417–421.
34. Moodie, S., Willumsen, B., Weber, M., and Wolfman, A. (1993). Complexes of Ras.GTP with Raf-1 and mitogen-activated protein kinase kinase. Science *260*, 1658–1661.
35. Vojtek, A.B., Hollenberg, S.M., and Cooper, J.A. (1993). Mammalian

Ras interacts directly with the serine/threonine kinase raf. Cell *74*, 205–214.

36. Rajalingam, K., Schreck, R., Rapp, U.R., and Albert, Š. (2007). Ras oncogenes and their downstream targets. Biochim. Biophys. Acta - Mol. Cell Res. *1773*, 1177–1195.
37. Rodriguez-Viciana, P., Warne, P.H., Dhand, R., Vanhaesebroeck, B., Gout, I., Fry, M.J., Waterfield, M.D., and Downward, J. (1994). Phosphatidylinositol-3-OH kinase direct target of Ras. Nature *370*, 527–532.
38. Kodaki, T., Woscholski, R., Hallberg, B., Rodriguez-Viciana Julian Downward, P., and Parker, P.J. (1994). The activation of phosphatidylinositol 3-kinase by Ras. Curr. Biol. *4*, 798–806.
39. Wolthuis, R.M.F., Zwartkruis, F., Moen, T.C., and Bos, J.L. (1998). Ras-dependent activation of the small GTPase Ral. Curr. Biol. *8*, 471–474.
40. Lambert, J.M., Lambert, Q.T., Reuther, G.W., Malliri, A., Siderovski, D.P., Sondek, J., Collard, J.G., and Der, C.J. (2002). Tiam1 mediates Ras activation of Rac by a PI(3)K-independent mechanism. Nat. Cell Biol. *4*, 621–625.
41. Kelley, G.G. (2001). Phospholipase Cepsilon: a novel Ras effector. EMBO J. *20*, 743–754.
42. Mo, S.P., Coulson, J.M., and Prior, I.A. (2018). RAS variant signalling. Biochem. Soc. Trans. *0*, 1–8.
43. Abankwa, D., Gorfe, A.A., and Hancock, J.F. (2007). Ras nanoclusters: Molecular structure and assembly. Semin. Cell Dev. Biol. *18*, 599–607.
44. Yan, J., Roy, S., Apolloni, A., Lane, A., and Hancock, J.F. (1998). Ras isoforms vary in their ability to activate Raf-1 and phosphoinositide 3-kinase. J. Biol. Chem. *273*, 24052–24056.
45. Newlaczyl, A.U., Coulson, J.M., and Prior, I.A. (2017). Quantification of spatiotemporal patterns of Ras isoform expression during development. Sci. Rep. *7*, 1–7.
46. Li, S., Balmain, A., and Counter, C.M. (2018). A model for RAS mutation patterns in cancers: finding the sweet spot. Nat. Rev. Cancer *18*, 767–

777.

47. Scheffzek, K. (1997). The Ras-RasGAP Complex: Structural Basis for GTPase Activation and Its Loss in Oncogenic Ras Mutants. Science (80-.). *277*, 333–338.
48. the C.O.S.M.I.C. v87 KRAS Gene - Somatic Mutations in Cancer. Available at: https://cancer.sanger.ac.uk/cosmic/gene/analysis?ln=KRAS [Accessed December 30, 2018].
49. the C.O.S.M.I.C. v87 NRAS Gene - Somatic Mutations in Cancer. Available at: https://cancer.sanger.ac.uk/cosmic/gene/analysis?ln=NRAS. [Accessed December 30, 2018].
50. the C.O.S.M.I.C. v87 HRAS Gene - Somatic Mutations in Cancer. Available at: https://cancer.sanger.ac.uk/cosmic/gene/analysis?ln=HRAS. [Accessed December 30, 2018].
51. Feramisco, J.R., Gross, M., Kamata, T., Rosenberg, M., and Sweet, R.W. (1984). Microinjection of the oncogene form of the human H-ras (t-24) protein results in rapid proliferation of quiescent cells. Cell *38*, 109–117.
52. Stacey, D.W., and Kung, H.-F. (1984). Transformation of NIH 3T3 cells by microinjection of Ha-ras p21 protein. Nature *310*, 508–511.
53. Gille, H., and Downward, J. (1999). Multiple Ras effector pathways contribute to G1 cell cycle progression. J. Biol. Chem. *274*, 22033–22040.
54. Diehl, J.A., Cheng, M., Roussel, M.F., and Sherr, C.J. (1998). Glycogen synthase kinase-3beta regulates cyclin D1 proteolysis and subcellular localization. Genes Dev. *12*, 3499–3511.
55. Yu, Q., Geng, Y., and Sicinski, P. (2001). Specific protection against breast cancers by cyclin D1 ablation. Nature *411*, 1017–1021.
56. Robles, A.I., Rodriguez-Puebla, M.L., Glick, A.B., Trempus, C., Hansen, L., Sicinski, P., Tennant, R.W., Weinberg, R.A., Yuspa, S.H., and Conti, C.J. (1998). Reduced skin tumor development in cyclin D1-deficient mice highlights the oncogenic ras pathway in vivo. Genes Dev. *12*, 2469–2474.

57. Choi, Y.J., Li, X., Hydbring, P., Sanda, T., Stefano, J., Christie, A.L., Signoretti, S., Look, A.T., Kung, A.L., von Boehmer, H., *et al.* (2012). The Requirement for Cyclin D Function in Tumor Maintenance. Cancer Cell *22*, 438–451.
58. McCarthy, S.A., Samuels, M.L., Pritchard, C.A., Abraham, J.A., and McMahon, M. (1995). Rapid induction of heparin-binding epidermal growth factor/diphtheria toxin receptor expression by Raf and Ras oncogenes. Genes Dev. *9*, 1953–1964.
59. Gangarosa, L.M., Sizemore, N., Graves-Deal, R., Oldham, S.M., Der, C.J., and Coffey, R.J. (1997). A Raf-independent epidermal growth factor receptor autocrine loop is necessary for Ras transformation of rat intestinal epithelial cells. J. Biol. Chem. *272*, 18926–18931.
60. Wu, L., Nam, Y.J., Kung, G., Crow, M.T., and Kitsis, R.N. (2010). Induction of the apoptosis inhibitor ARC by Ras in human cancers. J. Biol. Chem. *285*, 19235–19245.
61. Ahmed, M.M., Sheldon, D., Fruitwala, M.A., Venkatasubbarao, K., Lee, E.Y., Gupta, S., Wood, C., Mohiuddin, M., and Strodel, W.E. (2008). Downregulation of PAR-4, a pro-apoptotic gene, in pancreatic tumors harboring K-ras mutation. Int. J. Cancer *122*, 63–70.
62. Kennedy, N.J. (2003). Suppression of Ras-stimulated transformation by the JNK signal transduction pathway. Genes Dev. *17*, 629–637.
63. Vos, M.D., Ellis, C.A., Bell, A., Birrer, M.J., and Clark, G.J. (2000). Ras uses the novel tumor suppressor RASSF1 as an effector to mediate apoptosis. J. Biol. Chem. *275*, 35669–35672.
64. Fisher, G.H., Wellen, S.L., Klimstra, D., Lenczowski, J.M., Tichelaar, J.W., Lizak, M.J., Whitsett, J.A., Koretsky, A., and Varmus, H.E. (2001). Induction and apoptotic regression of lung adenocarcinomas by regulation of a K-Ras transgene in the presence and absence of tumor suppressor genes. Genes Dev. *15*, 3249–3262.
65. Chin, L., DePinho#, R.A., Tam, A., Pomerantz, J., Wong, M., Holash, J., Bardeesy, N., Shen, Q., O'Hagan, R., Pantginis, J., *et al.* (1999). Essential role for oncogenic Ras in tumour maintenance. Nature *400*,

468–472.

66. Giehl, K. (2005). Oncogenic Ras in tumour progression and metastasis. Biol. Chem. *386*, 193–205.
67. Liu, J., Yang, G., Thompson-Lanza, J.A., Glassman, A., Hayes, K., Patterson, A., Marquez, R.T., Auersperg, N., Yu, Y., Hahn, W.C., *et al.* (2004). A Genetically Defined Model for Human Ovarian Cancer. Cancer Res. *64*, 1655–1663.
68. Ancrile, B., Lim, K.H., and Counter, C.M. (2007). Oncogenic Ras-induced secretion of IL6 is required for tumorigenesis. Genes Dev. *21*, 1714–1719.
69. Sparmann, A., and Bar-Sagi, D. (2004). Ras-induced interleukin-8 expression plays a critical role in tumor growth and angiogenesis. Cancer Cell *6*, 447–458.
70. Cohen, T., Nahari, D., Cerem, L.W., Neufeld, G., and Levin, B.Z. (1996). Interleukin 6 induces the expression of vascular endothelial growth factor. J. Biol. Chem. *271*, 736–741.
71. Egeblad, M., and Werb, Z. (2002). New functions for the matrix metalloproteinases in cancer progression. Nat. Rev. Cancer *2*, 161–174.
72. Prete, A. Del, Allavena, P., Santoro, G., Fumarulo, R., Corsi, M.M., and Mantovani, A. (2011). Molecular pathways in cancer-related inflammation. Biochem. Medica *21*, 264–275.
73. Borrello, M.G., Alberti, L., Fischer, A., Degl'Innocenti, D., Ferrario, C., Gariboldi, M., Marchesi, F., Allavena, P., Greco, A., Collini, P., *et al.* (2005). Induction of a proinflammatory program in normal human thyrocytes by the RET/PTC1 oncogene. Proc. Natl. Acad. Sci. *102*, 14825–14830.
74. Ji, H., Houghton, A.M., Mariani, T.J., Perera, S., Kim, C.B., Padera, R., Tonon, G., McNamara, K., Marconcini, L.A., Hezel, A., *et al.* (2006). K-ras activation generates an inflammatory response in lung tumors. Oncogene *25*, 2105–2112.
75. Borrello, M.G., Degl'Innocenti, D., and Pierotti, M. a. (2008). Inflammation and cancer: The oncogene-driven connection. Cancer

Lett. *267*, 262–270.

76. Ancrile, B.B., Hayer, K.M.O., and Counter, C.M. (2008). Oncogenic Ras-Induced Expression of Cytokines. Mol Interv *1*, 22–27.
77. Shive, H.R., West, R.R., Embree, L.J., Sexton, J.M., and Hickstein, D.D. (2015). Expression of KRAS G12V in Zebrafish Gills Induces Hyperplasia and CXCL8 -Associated Inflammation. Zebrafish *12*, 221–229.
78. Grivennikov, S.I., Wang, K., Mucida, D., Stewart, C.A., Schnabl, B., Jauch, D., Taniguchi, K., Yu, G.-Y., Österreicher, C.H., Hung, K.E., *et al.* (2012). Adenoma-linked barrier defects and microbial products drive IL-23/IL-17-mediated tumour growth. Nature *491*, 254–258.
79. Ulrich, C.M., Bigler, J., and Potter, J.D. (2006). Non-steroidal anti-inflammatory drugs for cancer prevention: promise, perils and pharmacogenetics. Nat. Rev. Cancer *6*, 130–140.
80. Colotta, F., Allavena, P., Sica, A., Garlanda, C., and Mantovani, A. (2009). Cancer-related inflammation, the seventh hallmark of cancer: Links to genetic instability. Carcinogenesis *30*, 1073–1081.
81. Lin, R., Xiao, D., Guo, Y., Tian, D., Yun, H., Chen, D., and Su, M. (2015). Chronic inflammation-related DNA damage response: a driving force of gastric cardia carcinogenesis. Oncotarget *6*, 2856–64.
82. Kiraly, O., Gong, G., Olipitz, W., Muthupalani, S., and Engelward, B.P. (2015). Inflammation-Induced Cell Proliferation Potentiates DNA Damage-Induced Mutations In Vivo. PLoS Genet. *11*, 1–24.
83. Ostrand-Rosenberg, S. (2008). Immune surveillance: a balance between protumor and antitumor immunity. Curr. Opin. Genet. Dev. *18*, 11–18.
84. Pahl, H.L. (1999). Activators and target genes of Rel/ NFκB transcription factors. Oncogene *18*, 6853–6866.
85. Taniguchi, K., and Karin, M. (2018). NFκB, inflammation, immunity and cancer: Coming of age. Nat. Rev. Immunol. *18*, 309–324. Available at: http://dx.doi.org/10.1038/nri.2017.142.
86. Xia, L., Tan, S., Zhou, Y., Lin, J., Wang, H., Oyang, L., Tian, Y., Liu, L.,

Su, M., Wang, H., *et al.* (2018). Role of the NFκB-signaling pathway in cancer. Onco. Targets. Ther. *11*, 2063–2073.

87. Zhong, H., May, M.J., Jimi, E., and Ghosh, S. (2002). The phosphorylation status of nuclear NF-κB determines its association with CBP/p300 or HDAC-1. Mol. Cell *9*, 625–636.
88. Pal, S., Bhattacharjee, A., Ali, A., Mandal, N.C., Mandal, S.C., and Pal, M. (2014). Chronic inflammation and cancer: potential chemoprevention through nuclear factor kappa B and p53 mutual antagonism. J. Inflamm. *11*, 1–28.
89. Wang, V.Y.F., Huang, W., Asagiri, M., Spann, N., Hoffmann, A., Glass, C., and Ghosh, G. (2012). The Transcriptional Specificity of NF-κB Dimers Is Coded within the κB DNA Response Elements. Cell Rep. *2*, 824–839.
90. Siggers, T., Chang, A.B., Teixeira, A., Wong, D., Williams, K.J., Ahmed, B., Ragoussis, J., Udalova, I.A., Smale, S.T., and Bulyk, M.L. (2012). Principles of dimer-specific gene regulation revealed by a comprehensive characterization of NF-κB family DNA binding. Nat. Immunol. *13*, 95–102.
91. Bonizzi, G., and Karin, M. (2004). The two NF-κB activation pathways and their role in innate and adaptive immunity. Trends Immunol. *25*, 280–288.
92. Xiao, G., Harhaj, E.W., and Sun, S.-C. (2001). NF-κB-Inducing Kinase Regulates the Processing of NF-κB2 p100. Mol. Cell *7*, 401–409.
93. Karin, M., and Greten, F.R. (2005). NF-κB: Linking inflammation and immunity to cancer development and progression. Nat. Rev. Immunol. *5*, 749–759.
94. Rothwarf, D., Zandi, E., Natoli, G., and Karin, M. (1998). IKK-γ is an essential regulatory subunit of the IκB kinase complex. Nature *395*, 297–300.
95. Zandi, E., Rothwarf, D.M., Delhase, M., Hayakawa, M., Karin, M., Novack, D.V., Yin, L., Hagen-Stapleton, A., Schreiber, R.D., Goeddel, D. V, *et al.* (1997). The IκB Kinase Complex (IKK) Contains Two Kinase

Subunits, IKKα and IKKβ, Necessary for IκB Phosphorylation and NF-κB Activation. Cell *91*, 243–252.

96. Karin, M., and Ben-Neriah, Y. (2000). Phosphorylation Meets Ubiquitination: The Control of NF-κB Activity. Annu. Rev. Immunol. *18*, 621–663.
97. Senftleben, U., Cao, Y., Xiao, G., Greten, F.R., Krähn, G., Bonizzi, G., Chen, Y., Hu, Y., Fong, A., Sun, S.C., *et al.* (2001). Activation by IKKalpha of a second, evolutionary conserved, NF-kappa B signaling pathway. Science *293*, 1495–1499.
98. Cildir, G., Low, K.C., and Tergaonkar, V. (2016). Noncanonical NF-κB Signaling in Health and Disease. Trends Mol. Med. *22*, 414–429.
99. Adachi, O., Kawai, T., Takeda, K., Matsumoto, M., Tsutsui, H., Sakagami, M., Nakanishi, K., and Akira, S. (1998). Targeted Disruption of the MyD88 Gene Results in Loss of IL-1- and IL-18-Mediated Function. Immunity *9*, 143–150.
100. Burns, K., Martinon, F., Esslinger, C., Pahl, H., Schneider, P., Bodmer, J.-L., Di Marco, F., French, L., and Tschopp, J. (1998). MyD88, an Adapter Protein Involved in Interleukin-1 Signaling. J. Biol. Chem. *273*, 12203–12209.
101. Medzhitov, R., Preston-Hurlburt, P., Kopp, E., Stadlen, A., Chen, C., Ghosh, S., and Janeway, C.A. (1998). MyD88 is an adaptor protein in the hToll/IL-1 receptor family signaling pathways. Mol. Cell *2*, 253–258.
102. Newton, K., and Dixit, V.M. (2012). Signaling in innate immunity and inflammation. Cold Spring Harb. Perspect. Biol. *4*.
103. Lin, S.-C., Lo, Y.-C., and Wu, H. (2010). Helical assembly in the MyD88-IRAK4-IRAK2 complex in TLR/IL-1R signalling. Nature *465*, 885–890.
104. Tseng, P., Matsuzawa, A., Zhang, W., Mino, T., Vignali, D.A.A., and Karin, M. (2009). Different modes of ubiquitination of the adaptor TRAF3 selectively activate the expression of type I interferons and proinflammatory cytokines. Nat. Immunol. *11*, 70–75.
105. Laplantine, E., Fontan, E., Chiaravalli, J., Agou, F., Lopez, T., Lakisic, G., Ve, M., and Israe, A. (2009). NEMO specifically recognizes K63-

linked ubiquitin-binding domain. *28*, 2885–2895.

106. Xu, G., Lo, Y., Li, Q., Napolitano, G., Wu, X., Jiang, X., Dreano, M., Karin, M., and Wu, H. (2011). Crystal structure of inhibitor of κB kinase β. Nature *472*, 325–330.
107. Chen, Z.J. (2012). Ubiquitination in signaling to and activation of IKK. 95–106.
108. Gilmore, T.D. (2003). The Re1/NF-kappa B/I kappa B signal transduction pathway and cancer. Cancer Treat. Res. *115*, 241–265.
109. Neri, A., Chang, C.C., Lombardi, L., Salina, M., Corradini, P., Maiolo, A.T., Chaganti, R.S., and Dalla-Favera, R. (1991). B cell lymphoma-associated chromosomal translocation involves candidate oncogene lyt-10, homologous to NF-kappa B p50. Cell *67*, 1075–87.
110. Franzoso, G., Bours, V., Park, S., Tomfta-Yamaguchi, M., Kelly, K., and Siebenlist, U. (1992). The candidate oncoprotein Bcl-3 is an antagonist of pSO/NF-κB-mediated inhibition. Nature *359*, 339–342.
111. Reuther, J.Y., Reuther, G.W., Cortez, D., Pendergast, A.M., and Baldwin, A.S. (1998). A requirement for NF-kappaB activation in Bcr-Abl-mediated transformation. Genes Dev. *12*, 968–81.
112. Staudt, L.M. (2010). Oncogenic Activation of NF-κB. Cold Spring Harb Perspect Biol. 2:a000109.
113. Starczynowski, D.T., Lockwood, W.W., Deléhouzée, S., Chari, R., Wegrzyn, J., Fuller, M., Tsao, M., Lam, S., Gazdar, A.F., Lam, W.L., *et al.* (2011). TRAF6 is an amplified oncogene bridging the RAS and NF-κB pathways in human lung cancer. *121*, 4095–4105.
114. Weber, A.N.R., Cardona, Y., Özcan, G., Christian, Ç.H., Pezzutto, A., and Wolz, O.O. (2018). Oncogenic MYD88 mutations in lymphoma: novel insights and therapeutic possibilities. Cancer Immunol. Immunother. *67*, 1797–1807.
115. Zhu, S., Jin, J., Gokhale, S., Lu, A.M., and Shan, H. (2018). Genetic Alterations of TRAF Proteins in Human Cancers. *9*, 1–30.
116. Ben-Neriah, Y., and Karin, M. (2011). Inflammation meets cancer, with NF-κB as the matchmaker. Nat. Immunol. *12*, 715–723.

117. Bai, D., Ueno, L., and Vogt, P.K. (2009). Akt-mediated regulation of NFκB and the essentialness of NFκB for the oncogenicity of PI3K and Akt. Int. J. Cancer *125*, 2863–2870.
118. Lee, K.W., Kim, M.S., Kang, N.J., Kim, D.H., Surh, Y.J., Lee, H.J., and Moon, A. (2006). H-Ras selectively up-regulates MMP-9 and COX-2 through activation of EKK1/2 and NF-κB: An implication for invasive phenotype in rat liver epithelial cells. Int. J. Cancer *119*, 1767–1775.
119. Mahanivong, C., Chen, H.M., Yee, S.W., Pan, Z.K., Dong, Z., and Huang, S. (2008). Protein kinase Cα-CARMA3 signaling axis links Ras to NF-κB for lysophosphatidic acid-induced urokinase plasminogen activator expression in ovarian cancer cells. Oncogene *27*, 1273–1280.
120. Mayo, M.W., Wang, C.Y., Cogswell, P.C., Rogers-Graham, K.S., Lowe, S.W., Der, C.J., and Baldwin, A.S. (1997). Requirement of NF-kappaB activation to suppress p53-independent apoptosis induced by oncogenic Ras. Science *278*, 1812–5.
121. Chien, Y., Kim, S., Bumeister, R., Loo, Y.M., Kwon, S.W., Johnson, C.L., Balakireva, M.G., Romeo, Y., Kopelovich, L., Gale, M., *et al.* (2006). RalB GTPase-Mediated Activation of the IκB Family Kinase TBK1 Couples Innate Immune Signaling to Tumor Cell Survival. Cell *127*, 157–170.
122. Hill, C., and Carolina, N. (1993). Gene Expression by Diverse Inducers of Nuclear Factor κB Requires Raf-l. Science 17676–17679.
123. Finco, T.S., Westwick, J.K., Norris, J.L., Beg, A.A., Der, C.J., and Baldwin, A.S. (1997). Oncogenic Ha-Ras-induced Signaling Activates NF-κB Transcriptional Activity, Which Is Required for Cellular Transformation. J. Biol. Chem. *272*, 24113–24116.
124. Montaner, S., Perona, R., Saniger, L., and Lacal, J.C. (1998). Multiple signalling pathways lead to the activation of the nuclear factor κB by the Rho family of GTPases. J. Biol. Chem. *273*, 12779–12785.
125. Joneson, T.O.M. (1999). Suppression of Ras-Induced Apoptosis by the Rac GTPase. *19*, 5892–5901.
126. Bassères, D.S., Ebbs, A., Levantini, E., and Baldwin, A.S. (2010).

Requirement of the NF-κB subunit p65/RelA for K-Ras-induced lung tumorigenesis. Cancer Res. *70*, 3537–3546.

127. Meylan, E., Dooley, A.L., Feldser, D.M., Shen, L., Turk, E., Ouyang, C., and Jacks, T. (2009). Requirement for NF-κB signalling in a mouse model of lung adenocarcinoma. Nature *462*, 104–107.
128. Poligone, B., Hayden, M.S., Chen, L., Pentland, A.P., Jimi, E., and Ghosh, S. (2013). A role for NF-κB activity in skin hyperplasia and the development of keratoacanthomata in mice. PLoS One *8*, 1–12.
129. Kim, C., and Pasparakis, M. (2014). Epidermal p65/NF-κB signalling is essential for skin carcinogenesis. EMBO Mol. Med. *6*, 970–983.
130. Cataisson, C., Salcedo, R., Hakim, S., Moffitt, B.A., Wright, L., Yi, M., Stephens, R., Dai, R.-M., Lyakh, L., Schenten, D., *et al.* (2012). IL-1R–MyD88 signaling in keratinocyte transformation and carcinogenesis. J. Exp. Med. *209*, 1689–1702.
131. Erez, N., Truitt, M., Olson, P., and Hanahan, D. (2010). Cancer-Associated Fibroblasts Are Activated in Incipient Neoplasia to Orchestrate Tumor-Promoting Inflammation in an NF-κB-Dependent Manner. Cancer Cell *17*, 135–147.
132. Rakoff-Nahoum, S., and Medzhitov, R. (2007). Regulation of Spontaneous Intestinal Tumorigenesis Through the Adaptor Protein MyD88. Science *317*, 124–127.
133. Fearon, E.R., and Vogelstein, B. (1990). A genetic model for colorectal tumorigenesis. Cell *61*, 759–767.
134. Kinzler, K.W., and Vogelstein, B. (1996). Lessons from Hereditary Colorectal Cancer. Cell *87*, 159–170.
135. Holtorf, A., Conrad, A., Holzmann, B., and Janssen, K.-P. (2018). Cell-type specific MyD88 signaling is required for intestinal tumor initiation and progression to malignancy. Oncoimmunology *7*, e1466770.
136. Wang, K., Kim, M.K., Di Caro, G., Wong, J., Shalapour, S., Wan, J., Zhang, W., Zhong, Z., Sanchez-Lopez, E., Wu, L., *et al.* (2014). Interleukin-17 Receptor A Signaling in Transformed Enterocytes Promotes Early Colorectal Tumorigenesis. Immunity *41*, 1052–1063.

137. Tu, S., Bhagat, G., Cui, G., Takaishi, S., Kurt-Jones, E.A., Rickman, B., Betz, K.S., Penz-Oesterreicher, M., Bjorkdahl, O., Fox, J.G., *et al.* (2008). Overexpression of Interleukin-1β Induces Gastric Inflammation and Cancer and Mobilizes Myeloid-Derived Suppressor Cells in Mice. Cancer Cell *14*, 408–419.
138. Hagemann, T., Lawrence, T., McNeish, I., Charles, K.A., Kulbe, H., Thompson, R.G., Robinson, S.C., and Balkwill, F.R. (2008). "Re-educating" tumor-associated macrophages by targeting NF-κB. J. Exp. Med. *205*, 1261–1268.
139. Porta, C., Rimoldi, M., Raes, G., Brys, L., Ghezzi, P., Di Liberto, D., Dieli, F., Ghisletti, S., Natoli, G., De Baetselier, P., *et al.* (2009). Tolerance and M2 (alternative) macrophage polarization are related processes orchestrated by p50 nuclear factor κB. Proc. Natl. Acad. Sci. *106*, 14978–14983.
140. Maeda, S., Kamata, H., Luo, J., Leffert, H., and Karin, M. (2005). IKKβ Couples Hepatocyte Death to Cytokine-Driven Compensatory Proliferation that Promotes Chemical Hepatocarcinogenesis. Cell *121*, 977–990.
141. Hogerlinden, M. van, Rozell, B.L., Ährlund-Richter, L., and ToftgÅrd, R. (1999). Squamous Cell Carcinomas and Increased Apoptosis in Skin with Inhibited Rel/Nuclear Factor-κB Signaling. Cancer Res. *59*, 3299–3303.
142. Pasparakis, M., Courtois, G., Hafner, M., Schmidt-Supprian, M., Nenci, A., Toksoy, A., Krampert, M., Goebeler, M., Gillitzer, R., Israel, A., *et al.* (2002). TNF-mediated inflammatory skin disease in mice with epidermis-specific deletion of IKK2. Nature *417*, 861–866.
143. Kirkley, K.S., Walton, K.D., Duncan, C., and Tjalkens, R.B. (2017). Spontaneous Development of Cutaneous Squamous Cell Carcinoma in Mice with Cell- specific Deletion of Inhibitor of κB Kinase 2. *67*, 407–415.
144. Lind, M.H., Rozell, B., Wallin, R.P.A., van Hogerlinden, M., Ljunggren, H.-G., Toftgard, R., and Sur, I. (2004). Tumor necrosis factor receptor 1-mediated signaling is required for skin cancer development induced by

NF-κB inhibition. Proc. Natl. Acad. Sci. *101*, 4972–4977.

145. Kruger, P., Saffarzadeh, M., Weber, A.N.R., Rieber, N., Radsak, M., von Bernuth, H., Benarafa, C., Roos, D., Skokowa, J., and Hartl, D. (2015). Neutrophils: Between Host Defence, Immune Modulation, and Tissue Injury. PLOS Pathog. *11*, e1004651.
146. Powell, D.R., and Huttenlocher, A. (2016). Neutrophils in the Tumor Microenvironment. Trends Immunol. *37*, 41–52.
147. Uribe-Querol, E., and Rosales, C. (2015). Neutrophils in cancer: Two sides of the same coin. J. Immunol. Res. *2015,* Article ID 983698, 21 pages.
148. Jamieson, T., Clarke, M., Steele, C.W., Samuel, M.S., Neumann, J., Jung, A., Huels, D., Olson, M.F., Das, S., Nibbs, R.J.B., *et al.* (2012). Inhibition of CXCR2 profoundly suppresses inflammation-driven and spontaneous tumorigenesis. J. Clin. Invest. *122*, 3127–3144.
149. Powell, D., Lou, M., Barros Becker, F., and Huttenlocher, A. (2018). Cxcr1 mediates recruitment of neutrophils and supports proliferation of tumor-initiating astrocytes in vivo. Sci. Rep. *8*, 13285.
150. Freisinger, C.M., and Huttenlocher, A. (2014). Live imaging and gene expression analysis in zebrafish identifies a link between neutrophils and epithelial to mesenchymal transition. PLoS One *9*, 15–19.
151. Jablonska, J., Wu, C.F., Andzinski, L., Leschner, S., and Weiss, S. (2014). CXCR2-mediated tumor-associated neutrophil recruitment is regulated by IFN-β. Int. J. Cancer *134*, 1346–1358.
152. Raccosta, L., Fontana, R., Maggioni, D., Lanterna, C., Villablanca, E.J., Paniccia, A., Musumeci, A., Chiricozzi, E., Trincavelli, M.L., Daniele, S., *et al.* (2013). The oxysterol–CXCR2 axis plays a key role in the recruitment of tumor-promoting neutrophils. J. Exp. Med. *210*, 1711–1728.
153. Zhou, S.-L., Dai, Z., Zhou, Z.-J., Wang, X.-Y., Yang, G., Wang, Z., Huang, X., Fan, J., and Zhou, J. (2012). Overexpression of CXCL5 mediates neutrophil infiltration and indicates poor prognosis for hepatocellular carcinoma. Hepatology *56*, 2242–2254.

154. Feng, Y., Santoriello, C., Mione, M., Hurlstone, A., and Martin, P. (2010). Live imaging of innate immune cell sensing of transformed cells in zebrafish larvae: parallels between tumor initiation and wound inflammation. PLoS Biol. *8*, e1000562.
155. Fridlender, Z.G., Sun, J., Kim, S., Kapoor, V., Cheng, G., Ling, L., Worthen, G.S., and Albelda, S.M. (2009). Polarization of Tumor-Associated Neutrophil Phenotype by TGF-β: “N1” versus “N2” TAN. Cancer Cell *16*, 183–194.
156. Sagiv, J.Y., Michaeli, J., Fridlender, Z.G., Granot, Z., Sagiv, J.Y., Michaeli, J., Assi, S., Mishalian, I., Kisos, H., Levy, L., *et al.* (2015). Phenotypic Diversity and Plasticity in Circulating Neutrophil Subpopulations in Cancer Article Phenotypic Diversity and Plasticity in Circulating Neutrophil Subpopulations in Cancer. CellReports *10*, 562–573.
157. Mishalian, I., Bayuh, R., Levy, L., Zolotarov, L., Michaeli, J., and Fridlender, Z.G. (2013). Tumor-associated neutrophils (TAN) develop pro-tumorigenic properties during tumor progression. Cancer Immunol. Immunother. *62*, 1745–1756.
158. Wu, P., Wu, D., Ni, C., Ye, J., Chen, W., Hu, G., Wang, Z., Wang, C., Zhang, Z., Xia, W., *et al.* (2014). γδT17 Cells Promote the Accumulation and Expansion of Myeloid-Derived Suppressor Cells in Human Colorectal Cancer. Immunity *40*, 785–800.
159. Eruslanov, E.B., Bhojnagarwala, P.S., Quatromoni, J.G., Stephen, T.L., Ranganathan, A., Deshpande, C., Akimova, T., Vachani, A., Litzky, L., Hancock, W.W., *et al.* (2014). Tumor-associated neutrophils stimulate T cell responses in early-stage human lung cancer. J. Clin. Invest. *124*, 5466–5480.
160. Yan, C., Huo, X., Wang, S., Feng, Y., and Gong, Z. (2015). Stimulation of hepatocarcinogenesis by neutrophils upon induction of oncogenic kras expression in transgenic zebrafish. J. Hepatol. *63*, 420–428.
161. Antonio, N., Bonnelykke-Behrndtz, M.L., Ward, L.C., Collin, J., Christensen, I.J., Steiniche, T., Schmidt, H., Feng, Y., and Martin, P.

(2015). The wound inflammatory response exacerbates growth of pre-neoplastic cells and progression to cancer. EMBO J. *34*, 2219–2236.

162. Houghton, A.M., Rzymkiewicz, D.M., Ji, H., Gregory, A.D., Egea, E.E., Metz, H.E., Stolz, D.B., Land, S.R., Marconcini, L.A., Kliment, C.R., *et al.* (2010). Neutrophil elastase–mediated degradation of IRS-1 accelerates lung tumor growth. Nat. Med. *16*, 219–223.
163. Coussens, L.M., Tinkle, C.L., Hanahan, D., and Werb, Z. (2000). MMP-9 supplied by bone marrow-derived cells contributes to skin carcinogenesis. Cell *103*, 481–490.
164. Pliss, G.B., Zabezhinski, M.A., Petrov, A.S., and Khudoley, V. V (1982). Peculiarities of N-nitramines carcinogenic action. Arch. Geschwulstforsch. *52*, 629–634.
165. Kutok, J.L., Aster, J.C., Kanki, J.P., Lin, S., and Look, A.T. (2003). Myc-Induced T Cell Leukemia in Transgenic Zebrafish. *299*, 887–891.
166. Murphey, R.D., Wienholds, E., Neuberg, D., Kutok, J.L., Fletcher, C.D.M., Morris, J.P., Liu, T.X., Schulte-merker, S., Kanki, J.P., Plasterk, R., *et al.* (2005). tp53 mutant zebrafish develop malignant peripheral nerve sheath tumors. *102*, 407–412.
167. Reischauer, S., Levesque, M.P., Nüsslein-Volhard, C., and Sonawane, M. (2009). Lgl2 executes its function as a tumor suppressor by regulating ErbB signaling in the zebrafish epidermis. PLoS Genet. *5*.
168. White, R., Rose, K., and Zon, L. (2013). Zebrafish cancer: the state of the art and the path forward. Nat. Rev. Cancer *13*, 624–636.
169. Stoletov, K., and Klemke, R. (2008). Catch of the day : zebrafish as a human cancer model. 4509–4520.
170. Santoriello, C., Gennaro, E., Anelli, V., Distel, M., Kelly, A., Köster, R.W., Hurlstone, A., and Mione, M. (2010). Kita driven expression of oncogenic HRAS leads to early onset and highly penetrant melanoma in zebrafish. PLoS One *5*, 1–11.
171. Kaufman, C.K., Mosimann, C., Fan, Z.P., Yang, S., Thomas, A.J., Ablain, J., Tan, J.L., Fogley, R.D., Van Rooijen, E., Hagedorn, E.J., *et al.* (2016). A zebrafish melanoma model reveals emergence of neural

crest identity during melanoma initiation. Science. *351*.

172. Chew, T.W., Liu, X.J., Liu, L., Spitsbergen, J.M., Gong, Z., and Low, B.C. (2014). Crosstalk of Ras and Rho: Activation of RhoA abates Kras-induced liver tumorigenesis in transgenic zebrafish models. Oncogene *33*, 2717–2727.
173. Jung, I.H., Jung, D.E., Park, Y.N., Song, S.Y., and Park, S.W. (2011). Aberrant hedgehog ligands induce progressive pancreatic fibrosis by paracrine activation of myofibroblasts and ductular cells in transgenic zebrafish. PLoS One *6*.
174. Schiavone, M., Rampazzo, E., Casari, A., Battilana, G., Persano, L., Moro, E., Liu, S., Leach, S.D., Tiso, N., and Argenton, F. (2014). Zebrafish reporter lines reveal in vivo signaling pathway activities involved in pancreatic cancer. Dis. Model. Mech. *7*, 883–894.
175. Le Guellec, D., Morvan-Dubois, G., and Sire, J.Y. (2004). Skin development in bony fish with particular emphasis on collagen deposition in the dermis of the zebrafish (Danio rerio). Int. J. Dev. Biol. *48*, 217–231.
176. Chang, W.J., and Hwang, P.P. (2011). Development of zebrafish epidermis. Birth Defects Res. Part C - Embryo Today Rev. *93*, 205–214.
177. Lee, R.T.H., Asharani, P. V., and Carney, T.J. (2014). Basal keratinocytes contribute to all strata of the adult zebrafish epidermis. PLoS One *9*.
178. Eisenhoffer, G.T., Slattum, G., Ruiz, O.E., Otsuna, H., Bryan, C.D., Lopez, J., Wagner, D.S., Bonkowsky, J.L., Chien, C.-B., Dorsky, R.I., *et al.* (2017). A toolbox to study epidermal cell types in zebrafish. J. Cell Sci. *130*, 269–277.
179. Pellegrini, G., Dellambra, E., Golisano, O., Martinelli, E., Fantozzi, I., Bondanza, S., Ponzin, D., McKeon, F., and De Luca, M. (2001). p63 identifies keratinocyte stem cells. Proc. Natl. Acad. Sci. *98*, 3156–3161.
180. Bakkers, J., Hild, M., Kramer, C., Furutani-Seiki, M., and Hammerschmidt, M. (2002). Zebrafish ΔNp63 Is a Direct Target of Bmp Signaling and Encodes a Transcriptional Repressor Blocking Neural

Specification in the Ventral Ectoderm. Dev. Cell *2*, 617–627.

181. Krushna Padhi, B., Akimenko, M., and Ekker, M. (2006). Independent expansion of the keratin gene family in teleostean fish and mammals: An insight from phylogenetic analysis and radiation hybrid mapping of keratin genes in zebrafish. Gene *368*, 37–45.
182. McLeish, J.A., Chico, T.J.A., Taylor, H.B., Tucker, C., Donaldson, K., and Brown, S.B. (2010). Skin exposure to micro- and nano-particles can cause haemostasis in zebrafish larvae. Thromb. Haemost. *103*, 797–807.
183. Jevtov, I., Samuelsson, T., Yao, G., Amsterdam, A., and Ribbeck, K. (2014). Zebrafish as a model to study live mucus physiology. Sci. Rep. *4*, 1–6.
184. Pauley, G.B. (2011). Fish Immunology. J. Fish. Res. Board Canada *32*, 1674–1675.
185. Renshaw, S.A., and Trede, N.S. (2012). A model 450 million years in the making: zebrafish and vertebrate immunity. Dis. Model. Mech. *5*, 38–47.
186. Herbomel, P., Mordelet, E., Shinomiya, H., Colucci-Guyon, E., Murayama, E., Briolat, V., Redd, M.J., Kissa, K., Le Guyader, D., and Zapata, A. (2007). Origins and unconventional behavior of neutrophils in developing zebrafish. Blood *111*, 132–141.
187. Lieschke, G.J., Oates, A.C., Crowhurst, M.O., Ward, A.C., Layton, J.E., Lieschke, G.J., Oates, A.C., Crowhurst, M.O., Ward, A.C., and Layton, J.E. (2008). Morphologic and functional characterization of granulocytes and macrophages in embryonic and adult zebrafish. Blood *98*, 3087–3096.
188. Colucci-Guyon, E., Tinevez, J.-Y., Renshaw, S.A., and Herbomel, P. (2011). Strategies of professional phagocytes in vivo: unlike macrophages, neutrophils engulf only surface-associated microbes. J. Cell Sci. *124*, 3053–3059.
189. Brothers, K.M., Newman, Z.R., and Wheeler, R.T. (2011). Live Imaging of Disseminated Candidiasis in Zebrafish Reveals Role of Phagocyte Oxidase in Limiting Filamentous Growth. Eukaryot. Cell *10*, 932–944.

190. Palić, D., Andreasen, C.B., Ostojić, J., Tell, R.M., and Roth, J.A. (2007). Zebrafish (Danio rerio) whole kidney assays to measure neutrophil extracellular trap release and degranulation of primary granules. J. Immunol. Methods *319*, 87–97.
191. Jault, C., Pichon, L., and Chluba, J. (2004). Toll-like receptor gene family and TIR-domain adapters in Danio rerio. Mol. Immunol. *40*, 759–771.
192. Zhu, L.Y., Nie, L., Zhu, G., Xiang, L.X., and Shao, J.Z. (2012). Advances in research of fish immune-relevant genes: A comparative overview of innate and adaptive immunity in teleosts. Dev. Comp. Immunol. *39*, 39–62.
193. Phelan, P.E., Mellon, M.T., and Kim, C.H. (2005). Functional characterization of full-length TLR3, IRAK-4, and TRAF6 in zebrafish (Danio rerio). Mol. Immunol. *42*, 1057–1071.
194. Palti, Y. (2011). Toll-like receptors in bony fish : From genomics to function. Dev. Comp. Immunol. *35*, 1263–1272.
195. Kanwal, Z., Wiegertjes, G.F., Veneman, W.J., Meijer, A.H., and Spaink, H.P. (2014). Comparative studies of Toll-like receptor signalling using zebrafish. Dev. Comp. Immunol. *46*, 35–52.
196. Lam, S.H., Chua, H.L., Gong, Z., Lam, T.J., and Sin, Y.M. (2004). Development and maturation of the immune system in zebrafish, Danio rerio: A gene expression profiling, in situ hybridization and immunological study. Dev. Comp. Immunol. *28*, 9–28.
197. Renshaw, S.A., Loynes, C.A., Trushell, D.M.I., Elworthy, S., Ingham, P.W., and Whyte, M.K.B. (2006). A transgenic zebrafish model of neutrophilic inflammation. Blood *108*, 3976–3978.
198. Hall, C., Flores, M., Storm, T., Crosier, K., and Crosier, P. (2007). The zebrafish lysozyme C promoter drives myeloid-specific expression in transgenic fish. BMC Dev. Biol. *7*, 1–17.
199. Yang, C.-T., Cambier, C.J., and Davis, J.M. (2012). Neutrophils Exert Protection in the Early Tuberculous Granuloma by Oxidative Killing of Mycobacteria Phagocytosed from Infected Macrophages. Cell Host Microbe *12*, 301–312.

200. Ellett, F., Pase, L., Hayman, J.W., Andrianopoulos, A., and Lieschke, G.J. (2011). mpeg1 promoter transgenes direct macrophage-lineage expression in zebrafish. Blood *117*, e49–e56.
201. Walton, E.M., Cronan, M.R., Beerman, R.W., and Tobin, D.M. (2015). The Macrophage-Specific Promoter mfap4 Allows Live, Long-Term Analysis of Macrophage Behavior during Mycobacterial Infection in Zebrafish. PLoS One *10*, e0138949.
202. Kwan, K.M., Fujimoto, E., Grabher, C., Mangum, B.D., Hardy, M.E., Campbell, D.S., Parant, J.M., Yost, H.J., Kanki, J.P., and Chien, C. Bin (2007). The Tol2kit: A multisite gateway-based construction Kit for Tol2 transposon transgenesis constructs. Dev. Dyn. *236*, 3088–3099.
203. Balciunas, D., Wangensteen, K.J., Wilber, A., Bell, J., Geurts, A., Sivasubbu, S., Wang, X., Hackett, P.B., Largaespada, D. a., McIvor, R.S., *et al.* (2006). Harnessing a high cargo-capacity transposon for genetic applications in vertebrates. PLoS Genet. *2*, 1715–1724.
204. Westerfield, M. (2000). The zebrafish book. A guide for the laboratory use of zebrafish (Danio rerio) 4th Ed. (Univ. of Oregon Press, Eugene).
205. Kimmel, C.B., Ballard, W.W., Kimmel, S.R., Ullmann, B., and Schilling, T.F. (1995). Stages of embryonic development of the zebrafish. Dev. Dyn. *203*, 253–310.
206. Ramezani, T., Laux, D.W., Bravo, I.R., Tada, M., and Feng, Y. (2015). Live Imaging of Innate Immune and Preneoplastic Cell Interactions Using an Inducible Gal4/UAS Expression System in Larval Zebrafish Skin. J. Vis. Exp., 1–7.
207. Kanther, M., Sun, X., Mhlbauer, M., MacKey, L.C., Flynn, E.J., Bagnat, M., Jobin, C., and Rawls, J.F. (2011). Microbial colonization induces dynamic temporal and spatial patterns of NF-κB activation in the zebrafish digestive tract. Gastroenterology *141*, 197–207.
208. Hall, C., Flores, M.V., Chien, A., Davidson, A., Crosier, K., and Crosier, P. (2009). Transgenic zebrafish reporter lines reveal conserved Toll-like receptor signaling potential in embryonic myeloid leukocytes and adult immune cell lineages. J. Leukoc. Biol. *85*, 751–765.

209. Jonason, A.S., Kunala, S., Price, G.J., Restifo, R.J., Spinelli, H.M., Persing, J.A., Leffell, D.J., Tarone, R.E., and Brash, D.E. (1996). Frequent clones of p53-mutated keratinocytes in normal human skin. Proc. Natl. Acad. Sci. *93*, 14025–14029.
210. Ling, G., Persson, A., Berne, B., Uhlén, M., Lundeberg, J., and Ponten, F. (2001). Persistent p53 mutations in single cells from normal human skin. Am. J. Pathol. *159*, 1247–53.
211. Kandel, R., Li, S.-Q., Ozcelik, H., and Rohan, T. (2000). P53 Protein Accumulation and Mutations in Normal and Benign Breast Tissue. Int. J. Cancer *87*, 73–78.
212. Holst, C.R., Nuovo, G.J., Esteller, M., Chew, K., Baylin, S.B., Herman, J.G., and Tlsty, T.D. (2003). Methylation of p16 INK4a Promoters Occurs in Vivo in Histologically Normal Human Mammary Epithelia Methylation of p16 INK4a Promoters Occurs in Vivo in Histologically Normal Human. Cancer, 1596–1601.
213. Chen, X., Mitsutake, N., LaPerle, K., Akeno, N., Zanzonico, P., Longo, V.A., Mitsutake, S., Kimura, E.T., Geiger, H., Santos, E., *et al.* (2009). Endogenous expression of Hras(G12V) induces developmental defects and neoplasms with copy number imbalances of the oncogene. Proc. Natl. Acad. Sci. U.S.A. *106*, 7979–84.
214. Balmain, A., and Yuspa, S.H. (2014). Milestones in skin carcinogenesis: the biology of multistage carcinogenesis. J. Invest. Dermatol. *134*, E2–E7.
215. Seeburg, P.H., Colby, W.W., Capon, D.J., Goeddel, D. V., and Levinson, A.D. (1984). Biological properties of human c-Ha-ras1 genes mutated at codon 12. Nature *312*, 71–75.
216. Colby, W.W., Hayflick, J.S., Clark, S.G., and Levinson, A.D. (1986). Biochemical characterization of polypeptides encoded by mutated human Ha-ras1 genes. Mol. Cell. Biol. *6*, 730–734.
217. Balmain, A., and Pragnell, I.B. Mouse skin carcinomas induced in vivo by chemical carcinogens have a transforming Harvey-ras oncogene. Nature *303*, 72–4.

218. Quintanilla, M., Brown, K., Ramsden, M., and Balmain, A. (1986). Carcinogen-specific mutation and amplification of Ha-ras during mouse skin carcinogenesis. Nature *322*, 78–80.
219. Sukumar, S., Notario, V., Martin-Zanca, D., and Barbacid, M. (1983). Induction of mammary carcinomas in rats by nitroso-methylurea involves malignant activation of H-ras-1 locus by single point mutations. Nature *306*, 658–661.
220. Anderson, M.W. (1989). Activation of the Ki-ras protooncogene in spontaneously occurring and chemically induced lung tumors of the strain A mouse. *86*, 3070–3074.
221. Westcott, P.M.K., Halliwill, K.D., To, M.D., Rashid, M., Rust, A.G., Keane, T.M., Delrosario, R., Jen, K., Gurley, K.E., Kemp, C.J., *et al.* (2015). The mutational landscapes of genetic and chemical models of Kras-driven lung cancer. Nature *517*, 489–492.
222. Löhr, M., Klöppel, G., Maisonneuve, P., Lowenfels, A. B., & Lüttges, J. (2005). Frequency of K-ras mutations in pancreatic intraductal neoplasias associated with pancreatic ductal adenocarcinoma and chronic pancreatitis: a meta-analysis. Neoplasia *7,* 17–23.
223. Wistuba, I.I., and Gazdar, A.F. (2006). Lung Cancer Preneoplasia. Ann Rev of Path Mech of Dis *1*, 331-348.
224. Roh, M.R., Eliades, P., Gupta, S., and Tsao, H. (2015). Genetics of melanocytic nevi. Pigment Cell Melanoma Res. *28*, 661–672.
225. Kanda, M., Matthaei, H., Wu, J., Hong, S., Yu, J., Borges, M., Hruban, R.H., Maitra, A., Kinzler, K., Vogelstein, B., *et al.* (2012). Presence of Somatic Mutations in Most Early-Stage Pancreatic Intraepithelial Neoplasia. Gastroenterology *142*, 730-733.e9.
226. Guerra, C., Schuhmacher, A.J., Cañamero, M., Grippo, P.J., Verdaguer, L., Pérez-Gallego, L., Dubus, P., Sandgren, E.P., and Barbacid, M. (2007). Chronic Pancreatitis Is Essential for Induction of Pancreatic Ductal Adenocarcinoma by K-Ras Oncogenes in Adult Mice. Cancer Cell *11*, 291–302.
227. Hughley, C., Murphy, K.M., Shaw, A.S., and Unanue, E.R. (2001).

Somatic activation of the K-ras oncogene causes early onset lung cancer in mice. *410*, 1–6.

228. Brown, K., Strathdee, D., Bryson, S., Lambie, W., and Balmain, A. (1998). The malignant capacity of skin tumours induced by expression of a mutant H-ras transgene depends on the cell type targeted. Curr. Biol. *8*, 516–524.
229. Jackson, E.L., Willis, N., Mercer, K., Bronson, R.T., Crowley, D., Montoya, R., Jacks, T., and Tuveson, D.A. (2001). Analysis of lung tumor initiation and progression using conditional expression of oncogenic K-ras. 3243–3248.
230. Guerra, C., Mijimolle, N., Dhawahir, A., Dubus, P., Barradas, M., Serrano, M., Campuzano, V., and Barbacid, M. (2003). Tumor induction by an endogenous K-ras oncogene is highly dependent on cellular context. Cancer Cell *4*, 111–120.
231. Tuveson, D.A., Shaw, A.T., Willis, N.A., Silver, D.P., Jackson, E.L., Chang, S., Mercer, K.L., Grochow, R., Hock, H., Crowley, D., *et al.* (2004). Endogenous oncogenic K-rasG12Dstimulates proliferation and widespread neoplastic and developmental defects. Cancer Cell *5*, 375–387.
232. Hogan, C., Dupré-Crochet, S., Norman, M., Kajita, M., Zimmermann, C., Pelling, A.E., Piddini, E., Baena-López, L.A., Vincent, J.P., Itoh, Y., *et al.* (2009). Characterization of the interface between normal and transformed epithelial cells. Nat. Cell Biol. *11*, 460–467.
233. Kajita, M., Hogan, C., Harris, A.R., Dupre-Crochet, S., Itasaki, N., Kawakami, K., Charras, G., Tada, M., and Fujita, Y. (2010). Interaction with surrounding normal epithelial cells influences signalling pathways and behaviour of Src-transformed cells. J. Cell Sci. *123*, 171–180.
234. Norman, M., Wisniewska, K.A., Lawrenson, K., Garcia-Miranda, P., Tada, M., Kajita, M., Mano, H., Ishikawa, S., Ikegawa, M., Shimada, T., *et al.* (2012). Loss of Scribble causes cell competition in mammalian cells. J. Cell Sci. *125*, 59–66.
235. Leung, C.T., and Brugge, J.S. (2012). Outgrowth of single oncogene-

expressing cells from suppressive epithelial environments. Nature *482*, 410–413.

236. Distel, M., Wullimann, M.F., and Koster, R.W. (2009). Optimized Gal4 genetics for permanent gene expression mapping in zebrafish. Proc. Natl. Acad. Sci. *106*, 13365–13370.
237. Gerety, S.S., Breau, M.A., Sasai, N., Xu, Q., Briscoe, J., and Wilkinson, D.G. (2013). An inducible transgene expression system for zebrafish and chick. Development *140*, 2235–2243.
238. Akerberg, A.A., Stewart, S., and Stankunas, K. (2014). Spatial and temporal control of transgene expression in zebrafish. PLoS One *9*.
239. Abankwa, D., Gorfe, A.A., and Hancock, J.F. (2007). Ras nanoclusters: Molecular structure and assembly. Semin. Cell Dev. Biol. *18*, 599–607.
240. Plowman, S.J., Muncke, C., Parton, R.G., and Hancock, J.F. (2005). H-ras, K-ras, and inner plasma membrane raft proteins operate in nanoclusters with differential dependence on the actin cytoskeleton. Proc. Natl. Acad. Sci. *102*, 15500–15505.
241. Janosi, L., Li, Z., Hancock, J.F., and Gorfe, A.A. (2012). Organization, dynamics, and segregation of Ras nanoclusters in membrane domains. Proc. Natl. Acad. Sci. *109*, 8097–8102.
242. Rotblat, B., Prior, I.A., Muncke, C., Parton, R.G., Kloog, Y., Henis, Y.I., and Hancock, J.F. (2004). Three Separable Domains Regulate GTP-Dependent Association of H-ras with the Plasma Membrane. Mol. Cell. Biol. *24*, 6799–6810.
243. Sonawane, M. (2005). Zebrafish penner/lethal giant larvae 2 functions in hemidesmosome formation, maintenance of cellular morphology and growth regulation in the developing basal epidermis. Development *132*, 3255–3265.
244. Feng, Y., Renshaw, S., and Martin, P. (2012). Live imaging of tumor initiation in zebrafish larvae reveals a trophic role for leukocyte-derived PGE_2. Curr. Biol. *22*, 1253–9.
245. Webb, A.E., Driever, W., and Kimelman, D. (2008). Psoriasis Regulates Epidermal Development in Zebrafish. Dev. Dyn. *237*, 1153–1164.

246. Bartkova, J., Hořejší, Z., Koed, K., Krämer, A., Tort, F., Zleger, K., Guldberg, P., Sehested, M., Nesland, J.M., Lukas, C., *et al.* (2005). DNA damage response as a candidate anti-cancer barrier in early human tumorigenesis. Nature *434*, 864–870.
247. Bartkova, J., Rezaei, N., Liontos, M., Karakaidos, P., Kletsas, D., Issaeva, N., Vassiliou, L.V.F., Kolettas, E., Niforou, K., Zoumpourlis, V.C., *et al.* (2006). Oncogene-induced senescence is part of the tumorigenesis barrier imposed by DNA damage checkpoints. Nature *444*, 633–637.
248. Halazonetis, T.D., Gorgoulis, V.G., and Bartek, J. (2008). An Oncogene-Induced DNA Damage Model for Cancer Development. Science (80-.). *319*, 1352–1355.
249. de Oliveira, S., Reyes-Aldasoro, C.C., Candel, S., Renshaw, S.A., Mulero, V., and Calado, A. (2013). Cxcl8 (IL-8) Mediates Neutrophil Recruitment and Behavior in the Zebrafish Inflammatory Response. J. Immunol. *190*, 4349–4359.
250. Tauzin, S., Starnes, T.W., Becker, F.B., Lam, P. -y., and Huttenlocher, a. (2014). Redox and Src family kinase signaling control leukocyte wound attraction and neutrophil reverse migration. J. Cell Biol. *207*, 589–598.
251. White, A.C., Tran, K., Khuu, J., Dang, C., Cui, Y., Binder, S.W., and Lowry, W.E. (2011). Defining the origins of Ras/p53-mediated squamous cell carcinoma. Proc. Natl. Acad. Sci. *108*, 7425–7430.
252. Maurelli, R., Tinaburri, L., Gangi, F., Bondanza, S., Severi, A.L., Scarponi, C., Albanesi, C., Mesiti, G., Guerra, L., Capogrossi, M.C., *et al.* (2016). The role of oncogenic Ras in human skin tumorigenesis depends on the clonogenic potential of the founding keratinocytes. J. Cell Sci. *129*, 1003–1017.
253. Zhang, S., Yang, X., Wang, L., and Zhang, C. (2018). Interplay between inflammatory tumor microenvironment and cancer stem cells (Review). Oncol. Lett. *16*, 679–686.
254. Hagag, N., Diamond, L., Palermo, R., and Lyubsky, S. (1990). High

expression of ras p21 correlates with increased rate of abnormal mitosis in NIH3T3 cells. Oncogene *5*, 1481–1489.

255. Denko, N., Stringer, J., Wani, M., and Stambrook, P. (1995). Mitotic and post mitotic consequences of genomic instability induced by oncogenic Ha-Ras. Somat. Cell Mol. Genet. *21*, 241–253.
256. Knauf, J.A., Ouyang, B., Knudsen, E.S., Fukasawa, K., Babcock, G., and Fagin, J.A. (2006). Oncogenic RAS induces accelerated transition through G2/M and promotes defects in the G2 DNA damage and mitotic spindle checkpoints. J. Biol. Chem. *281*, 3800–3809.
257. Denko, N.C., Giaccia, A.J., Stringer, J.R., and Stambrook, P.J. (1994). The human Ha-ras oncogene induces genomic instability in murine fibroblasts within one cell cycle. Proc. Natl. Acad. Sci. *91*, 5124–5128.
258. Gorgoulis, V.G., Vassiliou, L.V.F., Karakaidos, P., Zacharatos, P., Kotsinas, A., Liloglou, T., Venere, M., DiTullio, R.A., Kastrinakis, N.G., Levy, B., *et al.* (2005). Activation of the DNA damage checkpoint and genomic instability in human precancerous lesions. Nature *434*, 907–913.
259. Tsantoulis, P.K., Kotsinas, A., Sfikakis, P.P., Evangelou, K., Sideridou, M., Levy, B., Mo, L., Kittas, C., Wu, X.R., Papavassiliou, A.G., *et al.* (2008). Oncogene-induced replication stress preferentially targets common fragile sites in preneoplastic lesions. A genome-wide study. Oncogene *27*, 3256–3264.
260. Federico, A., Morgillo, F., Tuccillo, C., Ciardiello, F., and Loguercio, C. (2007). Chronic inflammation and oxidative stress in human carcinogenesis. Int. J. Cancer *121*, 2381–2386.
261. Huang, Q., Li, F., Liu, X., Li, W., Shi, W., Liu, F.F., O'Sullivan, B., He, Z., Peng, Y., Tan, A.C., *et al.* (2011). Caspase 3-mediated stimulation of tumor cell repopulation during cancer radiotherapy. Nat. Med. *17*, 860–866.
262. Donato, A.L., Huang, Q., Liu, X., Li, F., Zimmerman, M.A., and Li, C.Y. (2014). Caspase 3 promotes surviving melanoma tumor cell growth after cytotoxic therapy. J. Invest. Dermatol. *134*, 1686–1692.

263. Cheng, J., Tian, L., Ma, J., Gong, Y., Zhang, Z., Chen, Z., Xu, B., Xiong, H., Li, C., and Huang, Q. (2015). Dying tumor cells stimulate proliferation of living tumor cells via caspase-dependent protein kinase Cδ activation in pancreatic ductal adenocarcinoma. Mol. Oncol. *9*, 105–114.
264. Yu, Y., Tian, L., Feng, X., Cheng, J., Gong, Y., Liu, X., Zhang, Z., Yang, X., He, S., Li, C.Y., *et al.* (2016). eIF4E-phosphorylation-mediated Sox2 upregulation promotes pancreatic tumor cell repopulation after irradiation. Cancer Lett. *375*, 31–38.
265. He, S., Cheng, J., Sun, L., Wang, Y., Wang, C., Liu, X., Zhang, Z., Zhao, M., Luo, Y., Tian, L., *et al.* (2018). HMGB1 released by irradiated tumor cells promotes living tumor cell proliferation via paracrine effect. Cell Death Dis. *9*, 648.
266. Watanabe, M., Hitomi, M., Wee, K. Van Der, Rothenberg, F., Fisher, S.A., Zucker, R., Svoboda, K.K.H., Goldsmith, E.C., Heiskanen, K.M., and Nieminen, A. (2002). The Pros and Cons of Apoptosis Assays for Use in the Study of Cells, Tissues, and Organs. Microscopy and Microanalysis *8*, 375-391.
267. Didenko, V. V (2011). DNA Damage Detection In Situ, Ex Vivo, and In Vivo. Methods and protocols 1st Ed. (Humana Press)
268. Didenko, V. V, and Hornsby, P.J. (1996). Presence of double-strand breaks with single -base 3’ overhang in cells with undergoing apoptosis but not necrosis. J. Cell Biol. *135*, 1369–1376.
269. Kockx, M.M., Muhring, J., Knaapen, M.W., and de Meyer, G.R. (1998). RNA synthesis and splicing interferes with DNA in situ end labeling techniques used to detect apoptosis. Am. J. Pathol. *152*, 885–8.
270. Tamura, T., Said, S., Lu, W., and Neufeld, D. (2000). Specificity of TUNEL method depends on duration of fixation. Biotech. Histochem. *75*, 197–200.
271. Jerome, K.R., Vallan, C., and Jaggi, R. (2000). The tunel assay in the diagnosis of graft-versus-host disease: Caveats for interpretation. Pathology *32*, 186–190.
272. Enomoto, M., Vaughen, J., and Igaki, T. (2015). Non-autonomous

overgrowth by oncogenic niche cells: Cellular cooperation and competition in tumorigenesis. Cancer Sci. *106*, 1651–1658.

273. Richardson, H.E., and Portela, M. (2018). Modelling Cooperative Tumorigenesis in Drosophila. Biomed Res. Int. *2018*, 23–25.
274. Herranz, H., Weng, R., and Cohen, S.M. (2014). Crosstalk between epithelial and mesenchymal tissues in tumorigenesis and imaginal disc development. Curr. Biol. *24*, 1476–1484.
275. Nakamura, M., Ohsawa, S., and Igaki, T. (2014). Mitochondrial defects trigger proliferation of neighbouring cells via a senescence-associated secretory phenotype in Drosophila. Nat. Commun. *5*, 1–11.
276. van der Aa, L.M., Chadzinska, M., Tijhaar, E., Boudinot, P., and Lidy verburg-Van kemenade, B.M. (2010). CXCL8 chemokines in teleost fish: Two lineages with distinct expression profiles during early phases of inflammation. PLoS One *5*.
277. Oehlers, S.H.B., Flores, M.V., Hall, C.J., O'Toole, R., Swift, S., Crosier, K.E., and Crosier, P.S. (2010). Expression of zebrafish cxcl8 (interleukin-8) and its receptors during development and in response to immune stimulation. Dev. Comp. Immunol. *34*, 352–359.
278. Sarris, M., Masson, J.B., Maurin, D., Van Der Aa, L.M., Boudinot, P., Lortat-Jacob, H., and Herbomel, P. (2012). Inflammatory Chemokines Direct and Restrict Leukocyte Migration within Live Tissues as Glycan-Bound Gradients. Curr. Biol. *22*, 2375–2382.
279. Deng, Q., Sarris, M., Bennin, D.A., Green, J.M., Herbomel, P., and Huttenlocher, A. (2013). Localized bacterial infection induces systemic activation of neutrophils through Cxcr2 signaling in zebrafish. J. Leukoc. Biol. *93*, 761–769.
280. de Oliveira, S., Lopez-Muñoz, A., Martínez-Navarro, F.J., Galindo-Villegas, J., Mulero, V., and Calado, Â. (2015). Cxcl8-l1 and Cxcl8-l2 are required in the zebrafish defense against Salmonella Typhimurium. Dev. Comp. Immunol. *49*, 44–48.
281. Torraca, V., Otto, N.A., Tavakoli-Tameh, A., and Meijer, A.H. (2017). The inflammatory chemokine Cxcl18b exerts neutrophil-specific

chemotaxis via the promiscuous chemokine receptor Cxcr2 in zebrafish. Dev. Comp. Immunol. *67*, 57–65.

282. Cavallo, F., De Giovanni, C., Nanni, P., Forni, G., and Lollini, P.L. (2011). 2011: The immune hallmarks of cancer. Cancer Immunol. Immunother. *60*, 319–326.
283. Duffey, D.C., Chen, Z., Dong, G., Ondrey, F.G., Wolf, J.S., Brown, K., Siebenlist, U., and Van Waes, C. (1999). Expression of a dominant-negative mutant inhibitor-κBα of nuclear factor-κB in human head and neck squamous cell carcinoma inhibits survival, proinflammatory cytokine expression, and tumor growth in vivo. Cancer Res. *59*, 3468–3474.
284. Loercher, A., Lee, T.L., Ricker, J.L., Howard, A., Geoghegen, J., Chen, Z., Sunwoo, J.B., Sitcheran, R., Chuang, E.Y., Mitchell, J.B., *et al.* (2004). Nuclear factor-κB is an important modulator of the altered gene expression profile and malignant phenotype in squamous cell carcinoma. Cancer Res. *64*, 6511–6523.
285. Aggarwal, S., Takada, Y., Singh, S., Myers, J.N., and Aggarwal, B.B. (2004). Inhibition of growth and survival of human head and neck squamous cell carcinoma cells by curcumin via modulation of nuclear factor-κB signaling. Int. J. Cancer *111*, 679–692.
286. Wullaert, A., Bonnet, M.C., and Pasparakis, M. (2011). NF-κB in the regulation of epithelial homeostasis and inflammation. Cell Res. *21*, 146–158.
287. Grinberg-Bleyer, Y., Dainichi, T., Oh, H., Heise, N., Klein, U., Schmid, R.M., Hayden, M.S., and Ghosh, S. (2015). Cutting Edge: NF-κB p65 and c-Rel Control Epidermal Development and Immune Homeostasis in the Skin. J. Immunol. *194*, 2472–2476.
288. Wang, D.J., Ratnam, N.M., Byrd, J.C., and Guttridge, D.C. (2014). NF-κB functions in tumor initiation by suppressing the surveillance of both innate and adaptive immune cells. Cell Rep. *9*, 90–103.
289. Hobbs, R.M., and Watt, F.M. (2003). Regulation of interleukin-1α expression by integrins and epidermal growth factor receptor in

keratinocytes from a mouse model of inflammatory skin disease. J. Biol. Chem. *278*, 19798–19807.

290. Cataisson, C., Ohman, R., Patel, G., Pearson, A., Tsien, M., Jay, S., Wright, L., Hennings, H., and Yuspa, S.H. (2009). Inducible cutaneous inflammation reveals a protumorigenic role for keratinocyte CXCR2 in skin carcinogenesis. Cancer Res. *69*, 319–328.
291. Ratnam, N.M., Peterson, J.M., Talbert, E.E., Ladner, K.J., Rajasekera, P. V., Schmidt, C.R., Dillhoff, M.E., Swanson, B.J., Haverick, E., Kladney, R.D., *et al.* (2017). NF-κB regulates GDF-15 to suppress macrophage surveillance during early tumor development. J. Clin. Invest. *127*, 3796–3809.
292. Lorenz, V.N., Schön, M.P., and Seitz, C.S. (2014). C-Rel downregulation affects cell cycle progression of human keratinocytes. J. Invest. Dermatol. *134*, 415–422.
293. Coste, I., Le Corf, K., Kfoury, A., Hmitou, I., Druillennec, S., Hainaut, P., Eychene, A., Lebecque, S., and Renno, T. (2010). Dual function of MyD88 in RAS signaling and inflammation, leading to mouse and human cell transformation. J. Clin. Invest. *120*, 3663–3667.
294. Kfoury, A., Le Corf, K., El Sabeh, R., Journeaux, A., Badran, B., Hussein, N., Lebecque, S., Manié, S., Renno, T., and Coste, I. (2013). MyD88 in DNA repair and cancer cell resistance to genotoxic drugs. J. Natl. Cancer Inst. *105*, 937–46.
295. Scheeren, F. a, Kuo, A.H., van Weele, L.J., Cai, S., Glykofridis, I., Sikandar, S.S., Zabala, M., Qian, D., Lam, J.S., Johnston, D., *et al.* (2014). A cell-intrinsic role for TLR2-MYD88 in intestinal and breast epithelia and oncogenesis. Nat. Cell Biol. *16*.
296. Wang, E.L., Qian, Z.R., Nakasono, M., Tanahashi, T., Yoshimoto, K., Bando, Y., Kudo, E., Shimada, M., and Sano, T. (2010). High expression of Toll-like receptor 4/myeloid differentiation factor 88 signals correlates with poor prognosis in colorectal cancer. Br. J. Cancer *102*, 908–915.
297. Je, E.M., Kim, S.S., Yoo, N.J., and Lee, S.H. (2012). Mutational and expressional analyses of MYD88 gene in common solid cancers. Tumori

98, 663–669.

298. Salcedo, R., Cataisson, C., Hasan, U., Yuspa, S.H., and Trinchieri, G. (2013). MyD88 and its divergent toll in carcinogenesis. Trends Immunol. *34*, 379–389.
299. Wu, X.Y., Liu, W.T., Wu, Z.F., Chen, C., Liu, J.Y., Wu, G.N., Yao, X.Q., Liu, F.K., and Li, G. (2016). Identification of HRAS as cancer-promoting gene in gastric carcinoma cell aggressiveness. Am. J. Cancer Res. *6*, 1935–1948.
300. Chun, K.S., Keum, Y.S., Han, S.S., Song, Y.S., Kim, S.H., and Surh, Y.J. (2003). Curcumin inhibits phorbol ester-induced expression of cyclooxygenase-2 in mouse skin through suppression of extracellular signal-regulated kinase activity and NF-κB activation. Carcinogenesis *24*, 1515–1524.
301. Zhang, X., Dong, Z., Zhang, C., Ung, C.Y., He, S., Tao, T., Oliveira, A.M., Meves, A., Ji, B., Look, A.T., *et al.* (2017). Critical Role for GAB2 in Neuroblastoma Pathogenesis through the Promotion of SHP2/MYCN Cooperation. Cell Rep. *18*, 2932–2942.
302. Van Antwerp, D.J., Martin, S.J., Kafri, T., Green, D.R., and Verma, I.M. (1996). Suppression of TNF-α-induced apoptosis by NF-κB. Science (80-.). *274*, 787–789.
303. Abbas, S., and Abu-Amer, Y. (2003). Dominant-negative IκB facilitates apoptosis of osteoclasts by tumor necrosis factor-α J. Biol. Chem. *278*, 20077–20082.
304. Espín-Palazón, R., Stachura, D.L., Campbell, C.A., García-Moreno, D., Del Cid, N., Kim, A.D., Candel, S., Meseguer, J., Mulero, V., and Traver, D. (2014). Proinflammatory signaling regulates hematopoietic stem cell emergence. Cell *159*, 1070–1085.
305. Karra, R., Knecht, A.K., Kikuchi, K., and Poss, K.D. (2015). Myocardial NF-κB activation is essential for zebrafish heart regeneration. Proc. Natl. Acad. Sci. *112*, 13255–13260.
306. Ogryzko, N. V., Renshaw, S.A., and Wilson, H.L. (2014). The IL-1 family in fish: Swimming through the muddy waters of inflammasome evolution.

Dev. Comp. Immunol. *46*, 53–62.

307. Ogryzko, N. V., Hoggett, E.E., Solaymani-Kohal, S., Tazzyman, S., Chico, T.J.A., Renshaw, S.A., and Wilson, H.L. (2014). Zebrafish tissue injury causes upregulation of interleukin-1 and caspase-dependent amplification of the inflammatory response. Dis. Model. Mech. *7*, 259–264.
308. Mittal, D., Saccheri, F., Vénéreau, E., Pusterla, T., Bianchi, M.E., and Rescigno, M. (2010). TLR4-mediated skin carcinogenesis is dependent on immune and radioresistant cells. EMBO J. *29*, 2242–2252.
309. Tang, D., Kang, R., Zeh III, H.J., and Lotze, M.T. (2010). High-mobility Group Box 1 [HMGB1] and Cancer. Biochem. Biophys. Acta *1799*, 1–22.
310. Guttridge, D.C., Albanese, C., Reuther, J.Y., Pestell, R.G., and Baldwin, A.S. (1999). NF-κB Controls Cell Growth and Differentiation through Transcriptional Regulation of Cyclin D1. Mol. Cell. Biol. *19*, 5785–5799.
311. Joyce, D., Albanese, C., Steer, J., FU, M., Bouzahzah, B., and Pestell, R. (2001). NF-κB and cell-cycle regulation: the cyclin connection. Cytokine Growth Factor Rev. *12*, 73–90.
312. Westerheide, S.D., Mayo, M.W., Anest, V., Hanson, J.L., and Baldwin, A.S. (2001). The putative oncoprotein Bcl-3 induces cyclin D1 to stimulate G(1) transition. Mol. Cell. Biol. *21*, 8428–8436.
313. Huitfeldt, H.S., Heyden, A., Clausen, O.P.F., Thrane, E.V., Roop, D., and Yuspa, S.H. (1991). Altered regulation of growth and expression of differentiation-associated keratins in benign mouse skin tumors. Carcinogenesis *12*, 2063–2067.
314. Schwitalla, S., Fingerle, A.A., Cammareri, P., Nebelsiek, T., Göktuna, S.I., Ziegler, P.K., Canli, O., Heijmans, J., Huels, D.J., Moreaux, G., *et al.* (2013). Intestinal tumorigenesis initiated by dedifferentiation and acquisition of stem-cell-like properties. Cell *152*, 25–38.
315. Niethammer, P., Grabher, C., Look, A.T., and Mitchison, T.J. (2009). A tissue-scale gradient of hydrogen peroxide mediates rapid wound detection in zebrafish. Nature *459*, 996–999.

316. Yoo, S.K., Starnes, T.W., Deng, Q., and Huttenlocher, A. (2011). Lyn is a redox sensor that mediates leukocyte wound attraction in vivo. Nature *480*, 109–112.
317. Deng, Q., and Huttenlocher, A. (2012). Leukocyte migration from a fish eye's view. J. Cell Sci. *125*, 3949–3956.
318. Sadik, C.D., and Luster, A.D. (2012). Lipid-cytokine-chemokine cascades orchestrate leukocyte recruitment in inflammation. J. Leukoc. Biol. *91*, 207–215.
319. Yoo, M.H., Song, H., Woo, C.H., Kim, H., and Kim, J.H. (2004). Role of the BLT2, a leukotriene B4 receptor, in Ras transformation. Oncogene *23*, 9259–9268.
320. Wang, D., and Dubois, R.N. (2010). Eicosanoids and cancer. Nat. Rev. Cancer *10*, 181–193.
321. Mathias, J.R., Dodd, M.E., Walters, K.B., Rhodes, J., Kanki, J.P., Look, A.T., and Huttenlocher, A. (2007). Live imaging of chronic inflammation caused by mutation of zebrafish Hai1. J. Cell Sci. *120*, 3372–3383.
322. Foxman, E.F., Kunkel, E.J., and Butcher, E.C. (1999). Integrating Conflicting Chemotactic Signals. J. Cell Biol. *147*, 577 – 588.
323. de Oliveira, S., Boudinot, P., Calado, Â., and Mulero, V. (2015). Duox1-Derived H_2O_2 Modulates Cxcl8 Expression and Neutrophil Recruitment via JNK/c-JUN/AP-1 Signaling and Chromatin Modifications. J. Immunol. *194*, 1523–1533.
324. Goll, M.G., Anderson, R., Stainier, D.Y.R., Spradling, A.C., and Halpern, M.E. (2009). Transcriptional silencing and reactivation in transgenic zebrafish. Genetics *182*, 747–755.
325. Akitake, C.M., Macurak, M., Halpern, M.E., and Goll, M.G. (2011). Transgenerational analysis of transcriptional silencing in zebrafish. Dev. Biol. *352*, 191–201.
326. Zhang, X., Zhang, W., Yuan, X., Fu, M., Qian, H., and Xu, W. (2016). Neutrophils in cancer development and progression: Roles, mechanisms, and implications (Review). Int. J. Oncol. *49*, 857–867.
327. Cloutier, A., Ear, T., Blais-Charron, E., Dubois, C.M., and McDonald,

P.P. (2007). Differential involvement of NF-kappaB and MAP kinase pathways in the generation of inflammatory cytokines by human neutrophils. J. Leukoc. Biol. *81*, 567–577.

328. Greten, F.R., Eckmann, L., Greten, T.F., Park, J.M., Li, Z.W., Egan, L.J., Kagnoff, M.F., and Karin, M. (2004). IKKβ links inflammation and tumorigenesis in a mouse model of colitis-associated cancer. Cell *118*, 285–296.
329. Takahashi, H., Ogata, H., Nishigaki, R., Broide, D.H., and Karin, M. (2010). Tobacco Smoke Promotes Lung Tumorigenesis by Triggering IKKβ- and JNK1-Dependent Inflammation. Cancer Cell *17*, 89–97.
330. Enzler, T., Sano, Y., Choo, M.K., Cottam, H.B., Karin, M., Tsao, H., and Park, J.M. (2011). Cell-selective inhibition of NF-κB signaling improves therapeutic index in a melanoma chemotherapy model. Cancer Discov. *1*, 496–507.
331. Yang, J., Hawkins, O.E., Barham, W., Gilchuk, P., Boothby, M., Ayers, G.D., Joyce, S., Karin, M., Yull, F.E., and Richmond, A. (2014). Myeloid IKKβ promotes antitumor immunity by modulating CCL11 and the innate immune response. Cancer Res. *74*, 7274–7284.
332. McLoed, A.G., Sherrill, T.P., Cheng, D.S., Han, W., Saxon, J.A., Gleaves, L.A., Wu, P., Polosukhin, V. V., Karin, M., Yull, F.E., *et al.* (2016). Neutrophil-Derived IL-1β Impairs the Efficacy of NF-κB Inhibitors against Lung Cancer. Cell Rep. *16*, 120–132.
333. Reilly, S.J., Odeberg, J., and Tornvall, P. (2011). Use of the Whole Leucocyte Population in the Study of the NFκB Pathway. Scand. J. Immunol. *73*, 338–343.
334. Vancurova, I., Miskolci, V., and Davidson, D. (2001). NF-κB activation in tumor necrosis factor α-stimulated neutrophils is mediated by protein kinase Cδ. Correlation to nuclear IκBα J. Biol. Chem. *276*, 19746–19752.
335. Zarember, K.A., and Godowski, P.J. (2002). Tissue Expression of Human Toll-Like Receptors and Differential Regulation of Toll-Like Receptor mRNAs in Leukocytes in Response to Microbes, Their

Products, and Cytokines. J. Immunol. *168*, 554–561.

336. Serezani, C.H., and Lewis, C. (2011). Leukotriene B4 amplifies NF-κB activation in mouse macrophages by reducing SOCS1 inhibition of MyD88 expression. J Clin Invest *121*, 671–682.
337. Wang, Z., Filgueiras, L.R., Wang, S., Serezani, A.P.M., Peters-Golden, M., Jancar, S., and Serezani, C.H. (2014). Leukotriene B4 Enhances the Generation of Proinflammatory MicroRNAs To Promote MyD88-Dependent Macrophage Activation. J. Immunol. *192*, 2349–2356.
338. Sareneva, T., Julkunen, I., and Matikainen, S. (2000). IFN- and IL-12 Induce IL-18 Receptor Gene Expression in Human NK and T Cells. J. Immunol. *165*, 1933–1938.
339. Riedl, J., Crevenna, A.H., Kessenbrock, K., Yu, J.H., Neukirchen, D., Bista, M., Bradke, F., Jenne, D., Holak, T.A., Werb, Z., *et al.* (2008). Lifeact: A versatile marker to visualize F-actin. Nat. Methods *5*, 605–607.
340. Xu, H., Ye, D., Behra, M., Burgess, S., Chen, S., and Lin, F. (2014). Gβ1 controls collective cell migration by regulating the protrusive activity of leader cells in the posterior lateral line primordium. Dev. Biol. *385*, 316–327.
341. Phng, L.-K., Stanchi, F., and Gerhardt, H. (2013). Filopodia are dispensable for endothelial tip cell guidance. Development *140*, 4031–4040.
342. McDonald, P.P. (1997). Activation of the NF-κB Pathway by Inflammatory Stimuli in Human Neutrophils. *70*, 1955–1958.
343. Miskolci, V., and Rollins, J. (2007). NFκB Is Persistently Activated in Continuously Stimulated Human Neutrophils. Mol. Med. *13*, 1.
344. Shive, M.S., Salloum, M.L., and Anderson, J.M. (2000). Shear stress-induced apoptosis of adherent neutrophils: A mechanism for persistence of cardiovascular device infections. Proc. Natl. Acad. Sci. *97*, 6710–6715.
345. Shive, M.S., Brodbeck, W.G., and Anderson, J.M. (2002). Activation of caspase 3 during shear stress-induced neutrophil apoptosis on biomaterials. J. Biomed. Mater. Res. *62*, 163–168.

346. Hattar, K., Franz, K., Ludwig, M., Sibelius, U., Wilhelm, J., Lohmeyer, J., Savai, R., Subtil, F.S.B., Dahlem, G., Eul, B., *et al.* (2014). Interactions between neutrophils and non-small cell lung cancer cells: enhancement of tumor proliferation and inflammatory mediator synthesis. Cancer Immunol. Immunother. *63*, 1297–1306.
347. Bekes, E.M., Schweighofer, B., Kupriyanova, T.A., Zajac, E., Ardi, V.C., Quigley, J.P., and Deryugina, E.I. (2011). Tumor-recruited neutrophils and neutrophil TIMP-free MMP-9 regulate coordinately the levels of tumor angiogenesis and efficiency of malignant cell intravasation. Am. J. Pathol. *179*, 1455–1470.
348. Sinha, P., Okoro, C., Foell, D., Freeze, H.H., Ostrand-Rosenberg, S., and Srikrishna, G. (2008). Proinflammatory S100 Proteins Regulate the Accumulation of Myeloid-Derived Suppressor Cells. J. Immunol. *181*, 4666–4675.
349. Brandau, S., Trellakis, S., Bruderek, K., Schmaltz, D., Steller, G., Elian, M., Suttmann, H., Schenck, M., Welling, J., Zabel, P., *et al.* (2011). Myeloid-derived suppressor cells in the peripheral blood of cancer patients contain a subset of immature neutrophils with impaired migratory properties. J. Leukoc. Biol. *89*, 311–317.
350. Ortiz, M.L., Kumar, V., Martner, A., Mony, S., Donthireddy, L., Condamine, T., Seykora, J., Knight, S.C., Malietzis, G., Lee, G.H., *et al.* (2015). Immature myeloid cells directly contribute to skin tumor development by recruiting IL-17–producing CD4 $^{+}$ T cells. J. Exp. Med. *212*, 351–367.
351. Wu, W.-C., Sun, H.-W., Chen, H.-T., Liang, J., Yu, X.-J., Wu, C., Wang, Z., and Zheng, L. (2014). Circulating hematopoietic stem and progenitor cells are myeloid-biased in cancer patients. Proc. Natl. Acad. Sci. *111*, 4221–4226.
352. Casbon, A.-J., Reynaud, D., Park, C., Khuc, E., Gan, D.D., Schepers, K., Passegué, E., and Werb, Z. (2015). Invasive breast cancer reprograms early myeloid differentiation in the bone marrow to generate immunosuppressive neutrophils. Proc. Natl. Acad. Sci. *112*, E566–

E575.

353. Singel, K.L., and Segal, B.H. (2016). Neutrophils in the tumor microenvironment: trying to heal the wound that cannot heal. Immunol. Rev. *273*, 329–343.
354. Patel, S., Fu, S., Mastio, J., Dominguez, G.A., Purohit, A., Kossenkov, A., Lin, C., Alicea-Torres, K., Sehgal, M., Nefedova, Y., *et al.* (2018). Unique pattern of neutrophil migration and function during tumor progression. Nat. Immunol. *19*.
355. Ortiz, M.L., Lu, L., Ramachandran, I., and Gabrilovich, D.I. (2014). Myeloid-Derived Suppressor Cells in the Development of Lung Cancer. Cancer Immunol. Res. *2*, 50–58.
356. Chen, Y., Corriden, R., Inoue, Y., Yip, L., Hashiguchi, N., Zinkernagel, A., Nizet, V., Insel, P.A., and Junger, W.G. (2006). ATP release guides neutrophil chemotaxis via P2Y2 and A3 receptors. Science *314*, 1792–1795.
357. Park, S.W., Davison, J.M., Rhee, J., Hruban, R.H., Maitra, A., and Leach, S.D. (2008). Oncogenic KRAS Induces Progenitor Cell Expansion and Malignant Transformation in Zebrafish Exocrine Pancreas. Gastroenterology *134*, 2080–2090.
358. Khavari, P.A. (2006). Modelling cancer in human skin tissue. Nat. Rev. Cancer *6*, 270–280.
359. Le, X., Langenau, D.M., Keefe, M.D., Kutok, J.L., Neuberg, D.S., and Zon, L.I. (2007). Heat shock-inducible Cre/Lox approaches to induce diverse types of tumors and hyperplasia in transgenic zebrafish. Proc. Natl. Acad. Sci. U. S. A. *104*, 9410–9415.
360. Kerr, E.M., Gaude, E., Turrell, F.K., Frezza, C., and Martins, C.P. (2016). Mutant Kras copy number defines metabolic reprogramming and therapeutic susceptibilities. Nature *531*, 110–113.
361. Chen, X., Makarewicz, J.M., Knauf, J.A., Johnson, L.K., and Fagin, J.A. (2013). Transformation by HrasG12V is consistently associated with mutant allele copy gains and is reversed by farnesyl transferase inhibition. Oncogene *33*, 5442–5449.

362. Varga, J., and Greten, F.R. (2017). Cell plasticity in epithelial homeostasis and tumorigenesis. Nat. Cell Biol. *19*, 1133–1141.
363. Natarajan, V., Komarov, A.P., Ippolito, T., Bonneau, K., Chenchik, A.A., and Gudkov, A. V. (2014). Peptides genetically selected for NF-κB activation cooperate with oncogene Ras and model carcinogenic role of inflammation. Proc. Natl. Acad. Sci. *111*, E474–E483.
364. Göktuna, S.I., Canli, O., Bollrath, J., Fingerle, A.A., Horst, D., Diamanti, M.A., Pallangyo, C., Bennecke, M., Nebelsiek, T., Mankan, A.K., *et al.* (2014). IKKα Promotes Intestinal Tumorigenesis by Limiting Recruitment of M1-like Polarized Myeloid Cells. Cell Rep. *7*, 1914–1925.
365. Oeckinghaus, A., and Ghosh, S. (2009). The NF-κB Family of Transcription Factors and Its Regulation. Cold Spring Harb. Perspect. Biol. *1*, 1–15.
366. Aguilera, C., Hoya-Arias, R., Haegeman, G., Espinosa, L., and Bigas, A. (2004). Recruitment of IκB to the hes1 promoter is associated with transcriptional repression. Proc. Natl. Acad. Sci. *101*, 16537–16542.
367. Mulero, M.C., Ferres-Marco, D., Islam, A., Margalef, P., Pecoraro, M., Toll, A., Drechsel, N., Charneco, C., Davis, S., Bellora, N., *et al.* (2013). Chromatin-bound IκBα regulates a subset of polycomb target genes in differentiation and cancer. Cancer Cell *24*, 151–166.